The role of a fungal-specific transcription regulator on vacuolar biology and host interaction in *Candida albicans*

Die Rolle eines pilzspezifischen Transkriptionsfaktors für die Vakuole und Wirtsinteraktion von *Candida albicans*

Doctoral thesis for a doctoral degree
at the Graduate School of Life Sciences,
Julius-Maximilians-University, Würzburg,
Section Infection and Immunity

Submitted by

Philipp Reuter-Weissenberger

From
Schweinfurt

Würzburg 2021

Für Elise

(Und für alle, die noch kommen mögen)

Submitted on:

Members of the Doctoral Thesis Committee

Chairperson: Prof. Dr. Thomas Dandekar

Primary Supervisor: Prof. Dr. J. Christian Pérez

Supervisor (Second): Prof. Dr. Bernhard Hube

Supervisor (Third): Prof. Dr. Joachim Morschhäuser

Supervisor (Fourth): Prof. Dr. Oliver Kurzai

Date of Public Defense:

Date of Receipt of Certificates:

Acknowledgements

I would like to start by thanking my primary supervisor Prof. Dr. J. Christian Pérez. Thank you for giving me the opportunity to work on this great project that allowed me to learn so many interesting things. I would also like to mention that I truly appreciate your constant support, in particular, during the last six month.

I thank Prof. Dr. Joachim Morschhäuser for always taking the time to discuss and talk about everything regarding *C. albicans* and beyond. It has been a pleasure!

I would also like to thank Prof. Dr. Bernhard Hube for hosting me in his laboratory. I truly enjoyed the time in Jena where I met great people and learned a lot about *C. albicans*.

A special thank you goes to Prof. Dr. Oliver Kurzai for his support and generosity while carrying out manuscript revisions. I feel honored to be now part of the IHM and I am looking forward to - hopefully - many interesting years!

I also want to thank the Graduate School of Life Sciences for their support and their well-organized study program.

I would like to give a huge thank you to all the members of the DNA-Labor of the IHM and Prof. Dr. Dr. Christoph Schoen for their support and patients during the last couple of months. I could not have ended up in a better team!

I am infinitely grateful for all the colleagues I have had the pleasure of working with in the Pérez lab: Sanda, Lena, Valentina, Marie, Juliane, and Sergio. It was amazing working with you. And for Valentina, I truly appreciated the time you spent lecturing this thesis and I cannot thank you enough for that! As well, I want to thank my former office neighbors and all the colleagues from the other working groups that became great friends to me namely Fabian, Gianluca, Falk, Yen, Elise, Youssef, Kotaro, Austin, Bernardo, and Mandela. I feel immensely lucky for knowing you all.

I would like to give a huge thanks to my family and friends and to my wife Isabell for her patience and constant support through all those years.

Summary

Microorganisms that colonize the human body face large fluctuations in their surroundings. Therefore, those microbes developed sophisticated mechanisms that allow them to adapt their cell biology and maintain cellular homeostasis. One organelle vital to preserve cell physiology is the vacuole. The vacuole exhibits a wide range of functions and is able to adjust itself in response to both external and internal stimuli. Moreover, it plays an important role in host interaction and virulence in fungi such as *Candida albicans*. Despite this connection, only a few regulatory proteins have been described to modulate vacuolar biology in fungal pathogens. Furthermore, whether such regulation alters fungus-host interplay remains largely unknown.

This thesis focuses on the characterization of *ZCF8*, a fungus-specific transcription regulator in the human-associated yeast *C. albicans*. To this end, I combined genome-wide protein-DNA interaction assays and gene expression analysis that identified genes regulated by Zcf8p. Fluorescence microscopy uncovered that several top targets of Zcf8p localize to the fungal vacuole. Moreover, deletion and overexpression of *ZCF8* resulted in alterations in vacuolar morphology and in luminal pH and rendered the fungus resistant or susceptible to a vacuole-disturbing drug. Finally, *in vitro* adherence assays showed that Zcf8p modulates the attachment of *C. albicans* to human epithelial cells in a vacuole-dependent manner.

Given those findings, I posit that the previously uncharacterized transcription regulator Zcf8p modulates fungal attachment to epithelial cells in a manner that depends on the status of the fungal vacuole. Furthermore, the results highlight that vacuolar physiology is a substantial factor influencing the physical interaction between *Candida* cells and mammalian mucosal surfaces.

Zusammenfassung

Mikroorganismen, die den Menschen besiedeln, sind großen Schwankungen in ihrer Umgebung ausgesetzt. Daher haben sie ausgeklügelte Mechanismen entwickelt, die es ihnen ermöglichen, ihre Zellbiologie anzupassen und die zelluläre Homöostase aufrechtzuerhalten. Eine für die Aufrechterhaltung der Zellphysiologie wichtige Organelle ist die Vakuole. Sie verfügt über ein breites Spektrum an Funktionen und ist in der Lage, auf externe und interne Stimuli zu reagieren. Außerdem spielt dieses Organell eine wichtige Rolle bei der Pilz-Wirt-Interaktion und somit für die Pathogenität von Pilzen wie *Candida albicans*. Trotz dieses Zusammenhangs wurden bisher nur wenige regulatorische Proteine beschrieben, welche die Biologie der Vakuolen in pathogenen Pilzen modulieren. Zudem ist weitgehend unbekannt, ob eine solche Regulierung das Zusammenspiel von Pilz und Wirt verändert.

Diese Arbeit konzentriert sich auf die Charakterisierung von *ZCF8*, einem pilzspezifischen Transkriptionsregulator in der pathogenen Hefe *C. albicans*. Zu diesem Zweck wurden Protein-DNA-Interaktionstests und Genexpressionsanalysen kombiniert, um Gene zu identifizieren, die direkt von Zcf8p reguliert werden. Fluoreszenzmikroskopie zeigte zudem, dass mehrere der wichtigsten Ziele von Zcf8p in der Pilzvakuole lokalisiert sind. Darüber hinaus führte die Deletion und Überexpression von *ZCF8* zu Veränderungen der Morphologie und des luminalen pH-Werts der Vakuole, und veränderte die Sensitivität des Pilzes gegenüber Stoffen, welche Funktionen der Vakuole beeinträchtigen. Schließlich deuteten *In-vitro*-Adhärenztests daraufhin, dass Zcf8p die Anheftung von *C. albicans* an menschliche Epithelzellen auf eine Weise moduliert, die abhängig von der Vakuole ist.

Angesichts dieser Ergebnisse kann davon ausgegangen werden, dass der bisher unbekannte Transkriptionsregulator *ZCF8* die Interaktion zwischen Pilz- und Epithelzellen des Wirts kontrolliert, und das auf eine Weise, die von der Pilzvakuole abhängig ist. Des Weiteren, unterstreichen die Ergebnisse, dass die Physiologie der Vakuole ein wesentlicher Faktor ist, welcher die Interaktion zwischen *C. albicans* und dem Wirt beeinflusst.

Abbreviation Index

% (v/v)	% (volume/volume)
°C	degree Celsius
Δ	delta; Deletion
^{32}P	radioactive isotope of phosphorus
BAM	Binary Alignment Map (file format, containing raw data from genome sequencing)
BCECF	2′,7′-bis-(2-carboxyethyl)-5-(and-6)-carboxyfluorescein
BED	Browser Extensible Data (file format to store information of a genome)
BFA	brefeldin A
BSA	Bovine Serum Albumin
CGD	*Candida* Genome Database
	ChIP-Seq chromatin immunoprecipitation followed by next generation sequencing
CO_2	carbon dioxide
DBD	DNA binding domain
DIC	differential interference contrast
DMEM	Dulbecco's Modified Eagle Medium
DMSO	dimethyl sulfoxide
DNA	deoxyribonucleic acid
dNTP	deoxyribonucloside triphosphate
DTT	dithiothreitol
EDTA	ethylenediaminetetra acetic acid
EMSA	electrophoretic mobility shift assay
EtOH	ethanol
FBS	fetal bovine serum
GFP	Green Fluorescent Protein
HCl	hydrochloric acid

HEPES	4-(2-hydroxyethyl)-1-piperazineethanesulfonic acid (buffer)
HRP	horseradish peroxidase
IP	immunoprecipitation
IPTG	isopropyl-β-D-thiogalactopyranosid
KOH	potassium hydroxide
LDH	lactate dehydrogenase
Log2FC	log2 fold change
LiCl	lithium chloride
$MgCl_2$	magnesium chloride
mNG	mNeonGreen
MOI	multiplicity of infection
mRNA	messenger RNA
MUSCLE	Multiple Sequence Comparison by Log-Expectation (Multiple sequence alignment tool provided by EMBL)
Na_2HPO_4	disodium phosphate
NaCl	sodium chloride
NaH_2PO_4	monosodium phosphate
NaOH	sodium hydroxide
NAT	nourseothricin
NCBI	National Center for Biotechnology Information
NGS	next generation sequencing
NS	not significant
nt	nucleotide(s)
OD_{600}	optical density at 600 nm
Oligo	oligonucleotide
ORF	open reading frame
P	*p*-value
PAGE	polyacrylamide gel electrophoresis
PAS	periodic acid-Schiff
PBS	phosphate buffered saline
PCA	principal component analysis

PCR	polymerase chain reaction
PMSF	phenylmethylsulfonylfluorid
PNK	polynucletide kinase
RNA	ribonucleic acid
RNA-Seq	RNA-sequencing
rpm	revolutions per minute
RT	room temperature
SAM	Sequence Alignment Map (storage format for DNA sequencing)
SD	standard deviation
SDS	sodium dodecyl sufate
TBS	tris-buffered saline
TBS-T	tris-buffered saline with Tween-20
TE	tris and EDTA containing buffer
TEER	transepithelial electrical resistance
Tris	tris(hydroxymethyl)aminomethane
ohm	SI derived unit of electrical resistance
V-ATPase	vacuolar-type ATPase
VPS	vacuolar protein sorting
WB	Western blot
WIG	wiggle (data format to plot quantitative data)
YFP	Yellow fluorescent protein
YM	yeast mold (agar)
YNB	yeast nitrogen base
YPD	Yeast Extract–Peptone–Dextrose
$ZnSO_4$	Zinc sulfate

List of figures

List of tables

Table of contents

1 Introduction

1.1 Living on the mammalian host

The mammalian host (such as the human body) is a complex habitat for any microbial colonizer. Depending on each niche nutrient availability, pH, oxygen, and CO_2 levels can be dramatically different (Brown *et al.*, 2014). The human oral mucosa, for example, is mildly acidic (pH 6) and saliva contains glycoproteins, mucins, and antimicrobial peptides, whereas the female genital tract is rather acidic (pH 4 - 5) and has lactate as the main carbon source (Hall, 2015). While lactate as well as acetate is also present in the stomach (Rowland *et al.*, 2018), microbes are here exposed to hypoxia (*i.e.* low oxygen levels) and an acidic pH of ~2 (Zwolińska-Wcisło *et al.*, 1998). Metabolic flexibility is required for microbial colonizers as they encounter a variety of both fermentable and nonfermentable carbon sources depending on each niche (Van Ende *et al.*, 2019). In addition, the host is able to withhold essential micronutrients, like iron, zinc, copper, and manganese a process named nutritional immunity (Hood and Skaar, 2012). Even if nutrients are available, there is a constant competition between host cells and microbes as well as within the microbial community for nutrients which leads to cooperative but also antagonistic interactions (Alves *et al.*, 2020). Bacteria and fungi might also be exposed to increased temperatures up to 42°C as the host responds to microbial infection with fever (Casadevall, 2016). If the immune system is activated, phagocytic cells attack microbes and expose them to oxidative, nitrosative, and cationic stresses in order to kill them (Alves *et al.*, 2020).

Microbes that colonize the mammalian host, therefore, have developed sophisticated mechanisms that allow a rapid and coordinated change of metabolism and the maintenance of cellular homeostasis that keeps their physiology intact. This is of particular interest for organisms that colonize different sites within the host such as the fungus *Candida albicans*.

1.2 The fungus *Candida albicans*

C. albicans is a prominent member of the human mycobiota, *i.e.* the composition of fungi associated with the human body. This opportunistic yeast is generally found as a harmless colonizer of a variety of different mammalian mucosae such as the oral cavity and gastrointestinal tract (Underhill and Iliev, 2014). The over proliferation of this fungus is kept under control by physical barriers (*e.g.*, the mucus layer in the intestine), the immune system, and competing microbes (Bougnoux *et al.*, 2006). Occasionally, when these mechanisms are disrupted, *e.g.*, in patients suffering from HIV, undergoing chemotherapy, or upon antibiotic treatments, the fungus can overgrow and cause diseases ranging from superficial to severe systemic infections (Brown *et al.*, 2012). *C. albicans* is polymorphic meaning that the fungus can adopt multiple morphologies. Each morphology interacts with host tissues in different ways. For example, while the oval-shaped yeast form is associated with harmless colonization of the gut (Pérez, 2019), filamentation has been described to play a major role during fungal infection (Gow *et al.*, 2012). However, both morphologies are relevant for virulence of *C. albicans* (Jacobson 2012). The fungus can also form pseudohyphae which are elongated ellipsoid cells that are connected to each other but remain separated by a septum (Gale and Berman, 2012), as well as thick-walled chlamydospores which survive unfavorable conditions and undergo phenotypic switching between white and opaque morphologies which is important for biofilm formation and mating.

C. albicans shares many core features with the related species *Saccharomyces cerevisiae*, a well-studied model organism. This allows for the application of many methodologies in *C. albicans* that were originally developed for *S. cerevisiae*. However, there is a large evolutionary distance of ~300 to 800 million years (Douzery *et al.*, 2004) and, in contrast to *S. cerevisiae*, *C. albicans* can survive in nearly every niche of the mammalian host and is able to cause severe diseases (Hernday *et al.*, 2010). Given the clinical relevance of *C. albicans* in human health and the availability of techniques that allow genome modification as well as high

quality sequencing, this fungus represents an important fungal pathogen for infection research.

1.3 Cellular biology of fungal adaptation

Possibly the most important challenge microbes face in the human host, is nutrient availability. Assimilation of nutrients including sugars, carboxylic acids, amino acids, lipids, or phospholipids is key to successfully colonize these microenvironments within host niches. The preferred carbon source for many cells is glucose. However, as glucose is either limited or absent from many sites, *C. albicans*, and other *Candida* species, have developed a strategy to assimilate glucose and alterative carbon sources such as galactose simultaneously (Barelle, *et al.*, 2006; Sandai *et al.*, 2012; Childers *et al.*, 2016). To do so, enzymes of the gluconeogenic and glyoxylate cycle that facilitate the assimilation of alterative carbon sources are, in contrast to *S. cerevisiae* (Gancedo, 1998), not ubiquitinylated and remain active in the presence of glucose (Sandai *et al.*, 2012; Childers *et al.*, 2016). In the gut, *C. albicans* is also able to take up and catabolize N-acetylglucosamine (GlcNAc) an amino sugar that is mainly produced by bacteria (Alvarez, 2007; Su *et al.*, 2016; Naseem *et al.*, 2017). The fungus also has specialized transporters to import further carbon sources such as lactate and acetate which are abundant in the gut and vaginal secretions (Owen *et al.*, 1999; Rowland *et al.*, 2018). In fact, the nature of the available carbon source induces not just metabolic adaptations, but niche-specific carbon sources are proposed to have a dramatic influence on the architecture and functionality of the fungal cell wall (Brown *et al.*, 2014). For example, while the structure remains similar, the thickness of the cell wall of *C. albicans* cells grown in lactate is only half of that grown with glucose (Ene *et al.*, 2012).

The acquisition and metabolism of nitrogen is also critical for *C. albicans*. To make amino acids in the surroundings accessible, the fungus releases **s**ecreted **a**spartyl **p**roteinases (SAPs) that degrade complement proteins and host connective tissue (Gropp *et al.*, 2009). Once the amino acids become available, they are sensed by the SPS complex which in turn activates transcription

regulators of extracellular proteases and peptide transporters as well as amino acid permeases to import the nutrients into the fungal cell (Martínez *et al.*, 2005).

C. albicans and other microbes face extreme changes in ambient pH, ranging from an acidic pH of 2 in the gastrointestinal tract (Zwolińska-Wcisło *et al.*, 1998) to the slightly alkaline human blood (pH 7.4) (Alves *et al.*, 2020). Adaptation to various pH levels is mediated by the Rim pathway (Cornet and Gaillardin, 2014). The pathway elicits the primary pH response in *C. albicans* and has been shown to be required not only for survival and growth in the host but also for virulence (Davis, 2003). While the mechanism of the Rim pathway is different depending on the pH, cell-wall remodeling seems to be relevant for fungal proliferation in acidic and alkaline milieus (Nobile *et al.*, 2008; Sherrington *et al.*, 2017). As a result, more chitin and β-glucans are added to the cell wall to provide rigidity and protection. However, both structures are key fungal PAMPs (**p**athogen-**a**ssociated **m**olecular **p**atterns) and the pH-dependent exposure at the cell surface consequently activates the immune system and attracts neutrophils and macrophages (Sherrington *et al.*, 2017). To reduce the local immune response again, chitin and β-glucans are “re-masked” over time (Pradhan *et al.*, 2018; Cottier *et al.*, 2019). Thus, the cell wall of *C. albicans* is a dynamic organelle that responds to changes in the ambient pH (Alves *et al.*, 2020).

Oxygen levels can vary dramatically between niches within the host, varying from the oxygen-rich oral cavity to hypoxic environments in the gastrointestinal tract. Moreover, biofilm formation and infection of host tissue also generates low-oxygen microenvironments. *C. albicans* cells can adapt to these variations but the molecular mechanisms are not fully understood (Alves *et al.*, 2020). When shifted from normal oxygen level (~21%) to hypoxic growth (≤1%), the expression of genes involved in multiple pathways is induced, including fatty acid metabolism (Setiadi *et al.*, 2006; Stichternoth and Ernst, 2009), heme and iron metabolism, cell-wall structure and sterol biosynthesis (Setiadi *et al.*, 2006; Askew *et al.*, 2009; Synnott *et al.*, 2010).

One way the human body responds to microbial infections is fever exposing the invading cells to temperatures up to 42°C (Alves *et al.*, 2020). In *C. albicans*, a shift

in temperature induces several processes including morphology, mating, and phenotypic switching (Shapiro *et al.*, 2011). The mechanisms that sense changes in the ambient temperature are rather diverse. The most studied pathway, however, is the heat shock response which induces early and long-term thermal adaptation (Lindquist, 1992; Leach *et al.*, 2012). The pathway monitors the number of molecular chaperones, named heat shock proteins, in the cytoplasm. Those proteins either maintain the function of other proteins by stabilizing their fold or target damaged proteins for degradation.

Another dynamic environmental factor *Candida* cells must cope with is the presence of surrounding microbial communities. While some interactions might be beneficial, others represent a serious obstacle for *Candida* that goes beyond metabolic competition (Alves *et al.*, 2020). Commensal bacteria such as *Lactobacillus* species produce antimicrobial peptides that appear to have high fungicidal activity (Graf *et al.*, 2019; Itapary Dos Santos *et al.*, 2019; Jang *et al.*, 2019). The mechanisms in *C. albicans* to avoid or counteract these antagonistic interactions remain unclear. Farnesol, a fungal quorum sensing molecule, is believed to play a role as it has strong antifungal and antibacterial activities against a range of different organisms (Polke and Jacobsen, 2017; Polke *et al.*, 2018).

The host immune defense is a ubiquitous factor for the microbial community. *C. albicans* has developed multiple strategies to either avoid recognition or escape host surveillance (Alves *et al.*, 2020). For example, PAMPs exposed on the cell surface such as chitin, β-glucans, and mannans are hidden or masked to avoid host recognition (Childers *et al.*, 2020). In addition, *Candida* cells can secrete proteases that degrade proteins of the complement system that would otherwise attract phagocytes (Speth *et al.*, 2008). If none of these strategies are successful, the fungus will be internalized by phagocytic cells and exposed to oxidative or nitrosative stresses in an attempt to kill the fungal cells. *C. albicans*' cellular response to counteract these stresses is the activation of genes that contribute to detoxification and reparation processes (Enjalbert *et al.*, 2006, 2007; Pradhan *et al.*, 2017).

In addition to the constant surveillance by the immune system, the host can actively withhold essential micronutrients from invading pathogens. This attempt of the immune system to restrict the access to iron, zinc, or manganese is called nutritional immunity (Hood *et al.*, 2012). These micronutrients are essential cofactors for enzymes, transcription factors, or other vital proteins (Gerwien *et al.*, 2018). Therefore, *C. albicans* has developed mechanisms to overcome this limitation by expressing specialized transporters and/or using alternative micronutrients (Crawford *et al.*, 2015; Li *et al.*, 2015). Sophisticated iron-uptake systems assimilate either free iron in the surroundings (Knight *et al.*, 2005; Chaves *et al.*, 2007) or exploit iron-binding proteins of the host such as hemoglobin (Kuznets *et al.*, 2014) and ferritin (Almeida *et al.*, 2008). A second interesting example is the use of alternative cofactors for enzymes that play important roles in antioxidant protection and cell signaling processes (Li *et al.*, 2015). For example, in the excess of copper, one form of the enzyme is active that uses copper as a cofactor. As levels of copper decline, a second copper-independent form of that enzyme is activated which allows to maintain functionality of the protein (Li *et al.*, 2015). The competition between the host and the fungus is even more drastic when it comes to zinc. The host follows multiple strategies to limit extracellular zinc levels either by releasing antimicrobial peptides that bind zinc (Urban *et al.*, 2009) and/or by pumping it into the Golgi apparatus of immune cells (Subramanian Vignesh *et al.*, 2013). As a response, the fungus overexpresses zinc uptake transporter systems and secrete proteins that bind zinc and sequester zinc from host cells (Citiulo *et al.*, 2012).

1.4 Fungal-specific family of transcription regulators

Transcription regulators are proteins present in all living organisms controlling the expression of specific genes. They determine how a cell functions and play a central part in responding to environmental factors. In *C. albicans*, around 4% of all transcripts code for these specialized proteins (Homann *et al.*, 2009). They recognize short non-coding DNA sequences usually located in intergenic loci upstream of the coding region of the gene they regulate. Through binding, these

proteins regulate the expression of their target genes by acting either as an activator or a repressor. When acting as activators, the regulators interact with the transcription machinery to initialize expression, whereas when they function as repressors, they block binding of the machinery either by chromatin condensation of the enhancer region or through allosteric competition with activator proteins (Carlberg *et al.*, 2020).

Transcription regulators have characteristic domains that define the general functionality of the protein such as the DNA binding domain, as well as other domains for dimerization, and for interaction with co-factors, and/or other nuclear proteins (Carlberg *et al.*, 2020). However, all transcription regulators share a protein structure (structural motif) which recognizes specific DNA sequence in the promoter region of the targeted gene (sequence or DNA motif). As the structure of those protein domains varies greatly, the most common way to classify transcription regulators is based on the protein structure of their DNA binding domain. One of the most abundant DNA binding motifs is the zinc finger. The classical zinc finger consists of about 30 amino acid residues of which two to four (either four cysteines or two cysteines and two histidine) interact with a single zinc ion that stabilizes the fold of the small motif (Carlberg *et al.*, 2020). Regulators with a zinc finger domain represent one of the largest classes of transcription regulators found in eukaryotes ranging from yeasts to humans (MacPherson *et al.*, 2006). However, one subfamily is exclusive to the kingdom of fungi (MacPherson *et al.,* 2006): $Zn(II)_2Cys_6$ or Zinc cluster proteins contain a well conserved and characteristic motif which consists of two zinc ions nested in six cysteine residues (Figure 1). They are best characterized for *S. cerevisiae* while they are also found in a variety of other fungi including *Kluyveromyces lactis*, *Schizosaccharomyces pombe*, and human pathogens such as *Aspergillus nibulans,* and *Candida albicans*. Moreover, zinc cluster transcription regulators are enriched in *Candida* species when compared to the non-pathogenic yeast *S. cerevisiae* suggesting they play key roles in adapting to the human host (Issi *et al.*, 2017).

Figure 1 illustrates a representation of a zinc cluster DNA binding domain. Such motifs are commonly found towards the 5’ end of the coding region but can be also

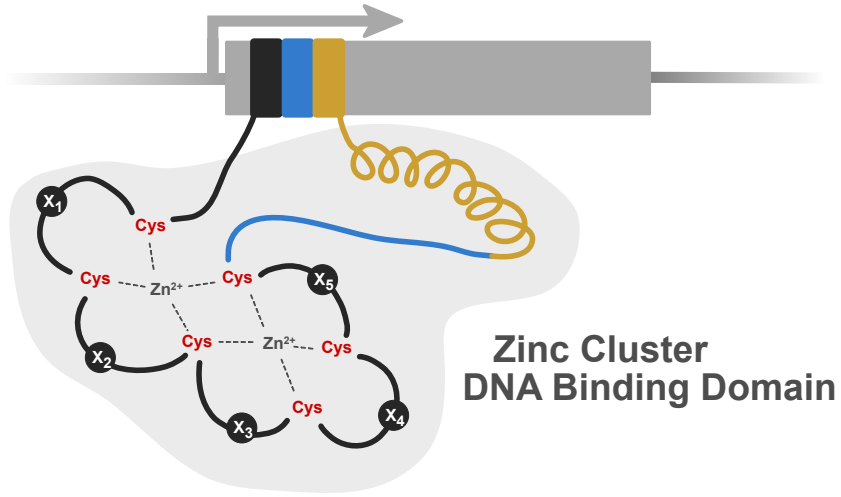

Figure 1: Common domains of a zinc cluster transcription regulator. Illustrated is an example of a zinc cluster proteins containing a distinct DNA binding domain towards the N-terminus which consists of a zinc finger domain (black), a linker sequence (blue), and a dimerization domain (yellow). The characteristic zinc finger has six cysteine residues (red) that interact with two zinc atoms. The amino acid sequence between the cysteines varies in sequence and length.

located close to the 3' end in some genes. The DNA binding domain consists of three regions: (a) the zinc finger motif, which contains the characteristic six cysteines with two nested zinc atoms, followed by (b) a linker sequence that provides a rigid scaffold and mediates sequence specific binding, and (c) dimerization regions which are responsible for dimerization and protein-protein interactions. Zinc cluster transcription regulators can bind the promoter region of their target genes solely as monomers, in protein complexes as homodimers or heterodimers, or even in combination with transcription regulators from other families (MacPherson *et al.*, 2006). There are also examples of networks of regulators that coordinate the transcription of a single shared target (*e.g.*, Pdr1p, Pdr3p, and Rdr1p regulate the expression of *PDR5*) (Katzmann *et al.*, 1994, 1996; Ha *et al.*, 1996; Akache *et al.*, 2002, 2004). Several members of the Zinc cluster family control their own gene expression generating a positive feedback loop (MacPherson *et al.*, 2006). Despite the vast repertoire of functions and functionalities of members within the family, a common feature of zinc cluster proteins is the recognition of DNA sequences harboring a 5'-CGG-3' triplet

(MacPherson *et al.*, 2006). This regulatory element within the DNA motif can be oriented everted or inverted, or as direct repeats depending on how the protein(s) binds to DNA (Mamane *et al.*, 1998; MacPherson *et al.,* 2006). In fact, two very important drivers of DNA-binding specificity are the orientation of the 5'-CGG-3' triplet and the spacing between the repeats (Vashee *et al.*, 1993). Despite the high similarity between these binding sites, the DNA motifs do display some degree of variations to guarantee that a specific regulator performs its own unique task. As mentioned above, the number and orientation of the triplet determines the specificity of the binding of protein to DNA, but some known DNA motifs do not even contain a strict CGG sequence but rather a GNCNC (*e.g.*, Arg81) (MacIsaac *et al.*, 2006), GCG (*e.g.*, Cha4p) (MacIsaac *et al.*, 2006), or CGCG (*e.g.*, Sut1p) (Régnacq *et al.*, 2001, MacIsaac *et al.*, 2006). Thus, it is very likely that sequence elements beyond the common 5'-CGG-3' triplet inside the binding site drive binding specificity and have not been characterized yet.

The family of zinc cluster proteins is best characterized in the model organism *S. cerevisiae*, of which genome contains 55 members (MacPherson *et al.,* 2006). Identified roles of these proteins in *S. cerevisiae* cover cellular processes ranging from sugar metabolism (*e.g.*, Gal4p, probably the most studied zinc cluster protein) (Marmorstein *et al.*, 1992) and nitrogen utilization (Bricmont *et al.*, 1991, Coornaert *et al.*, 1991) to regulating meiosis (*e.g.*, Ume6p) (Anderson *et al.*, 1995; Jackson *et al.,* 1996) and chromatin remodeling (Angus-Hill *et al.*, 2001). In contrast, the genome of the opportunistic human pathogen *C. albicans* contains 82 members that is 27 regulators more than in *S. cerevisiae* (Schillig *et al*, 2013). Among these 82 genes many are orthologs of *S. cerevisiae* and are implicated in similar processes (MacPherson *et al.,* 2006). However, multiple zinc cluster transcription regulators acquired novel functions in the human-associated fungus *C. albicans* most likely through a process named transcriptional (or evolutionary) rewiring. Examples of transcriptional rewiring can be found in the regulation of genes of alternative carbon metabolism (Ramírez *et al.*, 2009), allantoin catabolism (Tebung *et al.*, 2016), and ergosterol biosynthesis (Sellam *et al.*, 2010). Interestingly, some of these regulators play important roles in fungal virulence. For instance, Ume6p

mediates meiosis in *S. cerevisiae* but is a filament-specific regulator of hyphal extension and virulence in *C. albicans* (Banerjee *et al.*, 2008; Carlisle *et al.*, 2010).

1.5 Transcriptional control and host colonization

As mentioned above, morphological and metabolic adaptation are key for *C. albicans* to successfully proliferate on its mammalian host. Several transcription regulators have been identified so far to affect aspects of these cellular adaptation processes in the fungus. The morphological switch between yeast and hyphae, named yeast-to-hyphae transition, for example, is critical during gut colonization and orchestrated by an array of regulators (Gow and Yadav, 2017; Pérez, 2019). One of these transcription regulators is Flo8p. It is required for hyphal development because deleting the genes blocked hypha formation and rendered the mutant avirulent in a mouse model of systemic infection (Cao *et al.*, 2006). The role of the gene was further supported as its loss-of-function mutation, which was induced by continuously passages through the murine gut, showed increases fitness of *C. albicans* in that environment (Tso *et al.*, 2018).

Physiological adaptation of the fungus upon environmental changes regarding nutrient availability is modulated by another set of transcription regulators (Brown *et al.*, 2014). One example of regulators that modulate iron homeostasis in iron-rich environments as well as in niches where iron is sequestered by the host are the transcription regulators Sef1p, Sfu1p and Hap43p (Chen *et al.*, 2011). The presence of this essential metal triggers Sfu1p to directly repress Sef1p and iron uptake in general. In contrast, low concentrations of iron induce Sef1p to activate Hap43p and iron-uptake genes, and, moreover, Hap43p represses Sfu1p and iron-utilization (Chen *et al.*, 2011). This tripartite relationship is also one example on how multiple regulators interact in a network to orchestrate one trait.

In fact, there are several examples of transcriptional networks in *C. albicans*. Two well-studied regulators, Efg1p and Wor1p, are central in a global developmental process that primes the fungus for commensalism (Pande *et al.*, 2013): The gastrointestinal induced transition (GUT) phenotype regulates changes

on morphology and metabolism resulting in *Candida* cells which do not filament and are highly adapted to the nutrients available in the intestine (Pande *et al.*, 2013). In addition, Efg1p and Wor1p are suggested to coordinate another phenotypic adaptation characterized as white-gray-opaque tristable switching in *C. albicans* which enables the fungus to rapidly adjust cellular appearances, mating competency, and virulence (Tao *et al.*, 2014). Further research and understanding of regulatory proteins are crucial for the identification of key genes that orchestrate the biology of *C. albicans* during host colonization and/or virulence.

1.6 Biology of the vacuole

The vacuole is a dynamic, relatively large, spherical, or tubular organelle in eukaryotic cells of plants and fungi and analogous to the lysosome in animal cells (Klionsky *et al.*, 1990; Weber, 2002). The organelle's acidic lumen is separated from the surrounding neutral cytosol by a membrane, the tonoplast, which contains an array of embedded transporters for a wide variety of substrates (Li and Kane, 2009). The driving force for many membrane proteins is the proton gradient established by the **v**acuolar H^+-ATPase (V-ATPase) (Kane, 2006). Its activity generates an acidic pH of around 6.25 in the lumen which serves as the chemical basis for almost all functions of the vacuole: it provides an optimal milieu for the hydrolytic enzymes to mature, drives the uptake and storage of metabolites, and allows vesicle fusion. In fact, loss of vacuolar acidification is lethal in all organisms - except in fungi (Davies *et al.*, 1996; Sun-Wada *et al.*, 2000; Kane, 2006). In summary, the vacuole is a cellular multi-tool with four basic functions: It (a) degrades proteins and cellular components, (b) stores nutrients and ions, (c) maintains cellular homeostasis, and (4) detoxifies the cytosol (reviewed in Klionsky *et al.*, 1990; and Li and Kane, 2009).

1.6.1 Degradation of cytosolic proteins and organelles

The vacuole is a degradative organelle and hydrolases represent the major class of proteins in the acidic lumen that non-specifically break down the cargo

brought to it (Sarry *et al.*, 2007). Soluble and membrane-bound hydrolytic enzymes are amongst the best-characterized vacuolar proteins (Klionsky *et al.*, 1990; Jones, 1991; Knop *et al.*, 1993; Van Den Hazel *et al.*, 1996). They are delivered to the vacuole as proenzymes through specialized pathways and become mature inside the lumen. For example, the vacuolar protein **c**arboxy**p**eptidase **Y** follows the CPY pathway, one of several **v**acuolar **p**rotein **s**orting (VPS) pathways (Bryant and Stevens, 1998; Bryant *et al.*, 1998; Conibear *et al*, 1998; Wurmser *et al.*, 1999); or the **c**ytoplasm-to-**v**acuole **t**argeting (Cvt) pathway that is a biosynthetic route for vacuolar hydrolases and is related to autophagy (Wendland *et al.*, 1998; Strømhaug *et al.*, 2004). Autophagy is a process that enables the cell to sequester cytosolic proteins and organelles for degradation at the vacuole as part of both housekeeping and stress-response (Kim and Klionsky, 2000). There are two different types of autophagy, namely macroautophagy and microautophagy. In the latter, cytosolic material is “simply” engulfed by the vacuole and subsequently degraded. Conversely, macroautophagy is a more complex process: A double membrane vesicle named autophagosome forms **p**re-**a**utophagosomal **s**tructures (PAS) and encloses cytosolic cargo. Then the outer membrane of the vesicle fuses with the vacuole and releases the inner single-membraned vesicle (now named autophagic body) into the lytic lumen. The autophagic body containing the cargo is degraded as a whole by the resident hydrolases inside the vacuole (Kraft and Martens, 2012). The catabolites can be then exported to the cytosol and recycled providing a supplementary reserve for the cell. The terms autophagy and macroautophagy are often used synonymously as will be the case throughout this thesis.

1.6.2 Storage and cellular homeostasis

The vacuole is the main storage unit of the cell which is highlighted by the wide variety of transporters moving amino acids, phosphate, Ca^{2+}, and many ions over the membrane (Klionsky *et al.*, 1990; Li and Kane, 2009). A collection of broad or specific transporters localized at the fungal vacuole facilitate the accumulation of high levels of amino acids in it. In the yeast *Saccharomyces cerevisiae*, the

members of the major **f**acilitator **s**uperfamily (MFS) Vba1p (**v**acuolar **b**asic **a**mino acid transporter), Vba2p and Vba3p are responsible for the uptake of lysine, arginine and histidine (Shimazu *et al.*, 2005). Orthologs of the **a**mino acid **v**acuolar **t**ransporter (AVT) family, found in mammals, plants, and worms, are involved in bidirectional movement of large neutral amino acids across the vacuolar membrane (Russnak *et al.*, 2001). Bidirectional transport of amino acids is a critical feature of the vacuole. It allows the cell to maintain amino acid homeostasis by either storing an excess of amino acids inside the vacuole or recycling them from it. However, the mechanism for this balance remains poorly understood. Another metabolite that is highly abundant in the vacuolar lumen is phosphate, stored in the form of polyphosphate. Vacuolar polyphosphate acts as a macromolecular anion that imports and stabilizes positively charged ions and amino acids and thus represents a very efficient cytosolic phosphate buffer during periods of extracellular phosphate depletion (Thomas and O'Shea, 2005; Freimoser *et al.*, 2006). As a major calcium storage site, the vacuole regulates levels of free ionized calcium. Several ion transporters in the tonoplast operate to drive Ca^{2+} uptake as well as release into the cytosol (Miseta *et al.*, 1999; Denis and Cyert, 2002). Other metals, such as Zn^{2+}, are also stored and managed through the vacuole. As for zinc, cellular and vacuolar zinc levels can increase up to ten-fold due to activity of transporters in the tonoplast (MacDiarmid *et al.*, 2000, 2002; Simm *et al.*, 2007). In addition, the vacuole plays a central role for storage of the rare but essential nutrient iron which acts as a redox-active metal, that can be mobilized upon iron deprivation (Li *et al.*, 2001; Li and Kaplan, 2004; Singh *et al.*, 2007).

1.6.3 Detoxification of the cytosol

The last basic function of the fungal vacuole is detoxification, *i.e.*, cleaning toxic molecules as well as ions and excessive nutrients from the cytosol. Proton antiporters take up ions that are potentially toxic such as Ni^{2+}, Co^{2+} and Mn^{2+} and accumulate them in the vacuole (White *et al.*, 1986; Ramsay *et al.*, 1997). Two **A**TP **b**inding **c**assette (ABC) transporters residing in the tonoplast are dedicated to take up toxic metals like arsenite and cadmium, and other substrates such as

glutathione conjugates (Rebbeor *et al.*, 1998; Klein *et al.*, 2002; Sharma *et al.*, 2002).

1.6.4 Vacuolar morphology

The vacuolar morphology is dictated by an equilibrium of fission and fusion. Both are vital events for delivering cargo into and out of the vacuole and regulating vacuolar volume in response to cellular requirements. In proliferating cells, for example, high metabolic activity favors multiple medium-sized vacuoles whereas limitation of nutrients induces fusion events that tailor one single cell-filling organelle. The large volume is perfectly fitted to the enhanced need for breakdown of cellular material delivered to the vacuole via autophagy and/or the **m**ulti-**v**esicular **b**ody (MVB) pathway (Teichert *et al.*, 1989; Kim and Klionsky, 2000; Mijaljica *et al.*, 2007). The mechanism of homotypic vacuole fusion requires an array of molecular components and follows distinct steps (reviewed in Richards *et al.*, 2010): priming, tethering, docking and fusion. Simply put, once two nearby vacuoles are primed, *i.e.*, rearrangement of surface receptors in the tonoplast, they touch and are reversibly tethered together by the **ho**motypic fusion and **p**rotein **s**orting (HOPS) complex. During the next step, named docking, receptor complexes in the opposing membranes firmly assemble, the conformation of each complex are proof-read, and, eventually, fusion of the opposing membranes is facilitated mixing the content of both vacuolar vesicles. The antagonistic reaction to vacuolar fusion is called fission. Crucial factors for vacuolar fission have been identified through genetic and biochemical approaches, such as Vac14p, Vac7p, the kinase Fab1p and its product, as well as Atg18p (Efe *et al.*, 2005), and Vps1p (a dynamin-like protein that seems to be involved in fusion and fission of the vacuole) (Vater *et al.*, 1992; Baars *et al.*, 2007). In addition, the **TOR c**omplex **1** (TORC1), a key factor in nutrient sensing (Wullschleger *et al.*, 2006) that is down-regulated in response to starvation, stimulates fragmentation of the vacuole (Michaillat *et al.*, 2012). However, how these factors concert vacuolar fission remains elusive partly because the molecular elements required for vacuolar

fission upon hyperosmotic stress differs slightly from those for cell cycle-dependent fission (Aufschnaiter and Büttner, 2019).

Fusion and fission events dictate vacuolar morphology; however, it remains not fully understood how this balance is maintained. Controlling it enables the fungal cell to maintain organelle structure and function in response to internal and external stimuli. Hypotonic stress, for example, increases the rate and extent of fusion events in *S. cerevisiae* and *S. pombe* and, conversely, hypertonic conditions induce vacuolar fragmentation (Brett and Merz, 2008). Here, the equilibrium of fusion and fission is thought to allow the vacuole to rapidly readjust their surface-to-volume ratio that determines membrane tension which in turn influence functionality of transporter and ion channels in the membrane (Michaillat *et al.*, 2012). In response to starvation, however, the vacuoles in yeast cells fuse into a single big organelle most likely due to higher need for hydrolytic capacity for autophagy (Baba *et al.*, 1994).

There is one proton pump embedded in the tonoplast that is required for both vacuole fusion and fission: The vacuolar H^+-ATPase, a multi-subunit complex which directly maintains the low pH in the vacuolar lumen and of other endocytic vesicles (Baars et al., 2007; Li and Kane, 2009). It is composed of a cytosolic V_1 subunit that contains the site of ATP hydrolysis, and a membrane bound V_0 sector in the tonoplast that contains the proton pore (Banerjee and Kane, 2020). Activity of the complex moves protons into the vacuolar lumen which generates a pH between 5 and 6 depending on the growth conditions. Activity of the V-ATPase, and thereby to a great part vacuolar acidification, is regulated at the level of complex assembly. This describes the reversible dissociation of the ATP-hydrolytic V_1 domain from the proton-conducting V_0 domain. Regulation of vacuolar acidification upon V-ATPase assembly has been studied in mammalian lysosome extensively. For example, amino acid starvation leads to a rapid increase in V-ATPase assembly and activity of the complex (Collins *et al.*, 2018). Low pH of the lysosome is essential for proteolysis and the proton gradient drives the export of amino acids into the cytoplasm (Xu *et al.*, 2015). Glucose metabolism represents one example that regulates V-ATPase assembly in yeast, although the mechanisms of how glucose availability affects V-ATPase assembly are still

unknown (Li *et al.*, 2009). Nevertheless, assembly and subsequent activity of the complex provides the chemical basis for balancing fission and fusion events, is also important for degradation processes by hydrolytic enzymes. In addition, it introduces the H^+ electrochemical gradient over the tonoplast that energizes many vacuolar transporters that allow storage of metabolites (Li and Kane, 2009). For example, all members of the AVT family that are involved in amino acid homeostasis are believed to require an intact proton gradient, despite the fact that some function in the opposite direction (Russnak *et al.*, 2001). Furthermore, malfunctions of the vacuolar ATPase impinge on filamentation and virulence in *C. albicans* (Braun *et al.*, 2005; Rane *et al.*, 2013, 2014; Zhang *et al.*, 2017; Kim *et al.*, 2019).

1.7 Goal of this study

C. albicans is a normal resident on various mucosal surfaces of the human body including the oral cavity and the gastrointestinal tract. While a few genes have been reported to influence the proliferation of the fungus on these mucosae, the general biology of the fungus on these surfaces remains underexplored. In a genetic screening, the isogenic deletion mutant of a previously uncharacterized transcription regulator *ZCF8* displays two striking opposing phenotypes in mice: Firstly, *C. albicans* colonization of the intestine is impaired after oral gavage (Böhm *et al.*, 2017), and, secondly, fungal persistence on tongues in an oral infection model is increased (Meir *et al.*, 2018). How the zinc cluster transcription regulator Zcf8p contributes to these opposing phenotypes, remains unknown. My doctoral research aims to investigate the role(s) that *ZCF8* plays on fungal biology during host colonization. The general approach is to (a) identify genes that are bound by the regulator, (b) characterize transcriptional changes influenced by *ZCF8*, and (c) find the associated cellular process(es) and/or organelle(s) that can explain the opposing phenotype of *C. albicans* on different mammalian mucosae. Investigating genetic determinants such as *ZCF8* will help to understand cellular processes that are critical for fungal-host interactions.

2 Materials and Methods

2.1 *C. albicans* strains used in this study

Table 1: *C. albicans* strains used in this thesis

Name	Parent	Genotype	Source
JCP_398	SN152	$\frac{ura3\Delta::\lambda imm434::URA3-IRO1}{ura3\Delta::\lambda imm434}\ \frac{arg4::hisG}{arg4::hisG}\ \frac{his1::hisG}{his1::hisG}\ \frac{leu2::hisG}{leu2::hisG}$	Noble & Johnson, 2005
JCP_738	SN152	$\frac{ura3\Delta::\lambda imm434::URA3-IRO1}{ura3\Delta::\lambda imm434}\ \frac{arg4::hisG}{arg4::hisG}\ \frac{his1::hisG}{his1::hisG}\ \frac{leu2::hisG}{leu2::hisG}\ \frac{zcf8\Delta::CdHIS1}{zcf8\Delta::CmLEU2}$	Homann *et al.*, 2009
JCP_796	SN152	$\frac{ura3\Delta::\lambda imm434::URA3-IRO1}{ura3\Delta::\lambda imm434}\ \frac{arg4::hisG}{arg4::hisG}\ \frac{his1::hisG}{his1::hisG}\ \frac{leu2::hisG}{leu2::hisG}\ \frac{zcf8\Delta::YFP}{ZCF8}$	this study
JCP_936	SN152	$\frac{ura3\Delta::\lambda imm434::URA3-IRO1}{ura3\Delta::\lambda imm434}\ \frac{arg4::hisG}{arg4::hisG}\ \frac{his1::hisG}{his1::hisG}\ \frac{leu2::hisG}{leu2::hisG}\ \frac{zcf8\Delta::YFP}{zcf8\Delta::CmLEU2}$	this study
JCP_942	SN250	$\frac{ura3\Delta::\lambda imm434::URA3-IRO1}{ura3\Delta::\lambda imm434}\ \frac{arg4::hisG}{arg4::hisG}\ \frac{his1::hisG}{his1::hisG}\ \frac{leu2::hisG::CdHIS1}{leu2::hisG::CmLEU2}\ \frac{ZCF8-13xMYC}{zcf8\Delta}$	this study
JCP_520	SC5314		Gillum *et al.*, 1984
JCP_1072	SC5314	$\frac{TDH3p-YFP-ZCF8}{zcf8\Delta}$	this study
JCP_1102	SC5314	$\frac{zcf8\Delta}{zcf8\Delta}$	this study
JCP_1139	SC5314	$\frac{C\_13130C\_A-mNeonGreen}{C\_13130C\_B}$	this study
JCP_1140	SC5314	$\frac{DAL52-mNeonGreen}{DAL52}$	this study
JCP_1189	SC5314	$\frac{GFP-ATG8}{ATG8}$	this study
JCP_1190	SC5314	$\frac{zcf8\Delta}{zcf8\Delta}\ \frac{GFP-ATG8}{ATG8}$	this study

Construction of *C. albicans* strains generated in this study is described in more detail in the following section. All oligonucleotides and plasmids used in this thesis are listed in table 2 and table 3, respectively,

2.1.1 *zcf8* deletion mutant

I applied the well-established *SAT1* flipping method (Reuß *et al.*, 2004) to remove both *ZCF8* alleles in a two-step transformation process. The oligonucleotide pairs JCP_2162 and JCP_2163 or JCP_2164 and JCP_2165 were

used to amplify DNA fragments upstream or downstream of *ZCF8*, respectively, using genomic DNA as template. Both PCR products were digested and cloned into the respective restriction sites KpnI/XhoI or NotI/SacII of the pSFS2a plasmid. The wild-type reference strain was transformed with the KpnI/SacII-digested plasmid and the *SAT1* cassette was subsequently removed. Single deletion was verified through colony PCR using internal primer pairs JCP_1121 and JCP_2835 or JCP_1122 and JCP_2836. The transformation was repeated to remove the remaining allele of *ZCF8*. Double deletion was then confirmed by colony PCR with oligonucleotides JCP_2176 and JCP_2177, followed by removal of *SAT1* cassette and final colony PCR using flanking oligonucleotides JCP_2835 and JCP_2836.

2.1.2 Overexpression *ZCF8* mutant

To create a *C. albicans* mutant that overexpressed *ZCF8*, the wild-type strain was transformed with a PCR fusion product containing the *NAT1-TDH3* promoter sequence fused to *YFP* sequence. The *NAT1-TDH3* promoter sequence derived from the plasmid pCJN542 (Nobile *et al.*, 2008) using the oligonucleotide pair JCP_1563 and JCP_1478, and the *YFP* sequence was amplified from the plasmid pAJ2182 (Gerami-Nejad *et al.*, 2012) employing the oligonucleotides JCP_1564 and JCP_1479. Combination of the primers JCP_1563 and JCP_1564 generated a template that was inserted immediately upstream of *ZCF8* locus when transformed into *C. albicans*. The correct insertion was confirmed by colony PCR using the primer pair JCP_169 and JCP_2291.

2.1.3 *ZCF8*-MYC-tag for ChIP-Seq

This section focuses on the strain encoding a C-terminal 13xMYC tag, as it was the version used for the peak calling and follow-up data analysis. The *ZCF8* locus was genetically modified to encode a 13xMYC tag at the 3' end in the wild type strain SN250 following the strategy described previously (Hernday *et al.*, 2010). Briefly, the tag followed by a *SAT1*/flipper cassette was amplified from pADH34 employing the oligonucleotide pair JCP_1569 and JCP_1570. To delete the

untagged allele of *ZCF8*, homology regions upstream (JCP_2162 and JCP_2163) and downstream (JCP_2164 and JCP_2165) of *ZCF8* were PCR-amplified and cloned into KpnI/XhoI and NotI/SacII restriction sites of pSFS2a, respectively. The KpnI/SacII-digested plasmid was then transformed into *C. albicans*. The *SAT1*/flipper cassette was removed following Reuß *et al*. (2004). The correct insertion of the tag was verified by Sanger sequencing and Western Blot was used to confirm the expression of the tagged protein at the expected size.

2.1.4 Reporter strains to test autoregulation

To test whether Zcf8p regulates its own expression, two reporter strains were created. In “strain I”, one *ZCF8* allele in the *C. albicans* strain was replaced by *YFP*, amplified from pAJ2182 (Gerami-Nejad *et al*., 2012) using the primer pair JCP_1913 and JCP_1387, and fused to *SAT1*, from the plasmid pMBL179 (Dalal *et al*., 2016) employing oligonucleotides JCP1388 and JCP_1914. In “strain II”, the remaining *ZCF8* allele was deleted following the protocol by Noble and Johnson (2005) using the oligonucleotides JCP_2172 to JCP_2175. In both strains, the expression of the reporter is driven by the native *ZCF8* promoter.

2.1.5 Tagging *C1_13130C* and *DAL52* with mNeonGreen

To tag Dal52p with C-terminal mNeonGreen, the 3’ end of *DAL52* was PCR-amplified using the oligonucleotides JCP_2986 and JCP_2987 and genomic DNA as template. In addition, the oligonucleotides JCP_2988 and JCP_2980 amplified the sequence of mNeonGreen from the plasmid pRB895 (Frazer *et al*., 2019). Both PCR products were subsequently fused with oligonucleotides JCP_2986 and JCP_2980 and cloned in KpnI/XhoI restriction sites of pSFS2a. The DNA sequence downstream of *DAL52* was amplified employing the oligonucleotides JCP_2989 and JCP_2990 and cloned in NotI/SacII restriction site of pSFS2a. The *SAT1*/flipper cassette was removed following Reuß *et al*. (2004). Correct insertion was verified by colony PCR and Sanger sequencing using the oligonucleotides

JCP_2947 and JCP_2948. KpnI/SacII-digested plasmid was used to tag *DAL52* with C-terminal mNeonGreen.

Tagging *C1_13130C* with mNeonGreen was done similarly. The 3' end of *C1_13130C_A* was PCR-amplified using the oligonucleotides JCP_2981 and JCP_2982 and genomic DNA as template. The oligonucleotides JCP_2983 and JCP_2980 amplified the sequence of mNeonGreen from the plasmid pRB895 (Frazer *et al.*, 2019). Both PCR products were subsequently fused with oligonucleotides JCP_2981 and JCP_2980 and cloned in KpnI/XhoI restriction sites of pSFS2a. The DNA sequence downstream of *C1_13130C_A* was amplified employing the oligonucleotides JCP_2984 and JCP_2985 and cloned in NotI/SacII restriction site of pSFS2a. The correct insertion was verified by colony PCR and sequencing using the oligonucleotides JCP_2951 and JCP_2952. KpnI/SacII-digested plasmid was used to tag *C1_13130C* with C-terminal mNeonGreen.

2.1.6 Generation of strains to evaluate autophagy

Tagging Atg8p with mNeonGreen was done employing pSFS2a plasmid. The 5' end of *ATG8* (*C1_05700W_A*) was PCR-amplified using the oligonucleotides JCP_3104 and JCP_3105 and genomic DNA as template. The oligonucleotide pair JCP_3100 and JCP_3103 amplified the sequence of mNeonGreen from the plasmid pRB895 (Frazer *et al.*, 2019). Both PCR products were subsequently fused with oligonucleotides JCP_3100 and JCP_3105 and cloned in NotI/SacII restriction sites of pSFS2a. The DNA sequence upstream of *ATG8* was amplified employing the oligonucleotide pair JCP_3097 and JCP_3099 and cloned in KpnI/XhoI restriction site of pSFS2a. The *SAT1*/flipper cassette was removed following Reuß *et al.* (2004). Correct insertion was verified by colony PCR and sequencing using the oligonucleotides JCP_3102 and JCP_3106. KpnI/SacII-digested plasmid was used to tag Atg8p with N-terminal mNeonGreen.

Similarly, the pSFS2a plasmid was used to construct GFP-Atg8p. The 5' end of *ATG8* (*C1_05700W_A*) was PCR-amplified using the oligonucleotide pair JCP_3147 and JCP_3148 and genomic DNA as template. The oligonucleotides

JCP_3145 and JCP_3146 amplified the GFP sequence from the plasmid pNIM1 (Park *et al.*, 2005). Both PCR products were subsequently fused with oligonucleotides JCP_3145 and JCP_3148 and cloned in NotI/SacII restriction sites of pSFS2a. The DNA sequence upstream of *ATG8* was amplified employing the oligonucleotide pair JCP_3097 and JCP_3099 and cloned in KpnI/XhoI restriction site of pSFS2a. The *SAT1*/flipper cassette was removed following Reuß *et al.* (2004). Correct insertion was verified by colony PCR and sequencing using the oligonucleotides JCP_3149 and JCP_3150. KpnI/SacII-digested plasmid was used to tag Atg8p with N-terminal GFP.

2.1.7 Oligonucleotides used in this thesis

Table 2: List of oligonucleotides used in this thesis

Number	Description	Sequence (5'- 3')
***zcf8* deletion using pSFS2a**		
JCP_2162	Binds upstream of *ZCF8* with KpnI F	AGACTTGGTACCCGTGGCTGTATTGATGGATTGT
JCP_2163	Binds upstream of *ZCF8* with XhoI R	AGATTACTCGAGAGAAGTTTGTGGCTGTTGGA
JCP_2164	Binds downstream of *ZCF8* with NotI F	AGACGCGGCCGCTGCAAGATCAAACCCTTAGTCT
JCP_2165	Binds downstream of *ZCF8* with SacII R	AGCTAGCCGCGGACGAGTGTTGTGTTGAAAGGT
***ZCF8* ectopic overexpression (inserting *TDH3* promoter upstream *ZCF8*)**		
JCP_1563	*ZCF8*-specific, binds inside pCJN542 to amplify pTDH3 and fusion using JCP_1564 F	TTTCTTATATATATATTTTCTATTTAATTTAT ACTGGAATACATCAAGATTGATTGGAGATTGAATT GGCATCAAGCTTGCCTCGTCCCC
JCP_1478	Binds inside pCJN542 to amplify pTDH3 R	GAATAATTCTTCACCTTTAGACATATTTGAATTC AATTGTGATG
JCP_1479	Binds inside pAJ2181 to amplify YFP F	ATGTCTAAAGGTGAAGAATTATTC
JCP_1564	*ZCF8*-specific, binds inside pAJ2181 to amplify YFP and fusion using JCP_1563 R	GGGTAGCACTCGATGAAGGTGAAGATGGTGAAGGCGAAG GTGATTCAGTATTAGATAGATTACTTTCCATATTTG AATTCAATTGTGATG
Substitution of *ZCF8* by *YFP* and *ZCF8* deletion		
JCP_1913	ZCF8-specific, binds inside pAJ2182 to amplify *YFP* and fusion using JCP_1914 F	TATTTACTTTTCAATTCTTCCTTCCTTTTTCCCTGTCA AACTACATTCAACCTTAATTTTCATTCAA ATATGTCTAAAGGTGAATTATTC
JCP_1387	Binds inside pAJ2182 to amplify *YFP* R	CAAAACCAGATTTCCAGATTTCCAGTTATTTGTACAATTCATCCATACC

JCP_1388	Binds inside pMBLS179 to amplify Act1/Sat1 F	CTGGAAATCTGGAAATCTGGTTTTG
JCP_1914	ZCF8-specific, binds inside pMBSLS179 to amplify Act1/Sat1 and fusion JCP_1913 *R*	AATGATATTAACACTATTCTATCTATCTATATATA TATCAATACAATTTACCCATATGTTTCCCAAATTA GGCGTCATCCTGTGCTCCCG
JCP_2172	Primer 1 to delete *ZCF8* allele following Noble & Johnson, 2005	CGTGGCTGTATTGATGGATTGT
JCP_2173	Primer 3 to delete *ZCF8* allele following Noble & Johnson, 2005	CACGGCGCGCCTAGCAGCGGAGAAGTTTGTGGCTGTTGGA
JCP_2174	Primer 4 to delete *ZCF8* allele following Noble & Johnson, 2005	GTCAGCGGCCGCATCCCTGCTGCAAGATCAAACCCTTAGTCT
JCP_2175	Primer 6 to delete *ZCF8* allele following Noble & Johnson, 2005	ACGAGTGTTGTGTTGAAAGGT
C-terminal tagging of *ZCF8* with 13xMyc		
JCP_1569	*ZCF8*-specific, binds inside pADH34 to amplify 13xMYC F	ATTTAAATTTGATGAAAATGTCGTTAATGAATATTT CAAACATTGTGTTGAACCAAATATCTTTGAACG GATCCCCGGGTTAATTAACGG
JCP_1570	*ZCF8*-specific, binds inside pADH34 to amplify 13xMYC R	TGATATTAACACTATTCTATCTATCTATATATATATCAA TACAATTTACCCATATGTTTCCCAAGGCGGCCG CTCTAGAACTAGTGGATC
Tagging *C1_13130C_A* and *DAL52* with mNeonGreen		
JCP_2981	Binds in 5' of C1_13130C_A and fusion using JCP_2980 with KpnI F	ATATGGTACCCTATTGGTGGAGATTATGGAG
JCP_2982	Binds in 5' of C1_13130C_A with R	CCTTTAGAAACCATACCACTACCACCGCACCAGAAATTGACAAATC
JCP_2983	*C1_13130C_A*-specific, binds inside pRB895 to amplify mNeonGreen F	GATTTGTCAATTTCTGGTGCGGTGGTAGTGGTATGGTTTCTAAAGG
JCP_2980	Binds inside pRB895to amplify mNeonGreen and fusion with JCP_2981 or JCP_2986 with XhoI R	ATTACTCGAGCTATTTATACAATTCATCCATACC
JCP_2984	Binds downstream of *C1_13130C_A* with NotI F	TAATGCGGCCGCCATGATAAGAAATTTGTACG
JCP_2985	Binds downstream of *C1_13130C_A* with SacII R	TTATCCGCGGGTTGTTGTCTCTTTGTTCTG
JCP_2986	Binds in 5' of *DAL52* with KpnI F	TATAGGTACCTGTTTCTTCAAATGTTGC
JCP_2987	Binds in 5' of *DAL52* and 3' of mNeonGreen R	CCTTTAGAAACCATACCACTACCACCGAGACTATATCTA AAATTCAAATTTTC
JCP_2988	*DAL52*-specific, binds inside pRB895 to amplify mNeonGreen F	GAAAATTTGAATTTTAGATATAGTCTCGGTGGTAGTGGTAT GGTTTCTAAAGG
JCP_2989	Binds downstream of *DAL52* with NotI F	ATATGCGGCCGCATGAGATGATGAGTTATGTTG
JCP_2990	Binds downstream of *DAL52* with SacII R	TTTACCGCGGTGGATACAGATATTGATTCC
JCP_2947	Binds inside DAL52 to test insertion at 3' end F	AGCAAGATTAGCTGGTCTTTAT
JCP_2948	Binds downstream of DAL52 to test insertion at 3' end R	AGCTAATTGAACAGAACCATCT
Inserting *ZCF8* DNA binding domain sequence into pLIC-H3		

JCP_2024	Amplifies genomic sequence of putative Zcf8DBDp SmaI F	AGCAGCCCCGGGACAACAAAACCTAAACGTCAAAG
JCP_2026	Amplifies genomic sequence of putative Zcf8DBDp XhoI R	GTGGTGCTCGAGTTACTTTTCATAATTCTTCGAAGTAG
JCP_1357	Flank SmaI/XhoI cloning site on pLIC-H3 plasmid to test insertion F	GCACCATCATCATCACCATC
JCP_1358	Flank SmaI/XhoI cloning side on pLIC-H3 plasmid to test insertion R	CTTTCGGGCTTTGTTAGCAG
Oligonucleotides to test DNA-protein binding in EMSA, taken from *DAL52* promoter region		
JCP_2808	wild type sequence F	ACTGATTTTTCTAAATCCGTTCGAACTAAA
JCP_2809	wild type sequence R	TTTAGTTCGAACGGATTTAGAAAAATCAGT
JCP_2810	Point mutations in CCG F	ACTGATTTTTCTAAATAGATTCGAACTAAA
JCP_2811	Point mutations in CCG R	TTTAGTTCGAATCTATTTAGAAAAATCAGT
JCP_2812	Point mutations in AAA F	ACTGATTTTTCTGATTCCGTTCGAACTAAA
JCP_2813	Point mutations in AAA R	TTTAGTTCGAACGGAATCAGAAAAATCAGT
JCP_2814	Point mutations in CCG and AAA F	ACTGATTTTTCTGATTAGATTCGAACTAAA
JCP_2815	Point mutations in CCG and AAA R	TTTAGTTCGAATCTAATCAGAAAAATCAGT
Tagging *ATG8* with mNeonGreen or GFP		
JCP_3097	Binds upstream *ATG8*, with KpnI F	TTATGGTACCTTACATCACACATCACACGTTT
JCP_3099	Binds upstream *ATG8*, with XhoI R	ATAACTCGAGTATGAGTGATGTTTCTAAGTTCTG
JCP_3104	Binds inside 5'*ATG8*, F	TATGGATGAATTGTATAAAGGTGGTAGTGGTATGAGATCACAATTCAAAGACGAGCATC
JCP_3105	Binds inside 5'*ATG8*, with SacII, R	ATATCCGCGGGTCCTTGTGTTCTTCGTAGATT
JCP_3100	Binds inside pRB895 to amplify mNeonGreen and fusion with JCP_3105 with NotI F	TAATGCGGCCGCATGGTTTCTAAAGGTGAAGAAG
JCP_3103	*ATG8*-specific, binds inside pRB895to amplify mNeonGreen R	ATGCTCGTCTTTGAATTGTGATCTCATACCACTACCACCTTTATACAATTCATCCATACC
JCP_3102	Binds upstream *ATG8* F	CCAATGGCTGCTAATTATT
JCP_3106	Binds inside *ATG8* R	TGTGAAGAAAACTCTTAGGGTT
JCP_3147	Binds inside 5'*ATG8* F	CATGGATGAACTATACAAAAGATCACAATTCAAAGACGAGCATCC
JCP_3148	Binds inside 5'*ATG8* with SacII R	TATTCCGCGGTGTGAAGAAAACTCTTAGGGTT
JCP_3145	Binds inside pNIM1 to amplify *GFP* with NotI F	TAATGCGGCCGCATGAGTAAGGGAGAAGAACT
JCP_3146	*ATG8*-specific, binds inside pNIM1 to amplify *GFP* R	ATGCTCGTCTTTGAATTGTGATCTTTTGTATAGTTCATCCATGCC
JCP_3149	Binds upstream *ATG8* F	ATATATACATCCCCATCGATTC
JCP_3150	Binds inside *ATG8* R	CACCCACGAAAATGTTAGTATA

2.1.8 Plasmids used in this thesis

Table 3: List of plasmids used in this thesis

Number	Name	Description	Reference
JCP_054	pCJN542	Coding sequence for the *C. albicans TDH3* promoter	Nobile *et al*., 2008
JCP_002	pSFS2a	*SAT1*-flipper	Reuß *et al*., 2004
JCP_1118	pRB895	Coding sequence for *mNeonGreen* gene	Frazer *et al*., 2019
JCP_129	pMBL179	Coding sequence for *YFP*	Dalal *et al*., 2016
JCP_182	pAJ2182	Coding sequence for *NAT1*	Gerami-Nejade *et al*., 2012
JCP_080	pADH34	Coding sequence *13xMYC*	Hernday *et al*., 2010
JCP_233	pLIC-H3	Plasmid designed to produce recombinant N-terminal 6-His tagged proteins in *E. coli*, upon IPTG-induction	Cain *et al*., 2012
JCP_809	pLIC-H3-orf19.1718 DBD	Plasmid designed to produce recombinant N-terminal 6-His tagged proteins in *E. coli* of the putative Zn-cluster DNA binding domain (57-158aa), upon IPTG induction	this study
JCP_938	pSFS2a + upstream ORF19.1718 + downstream ORF19.1718	This plasmid can be used to replace *ZCF8* locus with *SAT1* flip recombinase cassette.	this study
JCP_1132	pSFS2a + DAL52-mNeonGreen + downstream DAL52	This plasmid can be used to tag *DAL52* with C-terminal *mNeonGreen*.	this study
JCP_1133	pSFS2a + ORF19.4940-mNeonGreen + downstream ORF19.4940	This plasmid can be used to tag *C1_13130C_A* with C-terminal *mNeonGreen*.	this study
JCP_1191	pNIM1	Coding sequence for *GFP*	Park *et al*., 2005

2.2 Chemicals, dyes, and antibodies used in this thesis

Table 4: List of chemicals, dyes, and antibodies used in this thesis

Name (ref. number)	Vender	Description	Reference
c-MYC Monoclonal antibody (#9E10.3)	Thermo Fisher Scientific (USA)	Antibody from mice against synthetic peptide from C-terminus of human c-myc	Manufactures description
FM4-64 (#T13320)	Thermo Fisher Scientific (USA)	N-(3-Triethylammoniumproply)-4-(6-(4-(Diethylamino) Phenyl) Hexatrienyl) Pyridinum Dibromide; lipophilic dye; internalized by the fungal cell *via* endocytosis, stains compartments of the endocytic pathway, and ultimately accumulates in the vacuolar membrane.	Manufactures description; Vida and Emr, 1995; Richards *et al.*, 2012
BCECF, AM (#B1170)	Thermo Fisher Scientific (USA)	2',7'-Bis-(2-Carboxythyl)-5-(and-6)-Carboxyfluorescein, Acetoxymethyl Ester; fluorescent pH-indicator; pH-dependent ratio of emission intensity from acidic to alkaline pH	Manufactures description; Boens *et al.*, 2006; Johnson *et al.*, 2010; Richards *et al.*, 2012
Nigericin (#SML1779)	Merck (Germany)	A K^+/H^+ ionophore that targets, among other organelles, the fungal vacuole	Jakubkova *et al.*, 2016,
Brefeldin A (#B6542)	Merck (Germany)	A drug that targets the Golgi apparatus and impairs vesicle formation and transport	Dinter and Berger, 1998
Anti-GFP antibody [E385] (#ab190584)	abcam (UK)	Recombinant HRP Anti-GFP antibody for Western blot, HRP rabbit monoclonal [E385] to GFP	Manufactures description
Anti-*Candida* antibody (#ab53891)	abcam (UK)	Anti-*C. albicans* antibody, rabbit polyclonal	Manufactures description

2.3 Media and growth conditions

C. albicans strains were routinely grown at 30°C in yeast-peptone-dextrose (YPD) media. When defined medium was employed, cells were collected from overnight cultures by centrifugation, washed twice with **p**hosphate-**b**uffered **s**aline (PBS) and diluted in nitrogen starvation medium (BD Difco™ YNB without amino acids and ammonium sulfate, and supplemented with 2% glucose) or medium containing ammonium sulfate as the only nitrogen source (DB Difco™ YNB without amino

acids, and supplemented with 2% glucose). Finally, cells were incubated for 6 hours at 30°C with shaking at 220 rpm.

2.4 Phylogeny

The protein sequences used in the phylogenetic analysis were retrieved from the *Candida* Genome Database (CGD) (Skrzypek *et al.*, 2017). Synteny was assessed using the *Candida* Gene Order Browser (Maguire *et al.*, 2013). The full-length protein sequence alignment of all orthologs and "best hits" was performed using MUSCLE (Edgar, 2004). Previous alignments revealed a mistake in the annotation of PGUG_013926 in *Candida guilliermondii* and CPAR2_807820 in *Candida parapsilosis,* since the protein sequence lacked the defining zinc cluster binding domain. Manual curation at the genomic localization of the erroneously annotated genes on the assemblies ASM18276v2:HE605205.1 (1.808 - 1.816 Mb) of *C. parapsilosis* and ASM14942v1:scaffold_2 (1.275 - 1.285 Mb) of *C. guilliermondii* (derived from the EnsemblFungi data base, http://fungi.ensembl.org/index.html), using NCBI's *Open Reading Frame Finder* (https://www.ncbi.nlm.nih.gov/orffinder/), identified alternative ORFs (HE605205.1: 1,812,795-1,810,240; scaffold_2: 1,281,667-1,280,114) that encoded zinc cluster binding domains. Protein sequences derived from these alternative ORFs were used in the alignments and the phylogenetic tree. To build the Maximum likelihood phylogenetic tree of *ZCF8*, protein sequences were aligned employing MAFFT (v.7.475) (Katoh and Standley, 2013). IQ-TREE 2 (v.2.1.2) (Nguyen *et al.*, 2015; Chernomor *et al.*, 2016; Kalyaanamoorthy *et al.*, 2017; Minh *et al.*, 2020) was used to predict the best-fitting model (VT+F+R4) according to Akaike Information Criterion (Akaike, 1973), and FigTree (v1.4.4) (http://tree.bio.ed.ac.uk/software/figtree/) was used to build and visualize the tree.

2.5 Chromatin immunoprecipitation followed by next-generation sequencing

The *ZCF8*-MYC-tagged strain, along with untagged controls, were grown in YPD broth overnight at 30°C. The chromatin immunoprecipitation procedure was carried out as described previously (Hernday *et al.*, 2010; Pérez *et al.*, 2013). Briefly, 20 ml of *C. albicans* culture was cross-linked with 37% formaldehyde for 15 minutes. Cross-linking was quenched by adding 2.5 M glycine to the cells. The samples were centrifuged down, washed with TBS and frozen at -80°C. The pellet was resuspended in lysis buffer and lysed mechanically with Zirconia beads for approximately 2 hours at 4°C. The lysate was recovered and subjected to two 1.5-minute rounds of sonication using a microtip sonicator followed by three 15-minute rounds of sonication using a Bioruptor (Diagenode, Belgium) (30 seconds ON / 30 seconds OFF). Part of the lysate was stored to be used as input control. Samples for **i**mmuno**p**recipitation (IP) were incubated with mouse anti-c-MYC antibody (Table 4) overnight. Sepharose beads were used to immunoprecipitate the DNA. The recovered DNA was washed and eluted. To reverse cross-linking, all samples were incubated in the presence of proteinase K at 37°C for two hours followed by 12 hours at 66°C. A PCR clean-up kit (Qiagen, Netherlands) was used to clean up the IP samples. Input and immunoprecipitated DNA samples were directly used to generate sequencing libraries using the NEBNext ChIP-Seq Library Prep Master Mix Set for Illumina (New England Biosciences, USA). DNA sequencing was carried out by GATC Biotech (Germany) using standard procedures.

Buffers and solutions used for ChIP:

TBS:

20 mM Tris-HCl (pH 7.5)

150 mM NaCl

Lysis buffer I:

50 mM HEPES-KOH (pH 7.5)

5 mM EDTA

150 mM NaCl

1% IGEPAL

0.5% Na-deoxycholate

0.1% SDS

Lysis buffer II:

50 mM HEPES-KOH (pH 7.5)

5 mM EDTA

500 mM NaCl

1% IGEPAL

0.5% Na-deoxycholate

0.1% SDS

Wash buffer:

10 mM Tris/HCl (pH 8.0)

250 mM LiCl

0.5% IGEPAL

0.5% Na-deoxycholate

1 mM EDTA

Elution buffer

50 mM Tris/HCL (pH 8.0)

10 mM EDTA

1% SDS

TE buffer:

10 mM Tris/HCl (pH 8.0)

1 mM EDTA

Processing raw sequencing data. Raw reads were downloaded and aligned to the *C. albicans* genome build 21 (obtained from CGD) and processed by the following steps (following: del Olmo Toledo *et al.*, 2018):

(a) the *C. albicans* genome file had to be indexed using Bowtie2 (v.2.3.5) (Langmead and Salzberg, 2013);

```
$ bowtie2-build <reference_genome.fasta> <indexed genome>
```

(b) raw, unpaired sequencing reads were aligned to the genome;

```
$ bowtie2 -t -local -x <indexed genome> -U <reads.fastq> -
S <output.sam>
```

(c) non-uniquely aligned reads and mismatches were removed from the SAM-file employing SAMtools (v.1.8) (Li *et al.*, 2009);

```
$ samtools view -Sh <input.sam> | grep -e "^@" -e
"XM:i:[012][^0-9]" | grep -v "XS:i:" > <output.filtered.sam>
```

(d) filtered SAM files were then converted to BAM format and sorted,

```
$ samtools view -bh <input.filtered.sam>  >
<output.filtered.bam>
```

```
$ samtools sort -o <output.sorted.bam>
<input.filtered.bam>
```

(e) PCR duplicates from library preparation were removed;

```
$ samtools rmdup -s <input.sorted.bam>
<output.noduplicates.bam
```

(f) the BAM files were indexed;

```
$ samtools index <input.noduplicates.bam> >
<output.indexed.bam>
```

(g) for visualization in MochiView (v.1.46) (Homann *et al.*, 2010), the BAM files were converted to coverage WIG files;

```
$ samtools mpileup <input.noduplicates.bam> | perl -ne
'BEGIN{print "track type=wiggle_0 name=fileName
description=fileName\n"};($c, $start, undef, $depth) =
split; if ($c ne $lastC) { print "variableStep chrom=$c\n";
};$lastC=$c;next unless $. % 10 ==0;print "$start\t$depth\n"
unless $depth<3;' > <output.wig>
```

(h) for peak calling using the R package “bPeaks”, BAM files were converted to BED files using BEDTools (v.2.29.2) (Quinlan *et al.*, 2010);

```
$ genomeCoverageBed -ibam <input.noduplicates.bam> -d >
<bed.txt>
```

Overall, between 3-6 million reads per sample were uniquely aligned to the genome.

Peak calling and DNA motif analysis. The R package “bPeaks” (v.1.2) (Merhej *et al.*, 2014) was employed to detect significantly enriched regions or “peaks” using the IP from the untagged strain as a control. Based on the selected parameters (T1: 2, T2: 1, T3: 1.8, T4: 0.9), 148 significant peaks were detected by the tool. All those peaks were visualized in MochiView (v.1.46) (Homann *et al.*, 2010) and refined based on the following criteria: (a) Only peaks located in intergenic regions were maintained; (b) peaks adjacent to highly expressed genes were removed because these places tend to be bound by almost all DNA binding proteins non-specifically (Zordan *et al.*, 2007; Tuch *et al.*, 2008; Nobile *et al.*, 2012; Pérez *et al.*, 2013); and (c) only peaks that were consistent in at least two out of the four replicates were kept for further analysis. This curation resulted in 42 peaks (Table 5) representing 48 genes (Table 6), 1 antisense target and 1 novel transcriptional active region (nTARs; Giosa *et al.*, 2017). To derive *de novo* a putative DNA binding motif, sequences of 500 nt centered on the midpoint of ~1/4 of the top scoring peaks (ranked on fold enrichment) were fed into the oligo-analysis tool of

the Regulatory Sequence Analysis Tools for fungal organism (http://rsat-tagc.univ-mrs.fr/oligo-analysis_form.cgi). The utility ran on default parameters with the background model for *C. albicans*.

2.6 Recombinant protein purification

To generate the expression plasmid, the putative DNA binding domain of Zcf8p (amino acids 57-158) was amplified by PCR using oligonucleotide pair JCP_2024 and JCP_2026 (Table 2) and *C. albicans* genomic DNA as template. The PCR fragment was subsequently digested and ligated into the SmaI/XhoI sites of plasmid pLIC-H3 (Table 3). This plasmid is designed to overproduce 6×His-tagged proteins in *E. coli* (Cain *et al.*, 2012). Correct amino acid sequence of the DNA binding domain was verified by sequencing using the oligonucleotides JCP_1357 and JCP_1358. The *E. coli* strain BL21 (Table 1) was used as the host of the expression plasmid. Transformed *E. coli* cells were grown to OD_{600} ~0.8 and expression was induced with 0.5 mM **I**so**p**ropyl-β-D-**t**hio**g**alactopyranosid (IPTG) (Sigma-Aldrich, USA). After ~3 hours induction at 25-30°C and at 200 rpm, cells were collected, washed once in cold 1x PBS, pelleted and stored at -80°C. Cells were resuspended in 15 ml of a fresh lysis buffer working solution (40 ml Lysis Buffer, 2 tablets protease inhibitor without EDTA, 0.5 mg/ml Lysozyme, 5 mM β-Mercaptoethanol and 1 mM **P**henyl**m**ethyl**s**ulfonyl**f**luorid (PMSF)), incubated on ice for 20 minutes and subsequently lysed by sonication (60 cycles, 1-2 minutes each, with 5 minutes of incubation on ice in between to prevent the sample from warming up and damaging of the proteins). Cell debris was removed by centrifugation (5000 rpm, 4°C, 20 minutes). The His-tagged protein was affinity purified from the lysate using Ni-NTA agarose beads (Qiagen, Netherlands) during 1 hour on a shaker at 4°C. After a series of washes (4 times, 10 minutes each with cold Washing Buffer containing 1 M PMSF, and frequent centrifugation at 4°C, 1000 rpm for 1 minute in between washes), proteins were eluted using 2 ml of a fresh elution buffer working solution (10 ml Elution Buffer, 1 tablet protease inhibitor without EDTA, and 1 mM PMSF) for 1 hour on a shaker at 4°C. The eluted protein was then transferred to Amicon Ultra-15 centrifugal filters (10K membrane) (Merck,

Germany) to exchange buffer and concentrate the protein in Storage Buffer. Protein concentration was estimated in Rothi-blue (Carl Roth, Germany) stained gels using known amounts of BSA as standards.

Buffers and solutions for protein purification:

Lysis Buffer:	**Washing Buffer:**	**Elution Buffer:**	**Storage Buffer:**
50 mM NaH_2PO	50 mM NaH_2PO_4	50 mM NaH_2PO_4	40 mM Tris
600 mM NaCl	600 mM NaCl	400 mM NaCl	400 mM NaCl
10 mM Imidazole	30 mM Imidazole	250 mM Imidazole	5 mM DTT
pH 8.0	pH 8.0	pH 8.0	pH 7

2.7 Gel shift assay

Gel shift assays were carried out as described previously (Cain *et al.*, 2012). Oligonucleotide pairs JCP_2808 and JCP_2809 (wilde-type), JCP_2810 and JCP_2811 (point mutation in CCG), JCP_2812 and JCP_2813 (point mutation in AAA) or JCP_2814 and JCP_2815 (point mutation in CCG and AAA) (Table 2) were combined equimolarly to a final concentration of 50 μM and annealed as follows: 95°C - 5 minutes, 90°C - 5 minutes, 85°C - 5 minutes, (...), 35°C - 5 minutes, 25°C - 30 minutes. Double-stranded DNA probes were radioactively labelled by combining the following reagents in this order:

1. 2.5 μl 10x PNK buffer (New England Biolabs, USA);
2. 2 μl DNA (1 μM);
3. 17.5 μl ddH_2O;
4. 2 μl ^{32}P radioactive isotope; and
5. 1 μl T4 polynucleotide kinase (New England Biolabs, USA).

Reaction tubes were then incubated at 37°C for 20 minutes, 65°C for 15 minutes, and 95°C for 5 minutes. After 10 minutes at room temperature the radiolabeled mix was filtered through a G25 column (Bio-Rad Laboratories, USA) by 4 minutes of centrifugation at 1000 g. The protein was diluted in 1x minimal buffer starting at 100 nM in 1:4 dilutions. Binding reactions, containing the diluted protein and radiolabeled DNA probe, were added to 10 µl of master mix and incubated for 15 minutes at room temperature. Then, the samples run on 6% polyacrylamide gels for 90 minutes, at 130 V. Dried gels were exposed to a phosphor imaging screen (GE Healthcare, USA) for at least 1 hour. Imaging was carried out with a Typhoon imager FLA 7000 (GE Healthcare, USA).

Buffer used for protein-DNA binding:

5x minimal buffer:	**Master mix:**
100 mM Tris pH 8.0	22.5% 5x minimal buffer
250 mM NaCl	5 mM $MgCl_2$
25% Glycerol	1 mM DTT
	0.1 NP-40
	1 mM $ZnSO_4$
	1 µg/µl BSA

2.8 Evaluation of autoregulation by *ZCF8*

Cells of a wild-type reference strain, a strain with one *ZCF8* allele replaced by *YFP* ("strain I"), and a strain with the second *ZCF8* allele removed ("strain II") were harvested from overnight cultures in YPD and diluted 1:1000 in 1x PBS. YFP fluorescence emitted by the reporter strains was measured using a Accuri™C6 Flow Cytometer (BD Biosciences, USA). The limit for each of the runs was set to 10,000 events. The experiment was conducted in three independent replicates. Statistical evaluation and plotting were done using GraphPad (v.9.1.0).

2.9 Transcriptome analyses

Cells harvested from overnight cultures in YPD were washed three times with PBS and diluted 1:10 in 3 ml defined medium without amino acids and ammonium sulfate. After 5.5 h incubation at 30°C in a shaker, nigericin at a final concentration of 15 *µ*g/ml, or an equal volume of DMSO/ethanol solution (used as mock control) were added and incubated for an additional 30 min. Cells were collected by centrifugation. RNA was prepared using the RiboPure™ Kit for yeast (Thermo Fisher Scientific, USA). Illumina library preparation and strand-specific sequencing were carried out by Novogene (UK) following standard operating procedures.

Processing raw sequencing data for differential expression analysis. After sequencing, an approximate amount of 41 to 48 million reads were obtained per sample (paired-end, 150 nt reads). QualiMap (v.2.2.1) (Okonechnikov *et al.*, 2016) was used to evaluate sequencing quality of each sample. Processing of reads, mapping, and differential gene expression analyses followed standard computational procedures described by our laboratory (del Olmo Toledo *et al.*, 2018; Moreno-Velásquez *et al.*, 2020). In brief:

(a) the reference genome was generated using STAR (v.2.7.3a) (Dobin *et al.*, 2013);

```
$ star --runMode genomeGenerate --genomeDir
<folder_for_reference_genome> --genomeFastaFiles
<transcriptome_sequence.fasta> --sjdbGTFfile
<transcriptome_annotation.gtf> --sjdbOverhang <read_length -
1>
```

(b) Illumina adaptor sequences were removed using the Trimmomatic tool (v.0.39) (Bolger *et al.*, 2014);

```
$ trimmomatic SE -phred33 <reads.fq.gz> <trimmed.fastq.gz>
ILLUMINACLIP:path/to/adapters/TruSeq2-PE.fa:2:30:10
LEADING:3 TRAILING:3 SLIDINGWINDOW:4:15
```

(c) trimmed reads were aligned to the *C. albicans* reference genome build 21 (www.candidagenome.org) using STAR (v.2.7.3a) (Dobin *et al.*, 2013);

```
$ star --genomeDir <folder_for_reference_genome> --
readFilesCommand gzcat --readFilesIn <trimmed.fastq.gz> --
outFileNamePrefix <output.bam> --outSAMtype BAM
SortedByCoordinate --outSAMstrandField intronMotif
```

(d) and count files were generated using HTSeq (v.0.11.2) (Anders *et al.*, 2015).

```
$ htseq-count -s no -f bam -r pos "${f}"
<transcriptome_annotation.gtf> > <output.counts>
```

Raw read counts were loaded onto R and analyzed employing the standard workflow for the DESeq2 package (v.1.28.1) (Love *et al.*, 2014). For visualization and ranking of genes according to their log-fold change, the *apeglm* method was applied (Zhu *et al.*, 2019) and volcano plots were created using the R package EnhancedVolcano (v.1.6.0) (https://github.com/kevinblighe/EnhancedVolcano). Two biological replicates were included in each RNA-Seq analysis.

Processing raw sequencing data for visualization in MochiView. For data visualization in MochiView (v.1.46) (Homann *et al.*, 2010), the reads were aligned strand-specifically to the full genome and not only to annotated features of the *Candida* genome. For this, the reads from the RNA-Seq were processed similarly to the sequencing reads from ChIP-Seq analysis but with some adaptations to the protocol:

(a) the indexed *C. albicans* genome file was generated using Bowtie2 (v.2.3.5) (Langmead and Salzberg, 2013);

```
$ bowtie2-build <reference_genome.fasta> <indexed_genome>
```

(b) the raw, unpaired sequencing reads were aligned to the indexed genome;

```
$ bowtie2 -t -local -x <indexed_genome> -U <reads.fastq> -S
<output.sam>
```

(c) files were converted to BAM format and reads were sorted strand-specifically;

```
$ samtools view -bhF 20 <input.sam> > <output.forward.bam>
$ samtools view -bhF 16 <input.sam> > <output.reverse.bam>
```

(d) reads in each BAM files were sorted relative to their position on the chromosome and subsequently indexed;

```
$ samtools sort <input.bam> <output.sorted.bam>
$ samtools index <input.bam> > <output.indexed.bam>
```

(g) the BAM files were - depending on the orientation - converted to coverage WIG files. Note that for the reverse-orientated reads, I inserted a "−" (minus) in in the second code in the segment `"$start\t-$depth\n"` which transforms all coverage values in the `input.reverse.bam` file to negative values. Negative coverage values are recognized by MochiView and plotted to the reverse strand which allows to view reads of both orientations in the same plot.

```
$ samtools mpileup <input.forward.bam> | perl -ne
'BEGIN{print "track type=wiggle_0 name=fileName
description=fileName\n"};($c, $start, undef, $depth) =
split; if ($c ne $lastC) { print "variableStep chrom=$c\n";
};$lastC=$c;next unless $. % 10 ==0;print "$start\t$depth\n"
unless $depth<3;' > <output.forward.wig>
```

```
$ samtools mpileup <input.reverse.bam> | perl -ne
'BEGIN{print "track type=wiggle_0 name=fileName
description=fileName\n"};($c, $start, undef, $depth) =
split; if ($c ne $lastC) { print "variableStep chrom=$c\n";
};$lastC=$c;next unless $. % 10 ==0;print "$start\t-
$depth\n" unless $depth<3;' > <output.reverse.wig>
```

2.10 Evaluation of vacuolar morphology

Vacuolar morphology was evaluated employing the membrane-selective dye FM4-64 (Table 4) to visualize the vacuolar membrane. *Candida* wild-type strain, *zcf8* deletion mutant strain and a strain overexpressing *ZCF8* were grown in YPD medium to stationary phase at 30°C overnight. Cells were washed three times with 1x PBS and diluted 1:10 in defined liquid medium either without ammonium sulfate and amino acids or in defined liquid medium complemented with ammonium sulfate and incubated at 30°C for 6 hours. Subsequently, cells were exposed to 10 μM FM4-64 during 30 minutes at 30°C. Samples were kept on ice until evaluation by fluorescence microscopy. Live-cell imaging at high resolution was performed using a wide-field epifluorescence microscopy (DMI6000 B, Leica, Germany) employing a 63X oil plan fluor objective. Excitation at 550 nm was used to detect the internalized FM4-64 dye. The fraction of *Candida* cells with a single, large vacuole was determined in contrast to cells with multiple, small compartments. More than 500 cells were scored deriving from at least three independent experiments. Statistical evaluation (Mann-Whitney U test) and plotting were done using GraphPad (v.9.1.0).

In addition, vacuolar morphology was evaluated in *Candida* cells attached to TR146 oral epithelial cells. *C. albicans* cultures and TR146 cell culture cells were prepared as described in section 2.17 with some modifications for microscopy purposes: (a) epithelial cells were seeded onto round, sterile cover slips placed in 24-well plates, and (b) *C. albicans* cells were treated with FM4-64 for 30 minutes prior to infection. After 1 hour of infection, wells were washed three times with 1x

PBS to remove non-adherent *C. albicans* cells. The cover slips carrying TR146 and attached fungal cells were removed and placed in inverted orientation onto a microscopy slide. Excitation at 550 nm was used to detect the internalized FM4-64 dye. The fraction of *Candida* cells with a single, large vacuole was determined in contrast to cells with multiple, small compartments. More than 30 cells were scored per strain and experiment in five independent replicates. Statistical evaluation (Mann-Whitney U test) and plotting were done using GraphPad (v.9.1.0).

2.11 Evaluation of endocytosis rate

Endocytosis rate was evaluated by assessing the internalization rate of the fluorescence dye FM4-64 (Table 4) and endocytic delivery to the vacuole (Vida and Emr, 1995). *C. albicans* wild-type strain, the *zcf8* deletion strain and a strain overexpressing *ZCF8* were grown in YPD medium to stationary phase at 30°C overnight, washed, and diluted 1:10 in defined liquid medium without amino acids and ammonium sulfate for 6 hours at 30°C. Cells were then incubated with 10 μM FM4-64 dye for 10 or 20 minutes at 37°C. After each time point, internalization was stopped by washing cells with ice-cold 1x PBS. Samples were kept on ice until evaluation by fluorescence microscopy. Live-cell imaging at high resolution was performed using a wide-field epifluorescence microscopy (DMI6000 B, Leica, Germany) employing a 63X oil plan fluor objective. Excitation at 550 nm was used to detect the internalized lipophilic dye. Image settings were retained for all samples to enable comparability between images. Fluorescence emitted by each cell was analyzed using FIJI (2.1.0) (Schindelin *et al.*, 2012; Schneider *et al.*, 2012). The fluorescence emitted from at least 400 cells derived from more than 20 microcopy fields was measured for each of the strains at each time point per experiment. Data was collected from four independent experiments. Statistical evaluation (Mann-Whitney U test) and plotting were done using GraphPad (v.9.1.0).

2.12 Atg8p autophagy assay

Fluorescence microscopy. mNeonGreen-Atg8p in a *C. albicans* wild-type background and *zcf8* deletion mutant was used to visualize the delivery of autophagosomes to the fungal vacuole and monitor autophagic activity. The two strains were grown overnight in YPD medium to stationary phase at 30°C, washed, diluted 1:10, and grown in 1 ml defined liquid medium without amino acids and ammonium sulfate for 6 hours at 30°C. Subsequently, cells were transferred to microscopy slides and observed under a fluorescence microscope (DMI6000 B, Leica, Germany). Percentage of cells in each microscopy field with a visible autophagosome was quantified as a proxy for autophagic activity. Only fields with more than 20 cells were taken into account for the analysis. Twenty fields were scored in each of five independent experiments. Statistical evaluation (Mann-Whitney U test) and plotting were done using GraphPad (v.9.1.0).

Western blot. GFP-Atg8p abundance was measured as a proxy for autophagy activity (Torggler *et al.*, 2017) in the wild-type background and in the *zcf8* deletion mutant. Both strains, as well as an untagged control, were grown overnight in YPD medium to stationary phase at 30°C. Cells were harvested, washed, diluted 1:10, and grown in 5 ml defined liquid medium without amino acids and ammonium sulfate for 3 and 6 hours at 30°C. Protein extraction followed the protocol described by Kushnirov (2000) with some modification. In brief, the culture was centrifuged and ~1/2 of the pellet was resuspended in 100 µl sterile water. Cells were lysed by mixing them with 100 µl 0.2 M NaOH followed by a 5-minute incubation step at room temperature. After centrifugation and removal of the supernatant the pellet was resuspended in sample buffer and boiled for 5 minutes. After a final centrifugation, 6 µl of the supernatant was loaded to a NuPAGE™ Bis-Tris 4 to 12% gel (Thermo Fisher Scientific, USA), and ran with 1x MES buffer (Thermo Fisher Scientific, USA) for 4 hours at 100 Volts. Afterwards, the proteins were transferred onto a PVDF membrane (pore size 0.45 µm) (Carl Roth, Germany) for 3 hours at 30V. The membrane was washed in distilled water and blocked with 5% milk powder in TBS-T for 1 hour. Afterwards, the membrane was incubated with a

1:2000 dilution of the anti-GFP antibody (Table 4) in mild solution. After 1 hour incubation, the membrane was washed three times with TBS-T, incubated with SuperSingalTM West Femto Maximum Sensitivity Substrate Kit (Thermo Fisher Scientific, USA), and imaged using an ImageQuant LAS 4000 system (GE Healthcare, USA).

Buffers and solutions used for Western Blot:

Sample buffer:

0.002 g bromophenol blue

0.6 g SDS

3 ml glycerol

1.5 ml ß-mercaptoethanol

3.9 ml 0.5 mM Tris (pH 6.8)

add 10 ml ddH_2O

Transfer buffer:

14 g glycine

3 g Tris base

100 ml Methanol

add 500 ml ddH_2O

1x TBS-T:

20 ml 1M Tris HCl (pH 7.5)

60 ml 2.5 M NaCl

add 1 L ddH_2O

500 µl Tween 20

2.13 Acidification of fungal vacuole

Flow cytometry. Differences in the luminal pH inside the fungal vacuole between the *Candida* strains was determined by employing the pH sensitive dye BCECF (Table 4) (Boens *et al.*, 2006; Johnson *et al.*, 2010). *Candida* wild-type strain, *zcf8* deletion mutant and a strain ectopically expressing *ZCF8* were grown in YPD medium to stationary phase at 30°C overnight. Cells were washed three

times in 1x PBS, diluted 1:10 in defined liquid medium either without ammonium sulfate and amino acids or complemented with ammonium sulfate, and incubated at 30°C for 6 hours. For the last 30 minutes of incubation, cells were co-incubated with 18 μM BCECF. Cells were then washed and diluted 1:500 in 1x PBS. Intensity of vacuolar fluorescence emitted by BCECF was quantified using a Accuri^{TM}C6 Flow Cytometer (BD Biosciences, USA). Each run's limit was set to 10,000 events. The experiment was conducted in four independent replicates. Statistical evaluation (Mann-Whitney U test) and plotting were done using GraphPad (v.9.1.0).

Fluorescence microscopy. To visualize changes in acidification of vacuolar lumen by fluorescence microscopy, nitrogen-starved *Candida* cells were prepared similarly as for flow cytometry and observed under a wide-field epifluorescence microscopy (DMI6000 B, Leica, Germany), with a 63X oil plan fluor objective (numerical aperture, 1.4) and excitation was set at 440 nm.

2.14 Microscopy analysis

Live-cell imaging of fungal cells at high resolution was performed using a wide-field epifluorescence microscopy (DMI6000 B, Leica, Germany). A 63X oil plan fluor objective (numerical aperture, 1.4) was employed. All the dyes and antibodies used in this thesis are listed in table 4. Excitation at 520 nm was used to visualize the subcellular localization of the mNeonGreen-tagged proteins. Excitation at 440 nm was used to visualize BCECF (18μM) in the vacuolar lumen and excitation at 550 nm was employed to detect vesicular/vacuolar membranes with FM4-64 (10 μM). Images were processed using FIJI (v.2.1.0) (Schindelin *et al.*, 2012; Schneider *et al.*, 2012).

2.15 Drug sensitivity assay

Drug sensitivity was established for a wild-type strain, the *zcf8* deletion mutant and a strain overexpressing *ZCF8* both on plate and in liquid medium employing

spot assays and growth curves, respectively. For spot assays, cells were grown overnight in YPD liquid medium, washed with PBS, serially diluted 10-fold from an initial cell concentration of 5×10^8 cells/ml and spotted onto YNB agar containing ammonium sulfate and nigericin at a final concentration of 1.5 μg/ml (2μM). Plates were incubated at 30°C for 48 hours prior imaging. Cells for growth curves were propagated similarly and adjusted to a cell concentration of $1x10^7$ cells/ml. In 96 well Nunclone™ plates (Thermo Fisher Scientific, USA), nigericin and brefeldin A were diluted in concentrations from 0.5 to 10 μg/ml and from 1 to 10 μg/ml, respectively, in 190 μl liquid YNB media containing ammonium sulfate. Eventually, 10 μl of cell stock dilution was added to each well. The plate was incubated for 24 hours at 30°C and measurements of OD_{600} were taken every 30 minutes using a plate reader (Infinite M Plex, Tecan, Switzerland).

2.16 Epithelial cell culture

The human oral buccal cell line TR146 (Sigma-Aldrich, USA) was cultured in DMEM/F12 medium (Gibco, Thermo Fisher Scientific, USA), supplemented with 10% FBS. The human Caucasian colon adenocarcinoma cell line Caco-2 (kindly provided by Prof. Dr. Cynthia Sharma, IMIB Würzburg, Germany) was cultured in DMEM medium (Gibco, Thermo Fisher Scientific, USA), supplemented with 10% FBS. HT29-MTX-E12 (Sigma-Aldrich, USA) cells were seeded on transwell membranes (Corning Transwell 0.4 μm pore polycarbonate membrane; 12 mm inserts purchased from Sigma-Aldrich, USA) and cultured in DMEM medium, supplemented with 10% FBS, 5 mM glutamine and 5 mM non-essential amino acids (Gibco, Thermo Fisher Scientific, USA) and were allowed to grow for 21 days with regular medium exchange twice per week. For *in vitro* translocation assay C2BBe1 cells were cultured in a collagen-coated transwell system in DMEM medium, supplemented with 10% FBS, and 0.01 mg/ml of holotransferrin. All cell lines were cultured in a humidified incubator at 37°C and 5% CO_2 and passaged three to four times to guarantee stable growth.

2.17 Adherence of *Candida albicans* cells to human epithelia

Attachment of *C. albicans* to epithelial cells was measured either through fluorescence microscopy as described earlier for TR146 cells (Meir et al., 2018), this protocol was also used to assess fungal adherence to the Caco-2 cell line, or plated in case of the HT29-MTX-E12 cell line. Briefly, cells of all three epithelial cell lines were challenged with *C. albicans* cells at a **m**ultiplicity **o**f **i**nfection (MOI) of 1. Prior to infection, epithelial cells were incubated in black 96-well plates to build a confluent monolayer. Growth medium was then replaced by medium lacking FBS. To prepare the *C. albicans* inoculum, cells were harvested from an overnight culture grown in liquid YPD medium, washed, and adjusted to $5x10^5$ cells per ml in the appropriate cell line medium. Epithelial cells were incubated with 100 µl of the *Candida* suspension. After 1 hour, cells were washed three times with 1x PBS to remove non-adherent *C. albicans* cells. TR146 and Caco-2 cells were fixed with 4% paraformaldehyde and incubated overnight with a primary rabbit anti-C albicans antibody (Table 4). Next day, cells were washed and stained with a secondary Alexa Fluor 594-conjugated goat anti-rabbit antibody (1:400) (Table 4). Imaging was done using a wide-field epifluorescence microscopy (DMI6000 B, Leica, Germany). The number of adhered fungal cells was measured in at least 30 fields per strain. *Candida* adherence to mucus covering the HT29-MTX-E12 transwell systems was assessed by scraping all cells from wells after extensive washing to remove non-adhered cells. Cell mixes were pelleted, plated on YPD plates, incubated for 48 h at 30°C, and colonies were counted. Adherence was determined in four independent experiments for each cell line.

Influence of nigericin on adherence. *C. albicans* cells treated with nigericin were also assayed for attachment to the oral epithelial cells TR146. Briefly, fungal cells were incubated with 15 µg/ml nigericin or a mock control (DMSO/ethanol) for 30 minutes or 2 hours at 30°C, washed twice, and added to TR146 cells. After the addition of *Candida*, cells were incubated for 2 hours at 37°C with 5% CO_2. Afterwards, cells were washed with PBS to remove non-adhered cells, fixed, stained, and quantified by microscopy as described above.

2.18 Evaluation of *in vitro* translocation

Tests assessing the ability of the *C. albicans* wild-type strain and the *zcf8* deletion mutant to translocate through the host epithelia and affect epithelial integrity were carried out by myself in the laboratory of Prof. Dr. Bernhard Hube at the Hans-Knöll Institut in Jena, under the supervision of Dr. Stefanie Allert and Dr. Toni Förster. The assay was done as described in Allert *et al.* (2018). Briefly, a subclone of Caco-2 cells, C2BBe1, was seeded with a concentration of $2x10^4$ cells per well in the upper compartment of a collagen-coated insert (5 μm pore size) of a transwell system (Sigma-Aldrich, USA). Cells were cultured in a humidified incubator at 37°C and 5% CO_2 for 14 days. On the day of infection, **t**rans**e**pithelial **e**lectrical **r**esistance (TEER) of the monolayer was measured using a volt-ohm meter (WPI, USA). Reduction of impedance (resistance) in TEER upon infection reflects the potential of the strain to translocate through the epithelium, thus reducing epithelial integrity. For that, one of the electrodes was dipped into the medium of the transwell insert, while the other one was dipped into the liquid medium in the lower compartment of the transwell system. *C. albicans* strains were grown overnight in YPD, washed, and adjusted to a concentration of $2x10^6$ cells/ml in DMEM without serum. The confluent C2BBe1 monolayer was challenged with $1x10^5$ *Candida* cells and incubated in an incubator at 37°C and 5% CO_2. After 24 hours, a second TEER-measurement was conducted to measure *Candida*-strain-specific changes on epithelial integrity (Ω*cm²) upon infection. In addition, a fresh Zymolyase solution (AMSBIO, UK) was added to the basolateral chamber of the transwell to a final concentration of 20 U/ml and incubated for an additional 2 hours at 37°C and 5% CO_2. The enzyme digests the fungal cell wall and, in this way, detaches filaments from the membrane of the transwell insert. Afterwards, the insert was removed and digested cell fragments of *Candida* hyphae in the lower compartment were counted under the microscope (to estimate dilution), diluted, and plated on YPD. The colony count was then used as a readout to determine translocation. Each *Candida* strain was tested for general growth in cell line medium, sensitivity against Zymolase, as well as translocation through a blank

insert which was used for data correction. Statistical evaluation (Wilcoxon matched-pairs signed rank test) and plotting were done using GraphPad (v.9.1.0).

2.19 Quantification of cytotoxicity

Cell damage was established by measuring **l**actate **d**e**h**ydrogenase (LDH) release as a proxy for cell damage of a epithelial cell line upon infection. C2BBe1 cells, TR146, and a mix of HT29-MTX-E12 and C2BBe1 (30:70) were co-incubated with *Candida* strains (Table 1), and LDH was monitored using a cytotoxicity detection kit (Roche, Switzerland). The experiment was conducted by me in the laboratory of Prof. Dr. Bernhard Hube at the Hans-Knöll Institut in Jena, under the supervision of Dr. Stefanie Allert and Dr. Toni Förster. The assay was done as described in Allert *et al.* (2018). Briefly, a collagen coated 96-well plate was seeded with $2x10^4$ cells per well of the C2BBe1 or the 70:30-mix, and with $1x10^5$ cells per well of TR146 cells, and incubated overnight in a humidified incubator at 37°C and 5% CO_2. *C. albicans* strains were grown in YPD, washed, and diluted in DMEM medium to a final concentration of $2x10^6$ cells/ml. All three cell lines were infected with $2x10^4$ cells per well and incubated at 37°C and 5% CO_2. After 24 hours, cells were centrifuged at 250g for 10 minutes and the LDH content in the supernatant was quantified using a cytotoxic detection kit according to the manufacturer's instructions and a standard solution of LDH. Untreated epithelial cells served as negative control whereas cells treated with 5% Triton-X 100 for 30 minutes at room temperature were used to determine the maximal release of LDH. Statistical evaluation (Mann-Whitney U test) and plotting were done using GraphPad (v.9.1.0).

2.20 Mouse model of oral infection

Murine oral infection was conducted as described by Solis and Filler (2012). The *C. albicans* inoculum for infection was prepared using a 1 ml overnight culture in YPD, washed twice with sterile 1x PBS, and serially diluted to a final concentration of $5x10^6$ cells/ml. A sterile cotton ball (~2.5 mg) was soaked for 1 hour in 100 μl of

the inoculum. The saturated cotton ball served as a carrier for the fungus to ensure that the cells are able to adhere to the epithelium and are not washed away by saliva. Six- to nine-week-old female C57BL/6J mice (Charles River, Germany) were anaesthetized with a mixture of Ketamin (100 mg/kg) (Zoetis, USA) and Xylazin (6 mg/kg) (CP-Pharma, Germany) in sterile PBS which was injected intraperitoneally. A cotton ball saturated with *C. albicans* cells was placed sublingually for 90 minutes. Animal weight was monitored daily. Animal weight is a well-documented proxy to track infection process in the mouse, as infected animals lose up to 10% of their weight in the beginning of an infection and start to gain weight as convalescence proceeds. Three days after inoculation, mice were euthanized, and tongues were removed and split sagittally. One half of the tongue was homogenized and plated on **y**east **m**old (YM) agar containing 0.1 μg/ml ampicillin and 0.01 μg/ml gentamicin to purge bacterial contamination. Plates were then incubated at 30°C to assess fungal fitness which was determined by the number of cells that managed to persist. The other half of the tongue was fixed for histology purposes.

Histology. As described above, the mural tongue was removed and split sagittally. Fixation was done overnight in 10% of buffered formalin (10% of a 37% formaldehyde solution, 0.65% Na_2HPO_4, and 0.4% NaH_2PO_4) and then washed several times with PBS. The tissue was embedded in paraffin on a paraffin embedding machine (Leica, Germany) using a standard program consisting of washing steps with increasing ethanol concentrations, xylol baths, and 3 hours in melted paraffin at 62°C. The resulting blocks were stored at room temperature. For microscopy, 4-μm sections were prepared, rehydrated in decreasing ethanol concentrations, stained applying the standard protocol for the **p**eriodic **a**cid-**S**chiff (PAS) method, and dehydrated using increasing ethanol concentrations, isopropanol, and xylol. Finally, samples were embedded in Entellan (Merck, Germany).

3 Results

3.1 Characterization of *ZCF8*

A collection of transcription regulator deletion mutants was tested in two independent genetic screenings for their ability to alter fitness of *C. albicans* on mammalian mucosae. The collection consists of isogenic mutants that did not exhibit a growth defect or any other abnormal phenotype under laboratory *in vitro* settings (Homann *et al.*, 2009) implying that these regulatory genes might be relevant in *in vivo* conditions. The genetic screens were conducted using murine models for **o**ro**p**haryngeal **c**andidiasis (OPC) (Meir *et al.*, 2018) and gut colonization (Böhm *et al.*, 2017) as both mucosae represent natural habitats of *C. albicans*. Interestingly, the putative zinc cluster transcription regulator *ZCF8* was described to exhibit opposing phenotypes in each of the infection settings: While the deletion of the gene increased persistence of the fungus in the oral cavity (Meir *et al.*, 2018), the same mutation reduced fungal fitness in the context of gut colonization (Böhm *et al.*, 2017). Additionally, *ZCF8* altered adherence of *C. albicans* to silicone surfaces *in vitro* (Finkel *et al.*, 2012). Finkel and colleagues screened a library of transcription regulator mutants and assessed their ability to adhere to a silicone substrate (polydimethylsiloxane) in a flow-cell assay. Adherence to silicone substrates is a critical step during biofilm formation and the basis for device-associated infections in humans. Mutation of *ZCF8* reduced adherence of fungal cells to 29% of wild-type adherence (Finkel *et al.*, 2012). However, the biology and role of the transcription regulator *ZCF8* remains to be elucidated.

ZCF8 is predicted to belong to the family of zinc cluster transcription regulators according to the ***C**andida* **G**enome **D**atabase (CGD) (Skrzypek *et al.*, 2017). As mentioned in the introduction, all members of this family contain a well-conserved and characteristic zinc finger DNA binding domain. A first scan of the protein sequence of Zcf8p revealed the presence of the six cysteine residues that are thought to interact with two zinc atoms (Figure 1 and 2A). In order to further

characterize *ZCF8* and shed light on its function, I sought to find homologs of the protein in closely related species. In fact, several members of the *Candida* clade harbor a *ZCF8* ortholog according to CGD, although, there are no predicted orthologs for this gene in the well-studied yeast *Saccharomyces cerevisiae*.

In order to reconstruct phylogeny for *ZCF8*, putative homologs within *C. albicans* were identified, by performing a BLASTP search of either full protein sequence

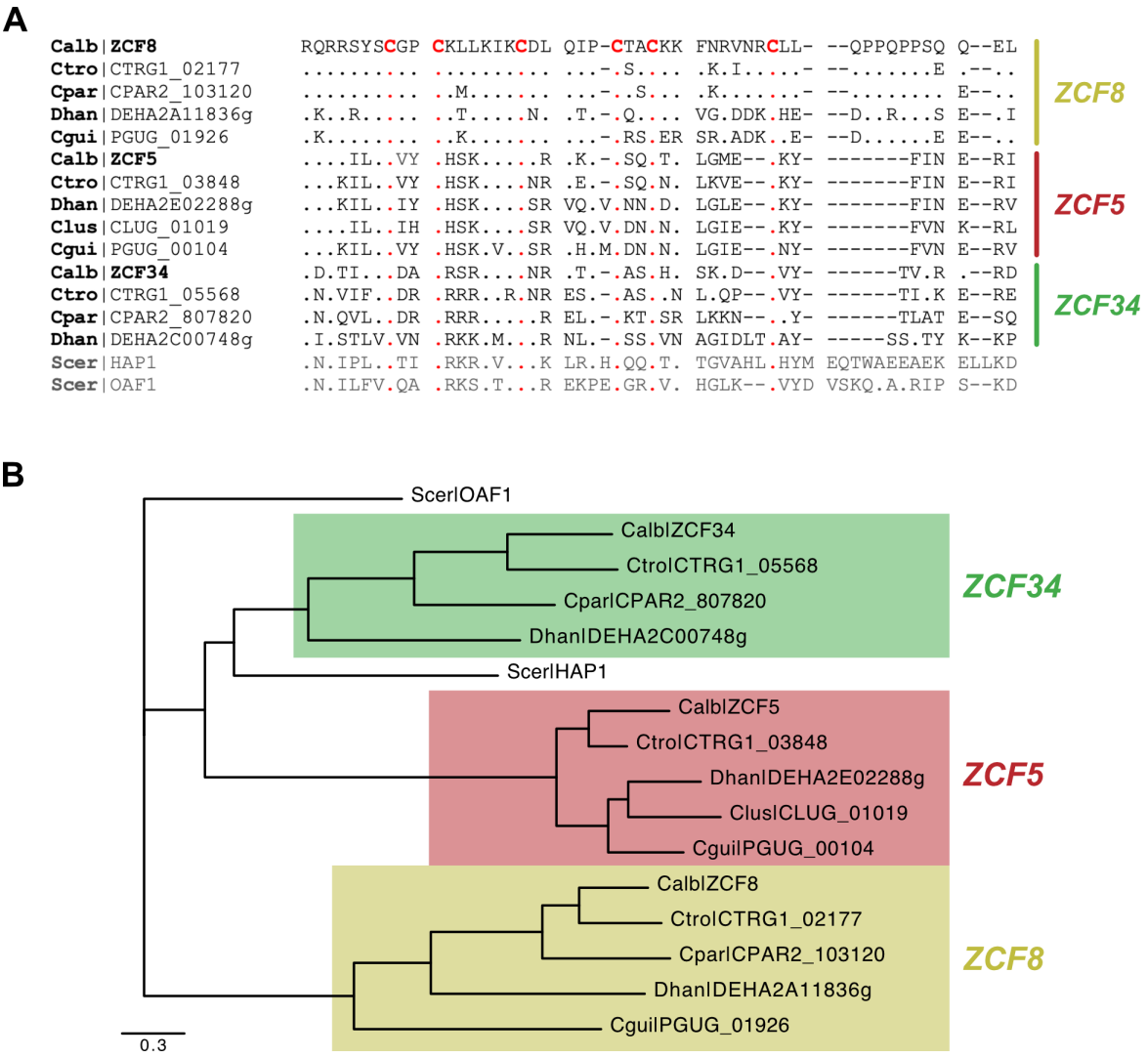

Figure 2: Low sequence identity between *ZCF8* and the two closest homologs. (A) Protein sequence of the putative DNA binding domains of *ZCF8* and its closest homologs. The characteristic six cysteine residues are highlighted in red. Identical amino acids are represented by dots whereas gaps are depicted as dashes. (B) Maximum likelihood phylogeny of *ZCF8* and its closest homologs. Three major clades are highlighted. (Reuter-Weissenberger *et al.*, *in press*)

(915 aa) or the predicted zinc finger domain (aa 61 - 110) as seed (Figure 2A). In both cases, the proteins identified with the highest sequence similarity were the zinc cluster transcription regulators Zcf5p (13.6% and 32.2% sequence identity of full protein length and of the DNA binding domain, respectively) and Zcf34p (14.9% and 36.0% for sequence identity of full protein length and of the DNA binding domain, respectively). The function of *ZCF5* is unknown, but *ZCF34* (also named *MRR2*) has been reported to be involved in regulating multidrug resistance via the drug efflux pump Cdr1p (Schillig and Morschhäuser, 2013) and is required for adherence to silicone surfaces (Finkel *et al.*, 2012). A similar adherence phenotype was also reported for *ZCF8* (Finkel *et al.*, 2012). However, unlike *ZCF34*, artificial activation of *ZCF8* does not lead to significant fluconazole resistance (Schillig and Morschhäuser, 2013).

To establish whether *ZCF8* shared a common origin with any of the two genes mentioned above, I identified additional orthologs and expanded the phylogenetic analysis to include species of the Hemiascomycetes group. This group includes the entire *Candida* clade as well as species closely related to *S. cerevisiae* (Figure 3). The reason for including more species into the phylogeny was to investigate whether *ZCF8* has orthologs in any extant species in the *Candida* and *Saccharomyces* clades. To illustrate the phylogenetic relationships between the proteins, I built a maximum likelihood tree based on the alignment of the full-protein sequences of Zcf8p, Zcf5p, and Zcf34p (Figure 2B). The tree shows the three proteins and their respective putative orthologs form distinct clades. Synteny analysis carried out using the ***C**andida* **G**ene **O**rder **B**rowser (CGOB) (Fitzpatrick *et al.*, 2010; Maguire *et al.*, 2013), which contains manually curated sets of orthologous *Candida* genes based on genomic context (*e.g.*, chromosomal location and adjacent genes) and sequence similarity, revealed no orthologs of these genes outside of the *Candida* clade (Figure 3).

According to CGD, *S. cerevisiae HAP1* and *OAF1* are designated “best hits” for *C. albicans ZCF5* and *ZCF34*, respectively. “Best hits” means that in a BLASTP sequence similarity search querying Zcf5p or Zcf34p against all protein sequences in *S. cerevisiae* the genes *HAP1* and *OAF1* represent the highest scoring hit, respectively. Although those results were confirmed by my own BLASTP search,

it is important to take into consideration that “best hits” are automatically generated by CGD when a protein with no known ortholog is queried, and it relies solely on sequence similarity without considering, for example, synteny. Both *HAP1* and *OAF1* encode a zinc cluster transcription regulator which harbors the characteristic six cysteine residues (Figure 2A). Based on the curated set of orthologous *Candida* genes provided by CGOB, the true orthologs of *S. cerevisiae HAP1* and *OAF1* in

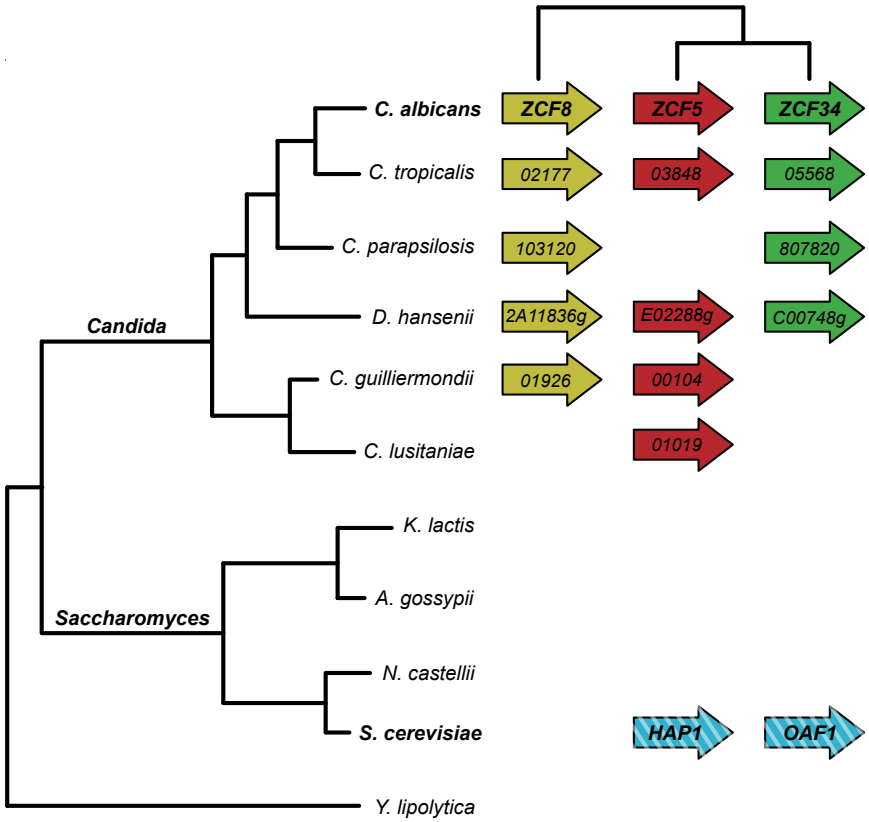

Figure 3: *ZCF8* might have a relatively recent origin arising by either gene duplication or horizontal gene transfer. Cladogram depicting the phylogenetic relationships among extant species of the *Candida* and *Saccharomyces* clade. Colored arrows represent *ZCF8* and its closest homologs according to the CGD Multi-Genome search using NCBI BLAST+ based on full-length protein sequences and/or sequence of the putative DNA binding domain. Gene orthology (same colors) is assigned following independent reconstructions generated by CGOB (Fitzpatrick *et al.*, 2010; Maguire *et al.*, 2013). *S. cerevisiae OAF1* and *HAP1* (stripped arrows) are the predicted “best hits” to *C. albicans ZCF34* and *ZCF5*, respectively. However, the phylogenetic tree of full-length protein sequence and synteny analysis indicates that neither can be considered true orthologs of the indicated *Candida* genes. (Reuter-Weissenberger *et al.*, *in press*)

C. albicans are *ZCF20* (C5_01500C) and *CTA4* (*C3_05930W*), respectively. Even though *CTA4* in *C. albicans* and *OAF1* in *S. cerevisiae* are not syntenic, the sequence identity between both proteins is slightly higher (16.48% and 41.18% sequence identity of full protein length and of the DNA binding domain, respectively) compared to the sequence identity between Zcf34p and Oaf1p (14.00% and 40.38% sequence identity of full protein length and of the DNA binding domain, respectively). In addition, the phylogenetic tree built in this study, based on protein sequence alignments, suggests that *HAP1* and *OAF1* cannot be assigned to any of the three clades. Therefore, the analysis above indicates that, like *ZCF8*, neither *ZCF5* nor *ZCF34* have orthologs in *S. cerevisiae* and that the true orthologs of *S. cerevisiae HAP1* and *OAF1* are *C. albicans ZCF20* and *CTA4,* respectively.

In summary, orthologs of the gene *ZCF8* could only be identified within the *Candida* clade. This result agrees with previous reports (Issi *et al.*, 2017) and suggests a rather recent origin of the gene. Issi and colleagues identified *ZCF8* as part of set of 35 zinc cluster DNA binding proteins that are (a) restricted to the fungal kingdom and (b) have homologs in pathogenic fungi while they are missing from nonpathogenic yeasts (Issi *et al.*, 2017). However, the origin of *ZCF8* remains unclear as both gene duplication and horizontal gene transfer are plausible.

3.2 ChIP-Seq revealed targets of regulation

To further characterize the role of *ZCF8* in *C. albicans*, I sought to identify genes regulated by the protein. Therefore, I conducted chromatin immunoprecipitation followed by next generation sequencing (ChIP-Seq). This method allows the isolation of fragments of genomic DNA physically bound by the protein, their purification, and high-throughput sequencing. Analysis of the resulting sequencing reads can be used to identify promoter regions bound by the protein. The extraction of the crosslinked DNA-protein aggregate from the lysed cell can be carried out by fusing the protein to an epitope tag that is recognized by a matrix-bound antibody. The ChIP-Seq strategy relies heavily on specific DNA binding by the tagged protein and on the quality and specificity of the used antibody. To optimize and increase

the outcome of the experiment, multiple epitope tags (13xMYC and GFP) at different locations on the protein were employed. Because the DNA binding domain of Zcf8p is localized towards the N terminus of the protein (Figure 1), the native *ZCF8* locus was genetically modified to encode a C-terminal epitope tag reducing the chances of steric hinderance. In addition, a second strain carrying an N-terminal 13xMYC tag was also generated. The expression of the gene, however, remained under the control of its native promoter. The different tagged *C. albicans* strains as well as a non-tagged control were grown overnight in YPD medium at 30°C and processed as described previously (Hernday *et al.*, 2010; Pérez *et al.*, 2013).

Two examples of the data generated by ChIP-Seq are illustrated in figure 4. Reads of DNA regions bound by Zcf8p are overrepresented and, therefore, appear as peaks in the upper panel of figure 4. In contrast, the grey line derived from a non-tagged control strain illustrates background noise due to non-specific antibody binding. The R package “bPeaks” (Merhej *et al.*, 2014) was employed to detect regions with a significant enrichment of mapped reads in the ChIP-Seq data. This tool is designed to find DNA binding sites in small eukaryotic genomes such as yeast genomes. It compares the height of each peak (*i.e.* number of reads aligned to that location) from an IP sample with the reads aligned to the same location in

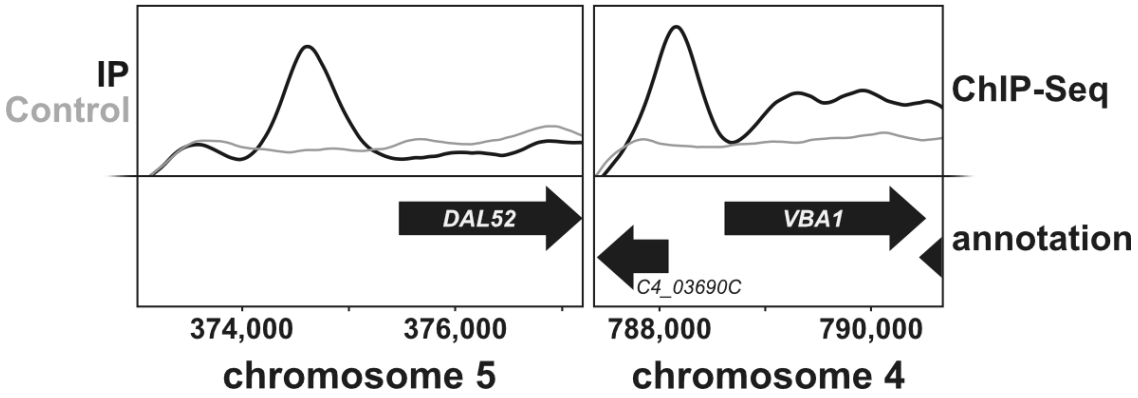

Figure 4: Two examples of peaks or regions bound by Zcf8p. The lines in the upper panel illustrates the IP signal in black and input control in grey. The lower part shows the genomic location in *C. albicans* with arrows representing open reading frames. Both peaks localize immediately upstream of *DAL52*, *VBA1,* and *C4_03690C*, respectively. (Reuter-Weissenberger *et al.*, *in press*)

the control strain. As mentioned above, several epitope tags were prepared and Zcf8p was C- and N-terminally tagged with the goal of increasing the chances of obtaining high quality data. At this point, having assessed the number of detected peaks and the consistency of particular enriched regions in the biological replicates, I decided to use the data derived from the C-terminal 13xMYC tag for further analysis. The N-terminal 13xMYC tag produced only few and small peaks which suggests that the tagged protein did not bind DNA properly. This is consistent with the relatively high background coverage which can result from the PCR amplification step during library preparation if no DNA fragments are overrepresented. Data derived from GFP tagged strain also showed poor data which might be caused by the protein being non-functional due to the localization of the tag or due to non-specific antibody binding. The list of enriched regions derived from the Zcf8p-13xMyc was refined by applying stringent criteria regarding the location of the peak and its consistency throughout the replicates. Therefore, all the peaks located within ORFs were discarded and only intergenic peaks located in regions upstream of genes were considered for the analysis. In addition, peaks adjacent to highly expressed genes were neglected since these regions tend to be bound by DNA binding proteins non-specifically (Zordan *et al.*, 2007; Tuch *et al.*, 2008; Nobile *et al.*, 2012; Pérez *et al.*, 2013). Finally, only peaks present in at least two of four replicates were kept. The final dataset consisted of 42 peaks or DNA regions which were then ranked by their fold enrichment (Table 5). Two of these regions are illustrated in figure 4.

In addition to applying stringent criteria to define peaks, a commonly used method to assess the quality of the called peaks is to derive DNA motifs overrepresented in the DNA regions bound by Zcf8p. To do this, I selected 500-nt-long DNA sequences centered on the highest point of each of the top scoring peaks (approximately 1/4 of the peaks). These sequences were then used as input and fed into the oligo-analysis tool of the **R**egulatory **S**equence **A**nalysis **T**ools (RSAT) for fungal organisms. The sequence 5'-TAATCCG-3' (Figure 5A) was overrepresented amongst the derived motifs. Interestingly, this putative DNA binding motif harbors a 5'-CCG-3' sequence, a well-established element of sequences bound by other zinc cluster transcription regulators (MacPherson *et al.*,

2006). This putative DNA binding motif was found in the promoter region of 21 of the 50 genes (46%). It is worth noticing that an alternative DNA binding motif containing a 5'-CCG-3' and 5'-AAA-3' triplet - but in flipped order - was overrepresented in the same set of sequences (Figure 5B), which implies that Zcf8p might be able to recognize and bind to variations of the motif within the target sequence.

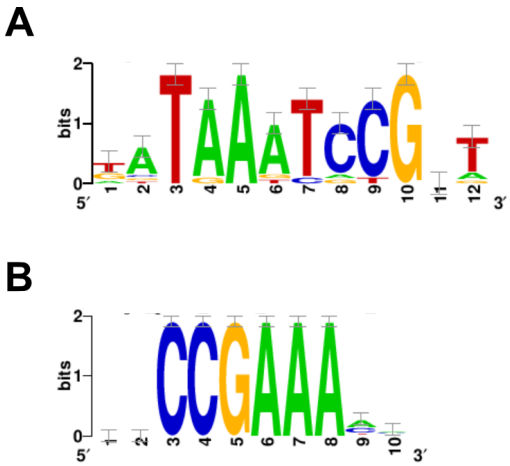

Figure 5: *Bona fide* DNA binding motif of Zcf8p derived *de novo*. (A) *Bona fide* motif derived by ~1/4 of the top peaks of *ZCF8*. (B) Alternative motif derived from the same set of sequences as for motif in A. (Reuter-Weissenberger *et al.*, *in press*)

In order to empirically validate this result, I conducted an **e**lectrophoretic **m**obility **s**hift **a**ssay (EMSA) to establish whether the derived DNA sequence was a *bona fide* binding site for Zcf8p. In this biochemical method, the purified protein (or its purified DNA binding domain) is incubated with radioactively labelled DNA sequences harboring instances of the putative DNA motif. The mixture is resolved by gel electrophoresis. Binding of the DNA probes to the protein can be assessed by the shift in size of the protein-DNA complex compared to the smaller, free-radiolabeled DNA.

As predicted, the purified DNA binding domain (aa 57 - 158) was able to recognize and bind instances of the sequence motif. Binding of the protein was specific as proven by the lack of binding when point mutations were inserted in the DNA motif (Figure 6A). Quantification of the signal intensity emitted by each protein-DNA complex was used to assess relative DNA binding (Figure 6B) which can be interpreted as a proxy for binding specificity. For example, the graph in figure 6B illustrates that the amount of protein (x-axis) needed to bind 25% of

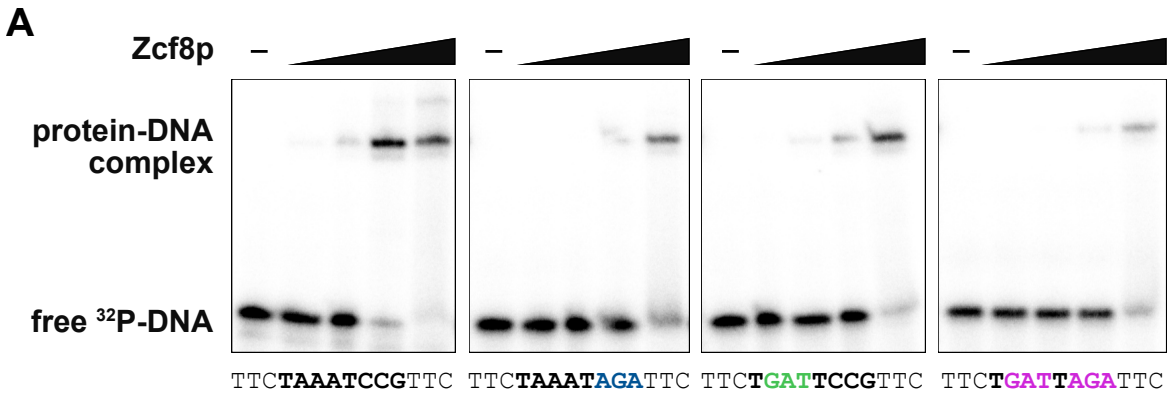

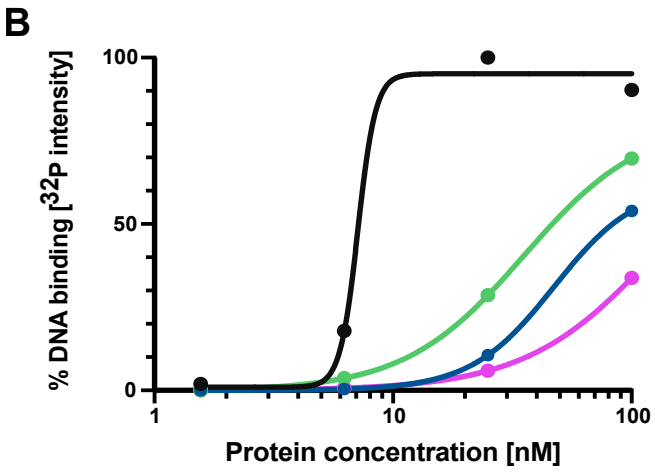

Figure 6: Electrophoretic mobility shift assay shows binding of the Zcf8 protein to its predicted binding site. (A) The purified DNA binding domain of Zcf8p in increasing concentrations was incubated with ^{32}P-labeled 30-nt-long oligonucleotides containing either the wild-type (black) or mutated DNA motif (color) (full sequence in table 2). (B) Quantification of gel shift in A. Colors correspond to DNA oligos. Notice the log scale in the X-axis. (Reuter-Weissenberger et al., *in press*)

labeled DNA (y-axis) is more than six-fold higher when interrupting the 5'-CCG-3' triplet (blue line) or three-fold higher when interrupting the 5'-AAA-3' triplet (green line). Therefore, specificity of Zcf8p is driven not just by the common regulatory element (5'-CCG-3') but also by the 5'-AAA-3' triplet.

In total, I was able to identify 48 genes, 1 antisense target, and 1 **n**ovel **t**ranscriptional **a**ctive **r**egion (nTAR) as putative targets of *ZCF8*'s regulation (Table 6). nTARs are transcriptionally active regions that map outside of annotated ORFs and are of unknown function (Giosa *et al.*, 2017). Gene ontology (GO) analysis of the 48 ORFs showed significant enrichment of multiple terms including cell adhesion (*e.g., AAF1*, *WOR4*), transmembrane transport (*e.g., SSA2*, *DAL8*,

MDR1), and biofilm formation (*e.g.*, *WOR1*, *TEC1*, *BRG1*). Notably, several targets of Zcf8p are known transcription regulators (*e.g., WOR1*, *BRG1*, *TEC1*) or putative regulatory proteins (*e.g., AAF1*, *TCC1*). This notion agreed with the overrepresentation of functions related to "sequence-specific DNA binding" and "transcription factor activity" terms of the GO search. In addition, a quarter of the annotated Zcf8p-regualted ORFs had roles connected to either vacuole or intracellular vesicle trafficking: The **v**acuolar **b**asic **a**mino acid transporter *VBA1* (Shimazu *et al.*, 2005); the **c**onserved **o**ligomeric **G**olgi complex *COG2* (Ram *et al.*, 2002; Loh and Hong, 2004), an essential component of a cytosolic tethering complex that functions in protein trafficking to mediate fusion of transport vesicles to Golgi compartments; the **u**nconventional **S**NARE in the **e**ndoplasmic reticulum *USE1* (Burri *et al.*, 2003; Dilcher *et al.*, 2003), which is involved in retrograde traffic from the Golgi to the ER; the putative oxidoreductase *C1_10840C* (Kanneganti *et al.*, 2011) which is involved in late endosome to Golgi transport; and the putative **c**arboxy**p**eptidase **S**, *CPS1*, which localizes to the vacuolar lumen (Bordallo *et al.*, 1993). Overall, the findings suggest that Zcf8p is part of a larger regulatory network that controls multiple traits including cell adhesion, biofilm formation, and filamentation. The data also shows that functional proteins of vacuole biology or intracellular trafficking are targets of Zcf8p which might reflect an alternative role of the regulator.

3.3 Transcriptome analysis connects *ZCF8* to the fungal vacuole

A complementary approach used to establish the role of *ZCF8* was a transcriptome analysis. RNA-Seq experiments were conducted using three *C. albicans* strains: a *zcf8* deletion mutant, a strain ectopically overexpressing *ZCF8,* and the wild-type reference strain. The reason for including mutants that either lack the regulator or have high levels of it was that one would expect targets of Zcf8p to display complementary expression profiles. *C. albicans* cells were incubated in defined medium either lacking any nitrogen source or supplemented with

ammonium sulfate to test the hypothesis that *ZCF8* might be connected to vacuolar biology or intracellular trafficking. As mentioned in the introduction, the vacuole is the cellular storage unit for amino acids and maintains homeostasis which is particularly important when cells face nitrogen-poor conditions (Mukaiyama *et al.*, 2010; Kawano-Kawada *et al.*, 2018). In addition, some top targets of genome-wide protein-DNA interaction data were predicted transporters of amino acids (*VBA1*) or of nitrogen-rich molecules (*DAL52*).

The **p**rincipial **c**omponent **a**nalysis (PCA) in figure 7 illustrates that both deleting and overexpressing *ZCF8* ("ectopic *ZCF8*") affect the fungal transcriptome in a somewhat opposing way. Surprisingly, the number of transcripts with significant changes in expression was rather low: Only 39 genes differently expressed in the deletion mutant when compared to the wild-type strain (negative $\log_{10}$ [p value] > 10 and $\log_2$ fold-change > |0.8|) (Figure 8A, Table 7); and in the overexpression strain, 45 genes passed the applied threshold (negative $\log_{10}$ [p value] > 10 and $\log_2$ fold change > |1.5|) (Figure 8B, Table 8). As expected, several transcripts were up-regulated in the *zcf8* deletion mutant and down-regulated in the strain overexpressing *ZCF8* and vice versa (*e.g., C4_05580C*, *CR_10320W*, and *DAL52*). Among this subset of genes (highlighted in figure 8A and 8B) were *VBA1* and *DAL52*, two top targets of Zcf8p identified in the ChIP-Seq data. The fact that these genes were also differently expressed in the RNA-Seq data indicated that both are indeed direct targets of Zcf8p's regulation, and that Zcf8p may function as a transcriptional repressor because both genes displayed increased expression levels in the *zcf8* deletion mutant. However, the function of the majority of the

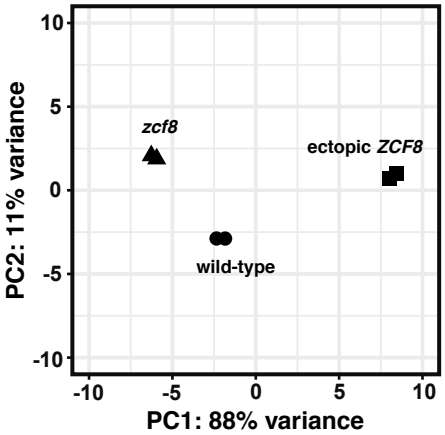

Figure 7: Zcf8p influences starvation response in *C. albicans*. PCA based on the *zcf8* deletion mutant, a strain ectopically overexpressing *ZCF8*, and the wild-type reference strain grown in defined medium lacking any nitrogen source. (Reuter-Weissenberger *et al.*, *in press*)

regulated genes in the deletion mutant is unknown (*e.g., C3_07670W, C4_01330W, CR_06500C*). Nonetheless, the addition of the strain overexpressing *ZCF8* expanded the list of putative *ZCF8*-regulated transcripts. For example, *YMX6* is the top down-regulated gene in the overexpression mutant. It encodes a predicted NADH dehydrogenase which is induced by nitric oxide, an antimicrobial compound produced by the innate immune system (Hromatka *et al.*, 2005), and does not have an assigned ortholog outside the *Candida* clade. Among other down-regulated genes is *C4_03050C*, the ortholog of the vacuolar carboxypeptidase *CPS1*, which was also a hit in the ChIP-Seq data (Table 6).

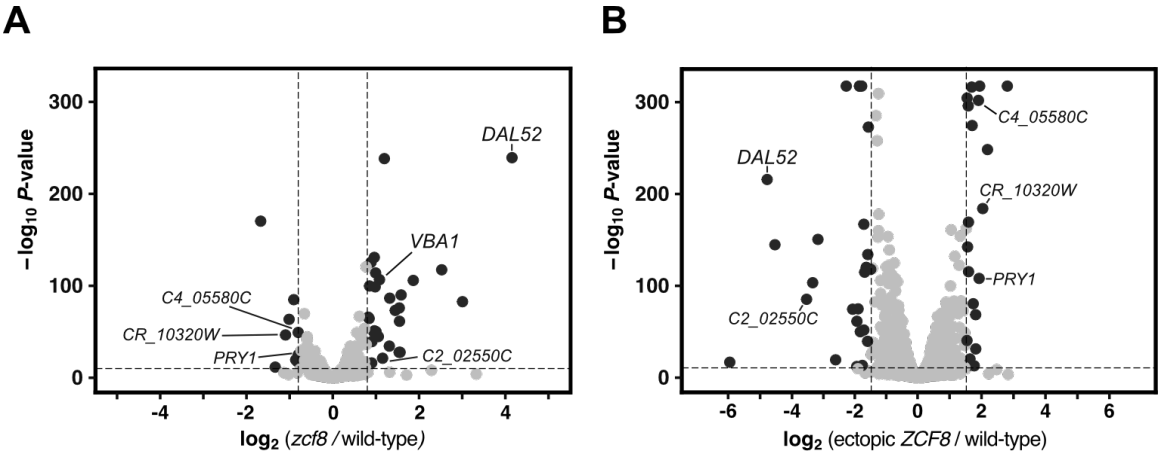

Figure 8: Differently regulated genes are linked to amino acid metabolism. Volcano plot depicting up- or down-regulated transcript in the *zcf8* deletion mutant (A) and in the strain ectopically overexpressing *ZCF8* (B). Each dot represents one transcript. Significantly up- or down-regulated transcripts are in black. (Reuter-Weissenberger *et al.*, *in press*)

GO searches, using the list of differently expressed ORFs in the deletion mutant as input, retrieved "amino acid biosynthesis*"* (*P* = 0.00193) and "amino acid metabolism*"* (*P* = 0.00927) as enriched terms in the dataset emphasizing *ZCF8*'s link to cellular amino acid homeostasis - processes mainly facilitated through the vacuole. The GO search also identified multiple terms related to biosynthetic and metabolic processes of vitamin B6 (also known as pyridoxine) or its active form pyridoxal phosphate. However, either term has in total only 4 and 3 genes assigned to it, respectively, and the enrichment is based on two genes (*SNZ1*, *SNO1*) that

are present in the data. Additional enriched terms are related to rather unspecific processes including biosynthesis of small molecules, carboxylic acids, or aldehydes. GO search with the set of ORFs that were differently expressed in the overexpression mutant did not add substantial information. The search retrieved terms of the ontology process regarding “oxidation-reduction process” (P = 0.01574) and “fluconazole transport” (P = 0.01623). The latter is based on only two genes that encode membrane transporter of the major facilitator superfamily (*MDR1*, *FLU1*). The fact that both genes are differently regulated exclusively in the overexpression strain and expression of *MDR1* is up-regulated while *FLU1* expression is down-regulated implies that they are not controlled by Zcf8p.

Overall, the genome-wide protein-DNA interaction and the gene expression data collectively suggest that Zcf8p - possibly as part of a regulatory network - regulates aspects of vacuolar biology (as targeted genes encode vacuolar proteins) that are linked to amino acid homeostasis (revealed by an overrepresentation of amino acid metabolism genes in the RNA-Seq data).

3.4 Zcf8p functions primarily as a transcriptional repressor

As mentioned in the previous section, several transcripts (*e.g., DAL52*, *VBA1*) were more abundant in the absence of Zcf8p, while the same genes were down-regulated when *ZCF8* was continuously expressed. This suggests that Zcf8p might function as a transcriptional repressor of these genes. In addition, the ChIP-Seq analysis allowed the detection of a peak in the intergenic region immediately upstream of *ZCF8*’s ORF (Table 5 and 6) suggesting autoregulation. In fact, multiple zinc cluster transcription regulators are known to activate their own gene’s expression by binding to their promoter (MacPherson *et al.*, 2006).

To assess whether Zcf8p binds its own promoter as an activator or repressor, two reporter strains were constructed: one strain where a copy of the *ZCF8* ORF was replaced by YFP while the other allele remained intact (“strain I”, Figure 9A), and a second strain where the remaining *ZCF8* was also deleted (“strain II”, Figure 9B). This setup allowed the use of fluorescence as a read out for transcriptional

regulation of the *ZCF8* locus. YFP levels were quantified by flow cytometry. The graph in figure 9C illustrates that fluorescence emitted by the heterozygous strain that harbors an intact *ZCF8* allele was significantly lower compared to the isogenic strain lacking *ZCF8* which is consistent with the hypothesis of the Zcf8 protein repressing its own expression. From these results I could conclude that *ZCF8* acts primarily as a transcriptional repressor generating a negative feedback loop.

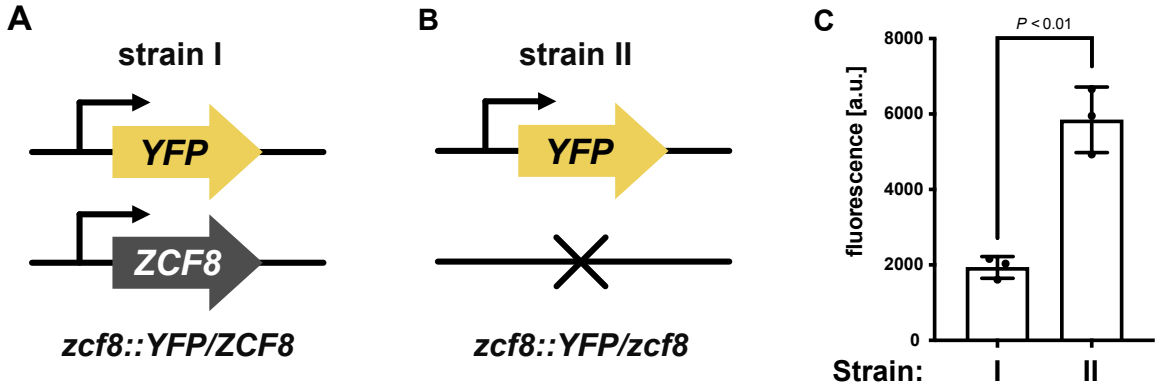

Figure 9: Zcf8p negatively regulates its own transcription. (A - B) Schematic of reporter strains used to evaluate autoregulation. (C) YFP fluorescence emitted by the reporter strains described in A. Plotted are the means ± SD. of three independent experiments. Statistical analysis by Student's *t*-test. (Reuter-Weissenberger *et al.*, *in press*)

3.5 Top targets of *ZCF8* accumulate in the vacuolar lumen

The predicted subcellular location of multiple targets of Zcf8p in *C. albicans* (*e.g.*, Vba1p, Cps1p) is the vacuole. In fact, some of these genes displayed the largest transcription changes when comparing deletion mutant vs. wild-type reference strain (Table 7) and, additionally, are associated with a peak in their 5' intergenic region (Table 6). Two of these "top targets" are *DAL52* and *VBA1*. The latter is a member of the **v**acuolar **b**asic **a**mino acid (VBA) transport family that facilitate vacuolar uptake of various amino acids in *S. cerevisiae* (Shimazu *et al.*, 2005). Interestingly, the expression of its ortholog *FNX1* is induced upon nitrogen starvation in the fission yeast *S. pombe* (Dimitrov *et al.*, 1998; Chardwiriyapreecha

et al., 2008). The biological function of *DAL52* is less apparent. CGD does not predict any ortholog for *DAL52* in a related species but suggests that the gene is "similar" to *DAL5* an allantoate permease which also transports dipeptides in *S. cerevisiae*. The amino acid sequences of both proteins share 43.37% sequence identity (*DAL5* in *S. cerevisiae* and its true ortholog *DAL5* in *C. albicans* share 46.73%). A database for eukaryotic pathogens (www.fungidb.org) predicts that, based on protein sequences, the ortholog of *DAL52* (as well as of *DAL5*, *DAL9*, *and DAL8*) in *S. pombe* is the putative dipeptide transmembrane transporter Dal5h2p. Therefore, it is plausible that Dal52p functions as a transporter of amino acids or peptides in *C. albicans* as well. However, the subcellular localization of the protein is unclear. The presence of 10 predicted transmembrane domains implies that the protein is targeted to either the plasma membrane or the membrane of any other internal organelle.

To establish its localization, the gene encoding Dal52p in its native chromosomal location was fused to a *Candida*-optimized version of the fluorescent reporter mNeonGreen (Frazer *et al.*, 2019). This modification was done in a wild-type *C. albicans* strain as well as in the *zcf8* deletion strain. To assess the environmental conditions under which *DAL52* is expressed, fungal cells were grown in nutrient rich (YPD) or defined medium either lacking nitrogen or supplemented with ammonium sulfate. The cellular growth was then evaluated at different growth phases (log phase or stationary phase) using fluorescence microscopy. Strikingly, Dal52p stably localized to the vacuolar lumen outlined by FM4-64 (Figure 10A). This membrane-specific dye is internalized by the fungus via endocytosis, transported to the vacuole, and accumulates in the vacuolar membrane (Vida *et al.*, 1995). Dal52p with a C-terminal mNeonGreen was targeted to the vacuolar lumen and fluorescence intensity was increased in the *zcf8* deletion background independently of the environmental conditions. An N-terminal YFP reporter misplaced the protein to subcellular structures that were identified as the endoplasmic reticulum. Since *DAL52* is annotated to be a putative permease of allantoate, one would expect the protein to be embedded in the plasma or the vacuolar membrane. A similar intracellular distribution pattern was observed for *C1_13130C* (Figure 10B) another gene identified as a target of Zcf8p regulation in

the ChIP-Seq experiment annotated as a putative histidine permease. Homologs of *C1_13130C* in *C. albicans*, *S. pombe*, and *S. cerevisiae* are reported or predicted fungal-specific transporters of amino acids with some being linked to the fungal vacuole (*e.g.*, *GAP1* in *S. cerevisiae*).

The fact that Dal52p and C1_13130C are targeted to the vacuole in *C. albicans* further supports a connection between this organelle and regulator.

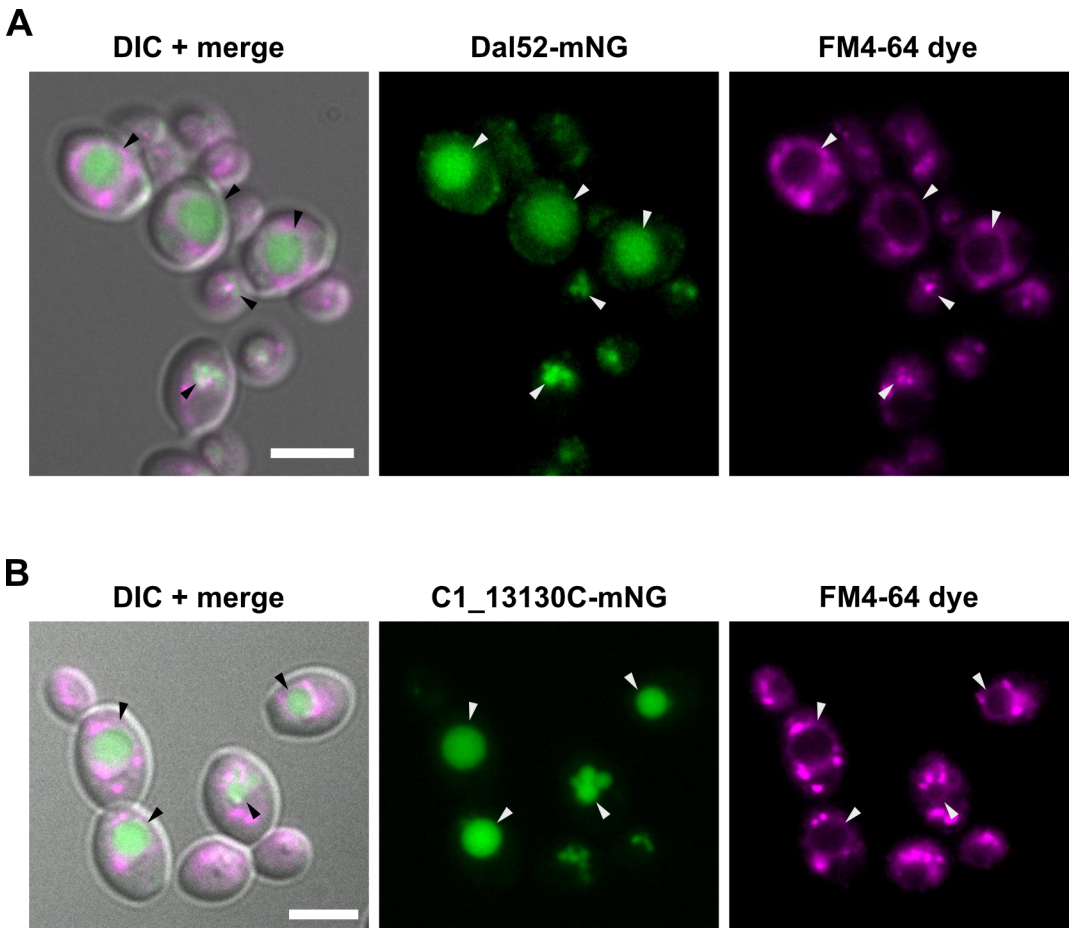

Figure 10: Putative allantoate and amino acid permeases are regulated by Zcf8p and targeted to the fungal vacuole. (A and B) Subcellular localization of Dal52p and C1_13130Cp tagged with a mNeonGreen reporter. Fungal vacuoles are marked with FM4-64 staining. Arrowheads point to vacuoles. Scale bars: 5 μm. (Reuter-Weissenberger *et al.*, *in press*)

3.6 Deletion of *ZCF8* results in altered vacuolar morphology

During the evaluation of the subcellular localization of Dal52p and C1_13130Cp, differences in vacuolar morphology became apparent: More cells of the *zcf8* deletion mutant seemed to display a single large vacuole compared to *C. albicans* wild-type cells when grown without an available nitrogen source. The presence of a single, large vacuole in yeast cells is thought to reflect nutrient limitation or other stress as these conditions induce vacuolar fusion events (Li *et al.*, 2009). In fact, the fungal vacuole is a dynamic organelle and yeast cells can contain up to five vacuoles per cell depending on extracellular and intracellular conditions (Warren *et al.*, 1996; Li *et al.*, 2009).

In order to find an explanation for the observed differences in vacuolar morphology, mutants of *ZCF8* and a wild-type strain were grown in defined medium lacking any nitrogen source or supplemented with ammonium sulfate. Figure 11 illustrates two examples of vacuole morphology in *C. albicans* cells under nitrogen-starved conditions after FM4-64 staining. The left panel displays how the vacuole fills most of the volume of the fungal yeast cell, whereas the smaller vacuoles on the right example occupy a minor fraction of the cell. As mentioned in the introduction, the large volume is perfectly fitted to increase hydrolytic capacity for

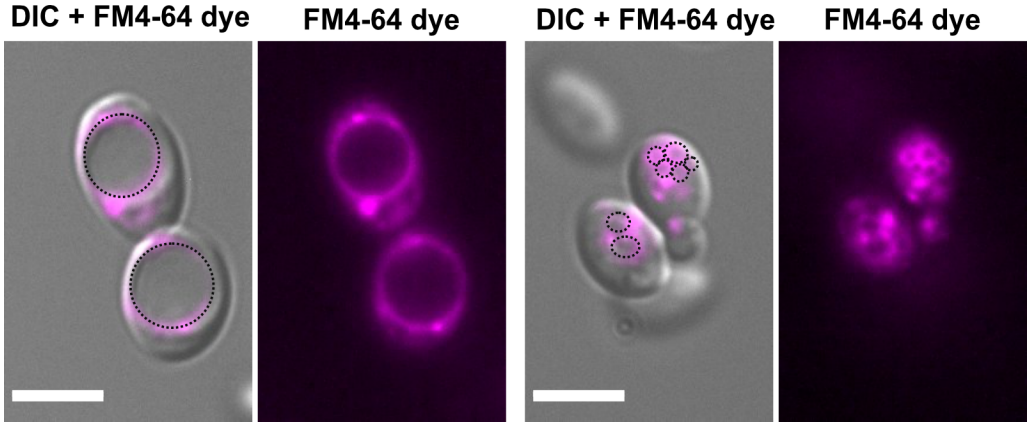

Figure 11: Fungal vacuoles come either as a single large vacuole or as multiple small vesicles depending on the cell's needs. Vacuolar membrane stained by FM4-64 is emphasized in the merged picture with dotted circles in black. Scale bars: 5 μm. (Reuter-Weissenberger *et al.*, *in press*)

the enhanced need of breakdown of cellular material that provides supplemental resources. In contrast, cells in the right panel of figure 11 display multiple smaller vacuoles suggesting that these cells are metabolically active. When cells were grown without any nitrogen source, the fraction of cells displaying a single large vacuole differed significantly between the *zcf8* mutant (39.10% ±2.01) and the wild-type reference strain (24,37% ±4.64) (Figure 12). In contrast, in the presence of ammonium sulfate, the *zcf8* mutant had less single-vacuolated cells (12.03% ±1.96). Thus, the fraction of cells that displayed a single large vacuole in the deletion mutant was more than 3-fold higher whereas overexpression *ZCF8* had no effect on vacuolar morphology as a response to changes in nitrogen availability. The results suggest that *ZCF8* is required for cellular homeostasis in *C. albicans* due to the deletion mutant being more susceptible to nutrient limitations as signs of starvation made evident by the formation of cell-filling vacuoles. It remains to be established whether the vacuolar phenotype is connected to a higher rate of vacuolar fusion or autophagy, defects in membrane recycling, or premature aging (Baars *et al.*, 2007; Li *et al.*, 2009; Aufschnaiter *et al.*, 2019). Since many of these processes rely on the acidic lumen of the vacuole, I sought to establish whether *ZCF8* alters vacuolar acidification.

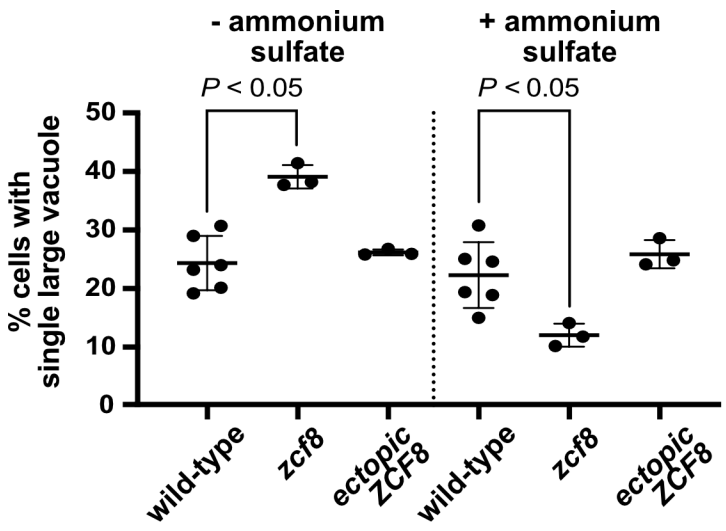

Figure 12: Vacuolar morphology in *C. albicans* depends on *ZCF8*. Plotted is the fraction of cells (%) displaying a single large vacuole ± SD. Each dot represents the mean of one experiment in which >500 cells were scored in at least three independent experiments. Statistical analysis by Mann-Whitney U test. (Reuter-Weissenberger *et al., in press*)

3.7 Vacuolar acidification in *C. albicans* is modulated by *ZCF8*

The acidic lumen of the vacuole is created by the activity of the vacuolar ATPase. Activity of the complex moves protons from the cytosol into the vacuolar lumen, thus creating the chemical basis which is vital not just for fusion and fission events. It also provides the optimal milieu for hydrolytic enzymes residing in the vacuolar lumen and the gradient over the membrane energizes many transporters and ion channels that maintain cellular homeostasis (Richards *et al.*, 2012). Therefore I sought to establish whether the vacuolar phenotype of the *zcf8* deletion mutant is based on alterations in vacuolar acidification.

To assess differences in vacuolar pH, *C. albicans* cells were evaluated again in defined medium lacking any nitrogen source or supplemented with ammonium sulfate and stained with the pH-sensitive fluorescent indicator BCECF (Figure 13). The cell-permeable molecule 2',7'-**b**is-(2-**c**arboxyethyl)-5-(and-6)-**c**arboxy-**f**luorescein **a**cetoxy**m**ethyl (BCECF-AM) ester is hydrolyzed in the vacuole by the resident esterases and the resulting BCECF is trapped in the organelle and can be used as a vacuolar marker (Boens *et al.*, 2006; Martínez-Muñoz *et al.*, 2008;

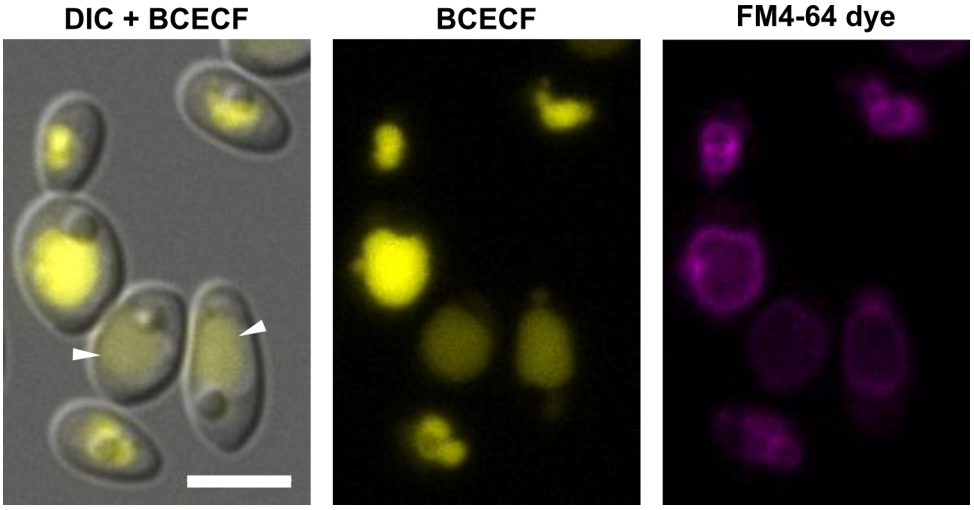

Figure 13: pH indicator BCECF visualizes vacuolar acidification by fluorescence intensity. FM4-64 staining marks vacuolar membrane inside the *Candida* cells. White arrowheads in the merged DIC point to a more acidic vacuolar lumen indicated by lower fluorescence intensity. The location of the vacuole is confirmed by FM4-64 staining. Scale bar: 5 *µ*m. (Reuter-Weissenberger *et al.*, *in press*)

Johnson *et al.*, 2010). Fluorescence intensity emitted by BCECF increases as pH increases from ~6 to ~9 (Boens *et al.*, 2006; Johnson *et al.*, 2010; Richards *et al.*, 2012). The vacuoles in figure 13 marked with a white arrowhead are, therefore, more acidic compared to the bright vacuole in the neighboring cells. While the assay does not provide absolute pH values, it allows the comparison of acidity between cell populations. Low levels of fluorescence emitted by the vacuole may indicate that the cell is catabolically more active. Flow cytometry was used to quantify the fluorescence emitted by each cell in the population. The observed distributions are shown in figure 14. This approach revealed that ectopically overexpressing *ZCF8* results in cells containing more alkalic vacuoles, while deleting *zcf8* significantly decreases the pH towards a more acidic vacuole. Therefore, vacuolar acidification changes in response to alterations in the expression of *ZCF8* regardless of nitrogen availability. Whether this response functions directly through assembly of V-ATPase or other indirect ways remains to be established. Differences in luminal pH may explain, at least in part, the vacuolar phenotype of the *zcf8* mutant as it affects several functions including storge of nutrients and maintaining homeostasis. Furthermore, other functions of the

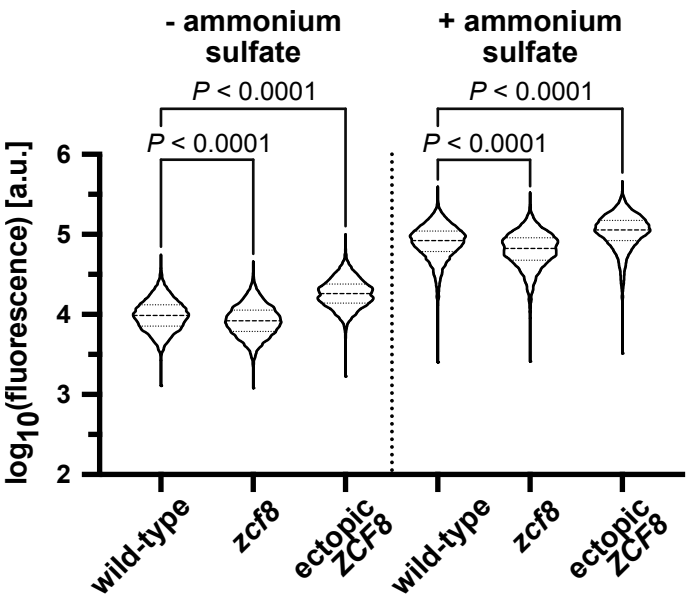

Figure 14: Vacuolar pH responses in *C. albicans* cells to alterations in *ZCF8* expression. Plotted is the quantification of fluorescence emitted by BCECF in cells grown in media either containing or lacking ammonium sulfate using flow cytometry. The median and quartiles are indicated with dashed and dotted lines, respectively. Data shown derived from four independent experiments. Statistical analysis by Mann-Whitney U test. (Reuter-Weissenberger *et al.*, *in press*)

organelle are likely to be influenced by *ZCF8* as well. The detected differences between the strains seemed to be minor although significant. However, the integrity and function of the vacuole depends heavily on the luminal pH and therefore I would not expect large differences.

3.8 Endocytosis and autophagy are not affected by *ZCF8*

As mentioned above, vacuolar acidification is a defining feature of the vacuole and essential for multiple functions of the organelle. Endocytosis, for example, is a cellular process in which extracellular substances are internalized by the cell, packed in vesicles (called endosomes), and transported to the vacuole. Another process is autophagy which is, as mentioned in the introduction, a process that enables the recycling of cytosolic proteins and organelles to provide supplemental resources as part of housekeeping and/or stress response. The final step for both pathways is the fusion of vesicles, either endosomes or autophagosomes, with the vacuolar membrane. Given that vesicle fusion relies on the luminal pH and *ZCF8* alters vacuolar acidification, I sought to examine both processes in *C. albicans*.

First, endocytosis was evaluated using the uptake of the fluorescent dye FM4-64 by the cells as a readout. The dye is not cell-permeable but lipophilic and thus integrates in the plasma membrane of the cell and can be used to trace the endocytic pathway from the membrane through endosomes to the vacuole (Vida *et al.*, 1995). It is a well-established method which has been used before in our laboratory to quantitatively analyze internalization of endocytic vesicles to the vacuole (Moreno-Velásquez et al., 2020). The *C. albicans* wild-type reference strain, a strain overexpressing *ZCF8* (“ectopic *ZCF8*”), and a *zcf8* deletion mutant strain were starved for nitrogen and incubated with FM4-64 for 10 and 20 minutes. To stop endocytosis, cells were washed with ice cold PBS and kept on ice until microscopy analyses were carried out. The assay evaluated the distribution of fluorescence in the endocytic vesicles (Figure 15A) and intensity emitted by the cell (Figure 15B). Figure 15A shows that after 10 minutes of staining several small endocytic vesicles were highlighted in the cytoplasm, while after 20 minutes the vacuolar membrane was clearly distinguishable. The distribution of fluorescence

inside the mutants was similar to the wild-type strains at both time points suggesting that internalization rate is unaffected by Zcf8p. As an alternative approach, fluorescence emitted by each cell was measured and used as a proxy to determine the rate of internalization as well as to assess the overall endocytic uptake. The data, plotted in figure 15B, indicate that neither internalization rate nor overall uptake is altered between the three strains. These results suggest that, under the experimental conditions evaluated here the regulator *ZCF8* does not affect endocytosis or fusion of endosomes with the vacuole in *C. albicans*.

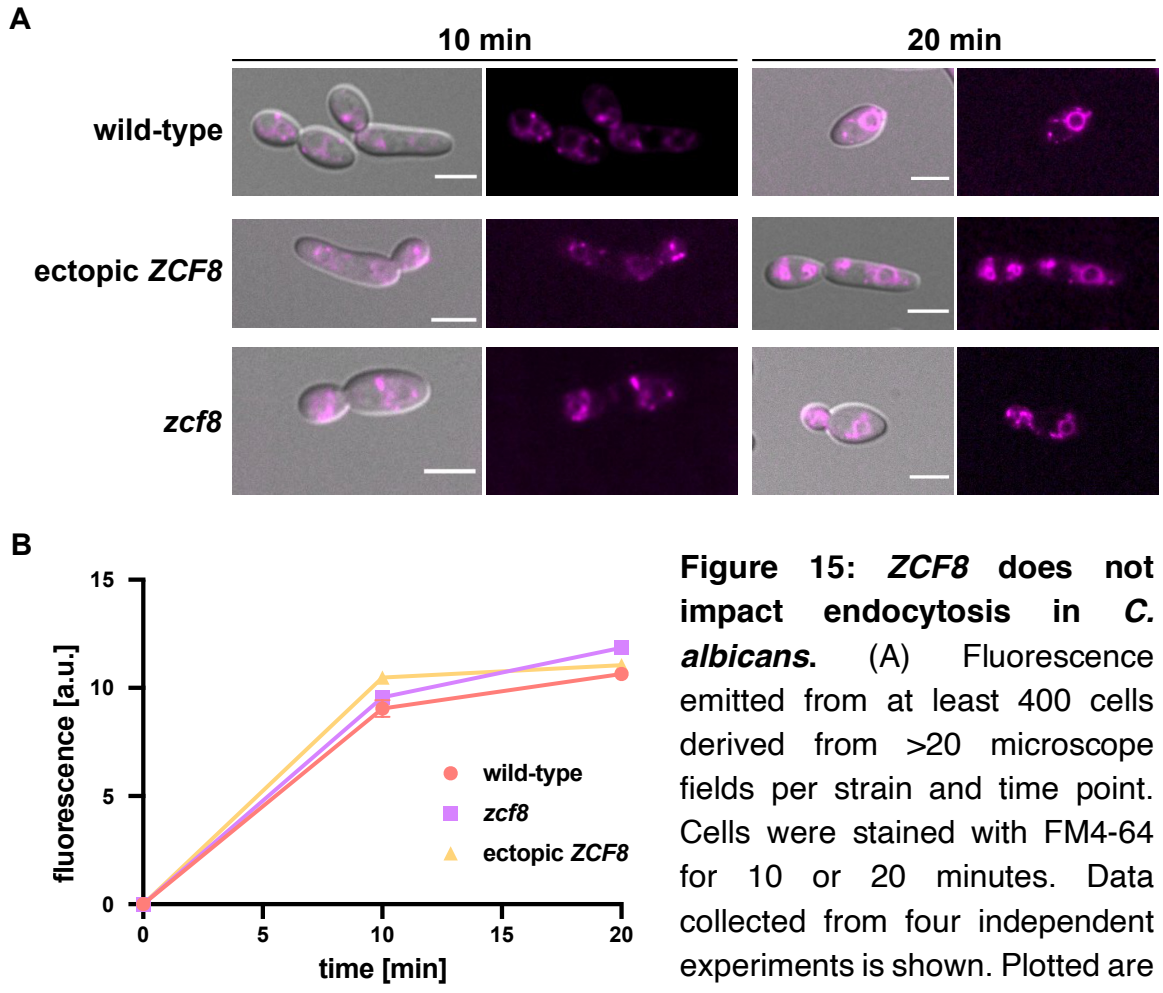

Figure 15: *ZCF8* does not impact endocytosis in *C. albicans*. (A) Fluorescence emitted from at least 400 cells derived from >20 microscope fields per strain and time point. Cells were stained with FM4-64 for 10 or 20 minutes. Data collected from four independent experiments is shown. Plotted are the means ± SD. (B) Representative images of cells stained with FM4-64 for 10 or 20 minutes. Internalization was monitored in cells from four different experiments. Scale bars: 5 µm. (Reuter-Weissenberger *et al.*, *in press*)

To evaluate whether *ZCF8* expression affects autophagy, I conducted a GFP-Atg8p assay. The assay allows to quantify the delivery of GFP-Atg8p as part of the autophagosome to the fungal vacuole by Western blotting (Torggler *et al.*, 2017). Atg8p is a well-established marker of autophagy in yeast (Delorme-Axford *et al.*, 2015; Torggler *et al.*, 2017). While its function is not clear, the protein is associated with the autophagosome (or the autophagic body to be more precise) and thus can be used as a reporter when fused to GFP or similar fluorophores. Figure 16A shows Atg8p fused N-terminally to mNeonGreen and incorporated into an autophagosome (arrowhead) in nitrogen-starved *C. albicans* cells. The unsharp fluorescence emitted by all four cells indicates free mNeonGreen in the vacuolar lumen suggesting some degree of autophagy taking place in all four cells. For Western blotting, a wild-type strain, the *zcf8* deletion mutant expressing *GFP-ATG8*, together with an untagged control strain were grown in defined media for 3 and 6 hours. Figure 16B shows that the GFP signal for both GFP-Atg8p and free GFP do not differ between the wild-type and the mutant. This shows that the abundance of Atg8p which is used to reflect autophagy is similar in the wild type

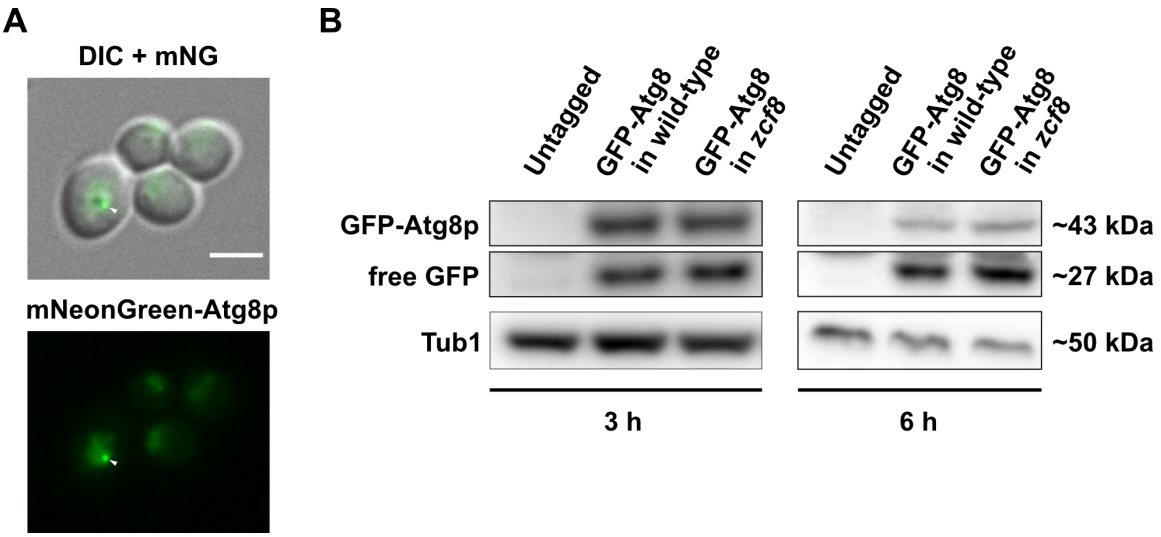

Figure 16: Autophagy acts independently of *ZCF8*. (A) Representative picture of a mNeonGreen-Atg8p incorporated into a autophagosome. The white arraw marks the distinctive autophagosome in contrast to the cloudy fluorescence emitted by free mNeonGreen in the vacular lumen. Scale bar: 5 μM (B) Western blotting of the autophagy marker GFP-Atg8p. Blotting anti-Tubulin 1 shows equal loading. (Reuter-Weissenberger *et al.*, *in press*)

and deletion mutant and, therefore, not altered by *ZCF8*. In addition, the ratio between both bands - which can be used as a readout for vacuolar degradation - is comparable between both strains suggesting no regulatory effect of *ZCF8* on autophagy.

Overall, the findings detailed in this section indicate that, under the experimental conditions employed here, neither endocytosis nor autophagy are influenced by Zcf8p in *C. albicans*.

3.9 *ZCF8* alters sensitivity to drugs targeting the vacuole

In an alternative approach to characterize the role of *ZCF8* on vacuolar biology, I tested *C. albicans'* response (in terms of growth) to the presence of the vacuole-disturbing agent nigericin or brefeldin A, a drug that impairs vesicle formation and transport. Nigericin is a K^+/H^+ ionophore that introduces additional “channels” into the vacuolar membrane which, consequently, alters vacuolar acidification and breaks down the pH gradient between cytoplasm and the organelle disrupting the function of the vacuole. It has been used to study the effects of ion perturbances, age-related processes, and autophagy in yeast (Stephan *et al.*, 2013; Jakubkova *et al.*, 2015). The motivation to test this drug on the *ZCF8* mutants was based on the hypothesis that *ZCF8* contributes to vacuolar homeostasis which relies on transporter activity energized by the proton gradient over the vacuolar membrane. Brefeldin A is a fungal metabolite that exhibits a wide range of antibiotic properties. The drug inhibits the proper formation of vesicles at the endoplasmic reticulum and transport to the Golgi apparatus which ultimately induces collapse and fusion of both organelles (Dinter *et al.*, 1998). This drug may reveal whether *ZCF8* influences vesicle-related processes associated with the fungal vacuole.

Interestingly, analysis of mutant strains grown on plates containing nigericin showed that deleting *ZCF8* rendered *C. albicans* cells resistant to nigericin (Figure 17A) while overexpressing it resulted in higher sensitivity to the drug. This result implies that *ZCF8* contributes to the maintenance of cell homeostasis in *C. albicans*. However, it remains unclear whether the phenotype is based solely on

the collapse of cellular homeostasis or on other vacuolar functions. Jakubkova *et al.* (2016) showed that defects in the vacuolar amino acid transporter Vba1p rendered *S. cerevisiae* cells resistant to nigericin. They also found that the drug induced rapid changes in vacuolar morphology (formation of single large vacuole) and pH (luminal pH increased along with acidification of the cytoplasm). These phenotypes strongly resemble those of the *zcf8* deletion mutant as shown by the morphology assay (Figure 12) and alterations in vacuolar pH (Figure 14). As for brefeldin A, the absence of the gene did not affect sensitivity while the contiguous expression reduced fungal growth in liquid media (Figure 17B). The fact that only the overexpression mutant ("ectopic *ZCF8*") showed higher sensitivity to this drug

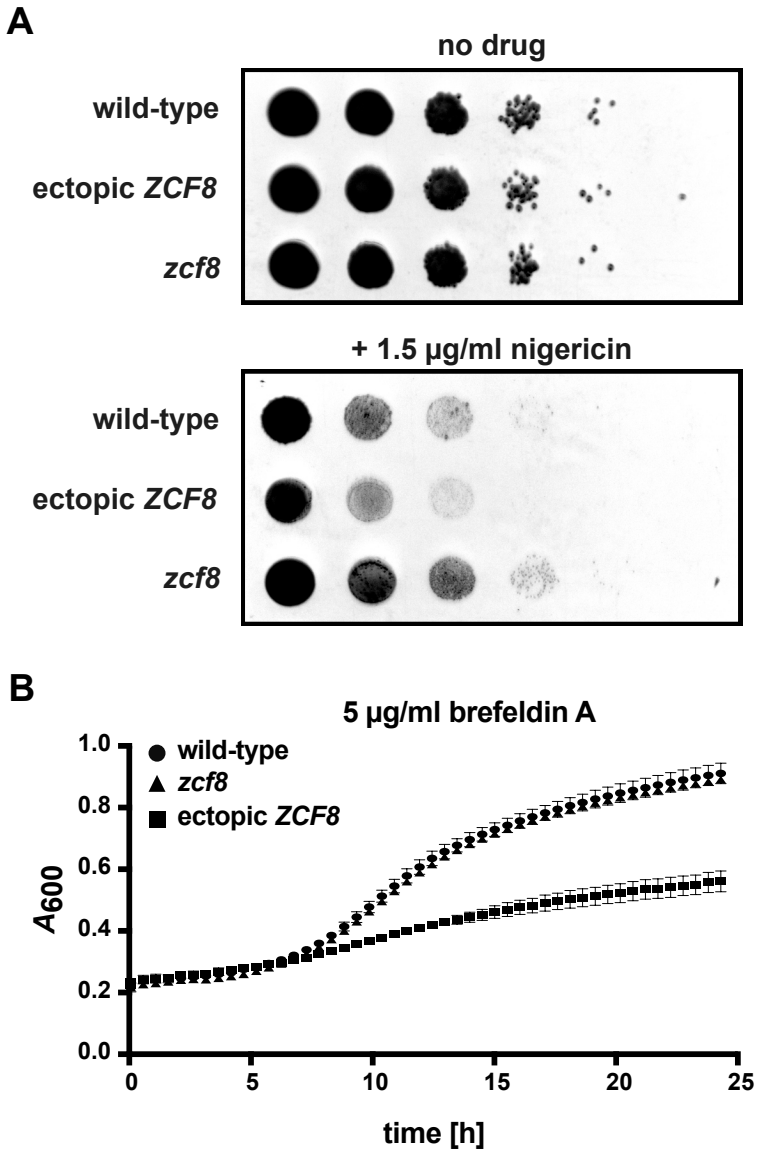

Figure 17: *ZCF8* alters sensitivity of *C. albicans* to vacuole-disturbing agent. (A) Spot assay of *Candida* mutants grown on agar plates with defined medium containing either no drug or nigericin. (B) Growth of *Candida* mutants in defined liquid medium containing brefeldin A. Plotted is the absorbance at 600 nm ± SD. (Reuter-Weissenberger *et al.*, *in press*)

suggests that indirect effects may be responsible for the phenotype, in particular, when comparing to the opposing phenotypes seen on nigericin.

3.10 *C. albicans*' transcriptional response upon nigericin treatment

Nigericin has been used to study mitochondrial ion homeostasis in *S. cerevisiae* (Kucejova *et al.*, 2005; Petrezselyova *et al.*, 2008). In a genetic screen in the fission yeast *S. pombe*, Stephan *et al.* (2013) showed that nigericin caused an extension of lifespan of the fungus by affecting vacuolar acidity and inhibiting vacuolar fission. To establish how the fungus *C. albicans* responds to this drug, I conducted a transcriptome analysis comparing *C. albicans* cells either treated with nigericin or a mock control. With the goal of minimizing secondary effects caused by the drug, cells were incubated for only 30 minutes with nigericin. To my knowledge there is no published dataset reporting the transcriptional response of any yeast to this drug.

The RNA-Seq experiment identified 188 genes with significantly altered expression in response to nigericin ($-\log_{10} p > 10$ and expression changes >2-fold (Figure 18A, Table 9). GO term searches showed that genes of "amino acid metabolism" and "transmembrane transport" were overrepresented in the dataset (Figure 16B). Genes assigned to the terms "transmembrane transport" ($P = 3x10^{-5}$) or "transmembrane transport activity" ($P = 2x10^{-5}$) were either activated (12) or repressed (18) in response to nigericin. Interestingly, of the 18 repressed genes code 7 (39%) for transporter of glucose, lactate, and glycerol. In contrast, 5 (42%) of the activated genes encoded transporter and permeases of amino acids and spermidine, a nitrogen-rich molecule. Consistently, all genes of the terms "cellular amino acid biosynthetic process" ($P = 7x10^{-9}$), "cellular amino acid metabolic process" ($P = 9x10^{-7}$), and "alpha-amino acid metabolic process" ($P = 5x10^{-6}$) were up-regulated, expect for *ADH2* that encodes an alcohol dehydrogenase. "Amino acid metabolism" was also overrepresented in the RNA-Seq dataset that identified *ZCF8*-regulated genes ($P = 9x10^{-3}$, Table 7 and 8) and some of the top target

genes regulated by Zcf8p encode transporters of amino acids or other nitrogen-rich molecules (*e.g.*, *C1_13130C*, *VBA1*) (Table 6). Surprisingly, the putative allantoate permease *DAL52* that is directly targeted by Zcf8p was down-regulated. In sum, the results indicate that to counteract the disruption of cellular physiology caused by nigericin, *C. albicans* requires access to available amino acids which seems to be more important than the availability of sugars. However, it remains unclear whether the need for amino acids is due to higher synthesis of proteins

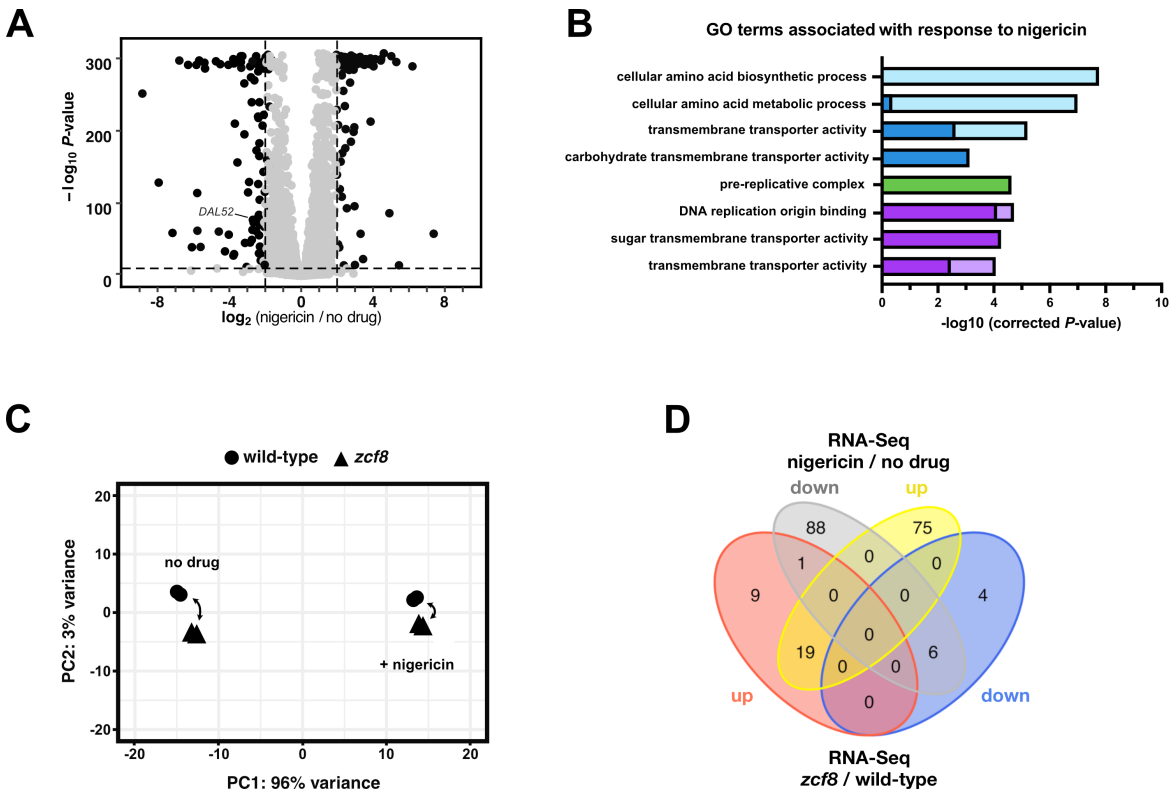

Figure 18: *Candida*'s response to nigericin on transcriptional level. (A) Volcano plot of genes differentially regulated in the presence of nigericin. Each dot represents one transcript. Significantly up- or down-regulated transcripts are in black. (B) GO term analysis of differently regulated genes. Bar colors correspond to the ontologies process (blue), component (green), and function (purple). Dark and light colors represent the fraction of transcripts that are down- or up-regulated, respectively (C) PCA to visualize the *ZCF8*-dependent transcriptional changes elicited by nigericin. Plotted data derived from samples of two independent experiments. (D) Venn diagram showing the overlap between the set of nigericin-regulated genes and up- or down-regulated transcripts following *ZCF8* deletion. (Reuter-Weissenberger *et al.*, *in press*)

(such as structural proteins to restore organelle integrity) or to buffer lowering pH in the cytoplasm.

The PCA in figure 18C visualizes an overall comparison of the responses to the drug at transcriptional level between the wild-type reference strain (Table 9) and the *zcf8* mutant (Table 10). It shows that nigericin explains a substantial portion of 96% of the variance in this experiment. However, the regulator *ZCF8* seems to participate in the response to nigericin as the transcriptome of the wild-type and the deletion mutant cluster closer together. The distance that separates the two samples in the PCA plot reflect their transcriptional differences/similarities. Therefore, the analysis indicates that the regulatory impact of *ZCF8* on the fungal biology is reduced by the drug. In fact, 19 of the 29 up-regulated transcripts in the deletion mutant were also up-regulated in response to the drug (Figure 18D). These 19 transcripts (Table 9, marked in red) are significantly enriched in genes contributing to cellular amino acid biosynthesis (*e.g.*, *ARO8*, *HIS5*, and *LYS22*) ($P = 0.00057$).

To assess the fungal response of nigericin on a cellular level, changes in vacuolar morphology were evaluated in *C. albicans* cells exposed to the drug. As mentioned in the previous section, nigericin alters vacuolar homeostasis as it introduces additional ion "channels" into the vacuole. Therefore, a *Candida* wild-type strain as well as the *zcf8* mutant were cultured in defined medium for 6 hours and stained using FM4-64 to allow visualization of the vacuolar membrane. After 30 minutes of nigericin treatment, vacuolar morphology was examined by live cell imaging. The results are presented in figure 19. The drug had no effect on vacuolar morphology of the deletion mutant. In contrast, the fraction of cells displaying a single large vacuole increased significantly in the wild-type strain exposed to nigericin. This rapid formation of single large vacuoles in wild-type cells is consistent with previous reports in *S. cerevisiae* (Jakubkova *et al.*, 2016). As for the *zcf8* deletion mutant, the fact that the ionophore nigericin had no additional

effect of the vacuole in the mutant further supports a connection between this organelle and the regulator.

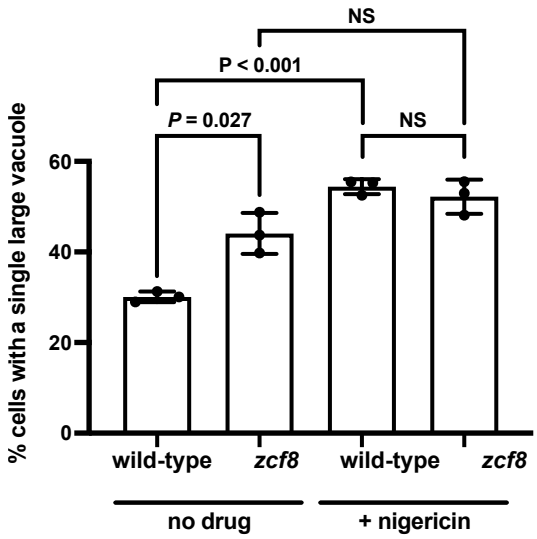

Figure 19: Altered vacuole morphology in response to nigericin. Plotted is the percentage of cells displaying a single large vacuole. Bars represent the mean ± SD of three independent experiments in which > 150 cell were scored per strain per condition. Statistical analysis by Student's t-test. (Reuter-Weissenberger *et al.*, *in press*)

Overall, the data so far suggest that the transcription regulator Zcf8p represses targets connected to vacuolar biology with consequences for morphology and acidification of this organelle. Furthermore, deletion of the gene rendered *C. albicans* cells resistant to the vacuolar-disturbing agent nigericin. The general transcriptional response to this drug is increased expression of genes related to amino acid metabolism and transport - a trait that seems to be targeted (repressed) by Zcf8p. Consistent with this, the drug reduced the regulatory impact of Zcf8p on fungal biology. Moreover, nigericin had no significant effect on vacuole morphology in the *zcf8* mutant. Collectively, all these findings characterize this transcription regulator as a repressor of vacuolar proteins that may contribute to some aspects of amino acid metabolism.

3.11 Zcf8p modulates host interactions in a vacuolar dependent manner

As previously mentioned, the reason to investigate the novel transcription regulator *ZCF8* in more detail were two striking opposing phenotypes of *C. albicans*

mutants in mice: While the deletion of the gene increased fungal persistence in an oropharyngeal infection model (OPC) (Meir *et al.*, 2018) the same mutation reduced fungal fitness in a gut colonization model (Böhm *et al.*, 2017). Additionally, Finkel *et al.* (2012) reported that the *zcf8* mutant showed reduced adherence of *C. albicans* to silicone substrates. Therefore, I hypothesized that the phenotypes of the *zcf8* deletion mutant in the mouse model could be explained through altered adhesion to mucosal surfaces.

To test this idea *in vitro*, the attachment of the fungus to intestinal and oral epithelial cells was assessed (Figure 20A). The cell line TR146 was used as a representative of the oral epithelium as it is derived from a buccal carcinoma (Rupniak *et al.*, 1985). The Caco-2 cell line is a traditional and commonly-used cell line that derived from colorectal carcinoma and represents an epithelium of the intestinal tract (Pinto *et al.*, 1983). However, in the gut, *C. albicans* cells do not directly interact with the intestinal epithelium as it produces a thick mucus layer that shields it from colonizing microbes (Böhm *et al.*, 2017; Eckstein *et al.*, 2020). Therefore, I included the mucus-secreting intestinal cell line HT-29-MTX-E12 (Navabi *et al.*, 2013). All three cell lines were incubated with a wild-type *C. albicans* strain and the *zcf8* deletion mutant for 1 hour. After extensive washing to remove non-adhered cells the number of adhered fungal cells was determined either by plating or microscopy. I found that the *zcf8* deletion mutant adhered significantly more to the oral epithelia cells (Figure 20B). Strikingly, while no differences in adherence were observed for the Caco-2 intestinal cells in presence of the mucus the deletion mutant adhered significantly less. These findings reflect the opposing phenotypes reported in the mouse models of oral infection (Meir *et al.*, 2018) and gut colonization (Böhm *et al.*, 2017), and altered adherence may provide one explanation for that. It seems likely that this phenotype is based on altered filamentation of the mutant as Zcf8p targets well-established regulators of yeast-to-filament transition (*e.g.*, *BRG1* and *RFG1*).

The results in this chapter link Zcf8p to two fungal traits: On the one hand, the regulator controls key properties of the fungal vacuole (*e.g.*, vacuolar morphology and acidification) (Figure 12 and Figure 14); and on the other hand, it alters fungal adhesion to mucosal surfaces (oral vs. intestinal epithelium) (Figure 20B). The

question is whether the *in vitro* characteristics of the vacuole are linked with the *in vivo* phenotypes.

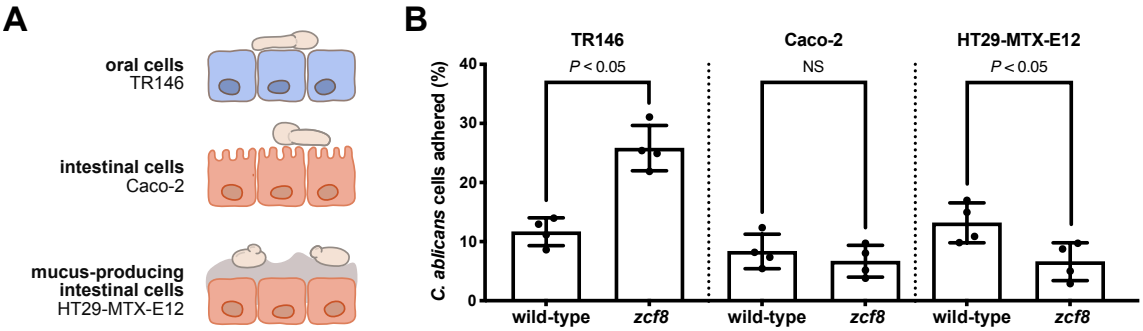

Figure 20: Zcf8p modulates *Candida* adherence to host epithelial cells. (A) Diagram illustrating the three epithelial cell systems employed to probe fungal interactions. (B) Adhesion of *C. albicans* to intestinal and oral epithelial cells. Each dot represents the percentage of adhered cells in one of four independent experiments. Bars represent the mean ± SD. Statistical analysis by Mann-Whitney U test. (Reuter-Weissenberger *et al.*, *in press*)

In an approach to answer this question, I evaluated whether disrupting the fungal vacuole and/or vacuolar functions had any consequences on adherence of *C. albicans* to epithelial cells. Wild-type *C. albicans* strain and the *zcf8* deletion mutant were incubated for 30 minutes with nigericin to disrupt the fungal vacuole. A rather short period of time was chosen as short exposure times had been previously shown to alter vacuolar function in yeast (Jakubkova *et al.*, 2016). Washed cells were transferred to a confluent layer of TR146 cells and incubated at 37°C in a humidified incubator. In contrast to the above-mentioned adherence assay illustrated in figure 20B, nigericin-treated cells were incubated for 2 hours on TR146 cells. Figure 21A shows that the enhanced adherence of the *zcf8* deletion mutant to the oral epithelial cells vanished when the fungus was treated with the vacuole-disturbing agent nigericin. Therefore, a functional vacuole seems to be crucial for *C. albicans*' adhesion to host epithelial cells.

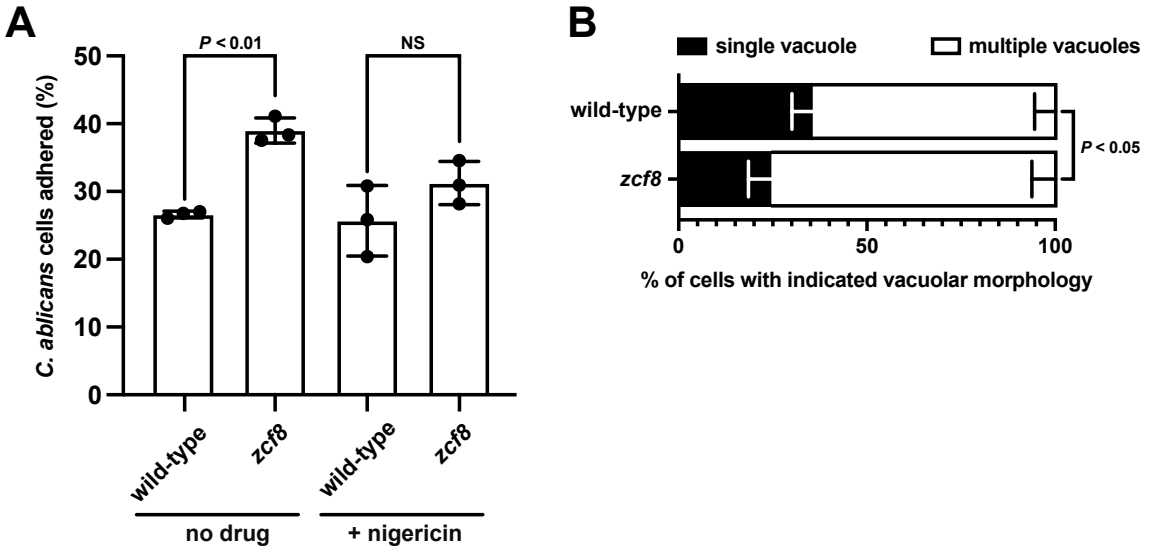

Figure 21: Increased adherence of *zcf8* mutant cells to oral epithelial cells requires an intact vacuole. (A) *C. albicans* were either treated with nigericin or a mock control and added to oral epithelial cells to evaluate adhesion. Bars represent mean ± SD. Statistical analysis by Mann-Whitney U test. (B) Plotted is the percentage of fungal cells adhered to TR146 cells displaying either a single vacuole or multiple vacuoles. Bars represent means ± SD of three independent experiments in which at least 150 cells were scored per strain and condition. Statistical analysis by Student's t-test. (Reuter-Weissenberger *et al.*, *in press*)

A second approach to link the *in vivo* and *in vitro* phonotypes focused on vacuolar morphology during fungal-host interplay. *Candida* cells were stained using FM4-64 to highlight the vacuolar membrane. After incubating the fungal cells on TR146 cells for 1 hour at 37°, non-adhered *C. albicans*-cells were removed by extensive washing. Live cell imaging allowed the characterization of the fungal vacuole when *Candida* cells were in direct contact with oral epithelial cells. The data is illustrated in figure 21B and shows that the number of vacuoles per cell differed between deletion mutant and wild-type strain. Mutant cells, which tent to adhered better to oral epithelium, displayed significantly fewer single vacuoles (24.72% ±6.33) than wild-type cells (35.51% ±5.56). In fact, vacuolar morphology matches the phenotype when the mutant was cultured in medium supplemented with ammonium sulfate as a nitrogen source (Figure 12). This is coherent with the fact that the medium used to culture epithelial cells contained nutrients such as

non-essential amino acids. The data shows, however, that *ZCF8* alters vacuolar homeostasis in the fungus.

The results obtained by both assays indicate, therefore, that the role of Zcf8p on adherence in *C. albicans* relies, at least in part, on the integrity and functionality of the fungal vacuole.

3.12 *In vitro* translocation and cytotoxicity are independent of *ZCF8*

I established in the previous section that Zcf8p modulates adherence of *C. albicans* to epithelial cells in a vacuole-dependent manner. Adhesion to mucosal surfaces is a first central and necessary step for host colonization by the fungus. However, I sought to investigate whether other non-commensal traits such as translocation and/or cell damage are also influenced by Zcf8p. *C. albicans* can translocate through the intestinal epithelium under particular conditions (*e.g.*, imbalances of microbiota or compromised immune system) which provide the basis for bloodstream infections (Brown *et al.*, 2012; Williams *et al.*, 2013; Allert *et al.*, 2018). To test whether Zcf8p participates in any of the stages of translocation, I conducted an *in vitro* assay on C2BBe1 cell, a subclone of the intestinal epithelial cell line Caco-2 (Peterson *et al.*, 1992). In addition, the release of LDH was quantified as a readout for cellular damage exhibited by the deletion mutant. Both assay were performed in the laboratory of Prof. Dr. Bernhard Hube at the HKI in Jena, Germany, under the supervision of Dr. Stefanie Allert and Dr. Toni Förster following their protocol (Allert *et al.*, 2018). Furthermore, **t**rans**e**pithelial **e**lectrical **r**esistance (TEER) of the confluent epithelial layer was measured before and after infection using a volt-ohm meter (WPI, USA) to test integrity of the epithelium. Reduction of impedance (~ electrical resistance) in TEER upon infection reflects the potential of the strain to translocate through the epithelium and thus perforate the otherwise intact monolayer. Impedance of an intact monolayer ranges from 2500 to 3500 ohm. In the first experiment the impedance of all prepared epithelial monolayers stayed below this range indicating that the monolayer was not intact.

Therefore, I excluded the entire TEER data from the analysis. For the translocation assay, the C2BBe1 cells were challenged with a *C. albicans* wild-type strain and the *zcf8* deletion mutant. After 24 hours, the hyphae that grew through the epithelia from the lower side of the insert were detached, the fragments from the basolateral chamber of the trans-well system were recovered, and plated on YPD. The number of colonies of the *zcf8* deletion mutant relative to the recovered wild-type cells is plotted in figure 22 which shows that Zcf8p or its regulation upon the vacuole influences *in vitro* translocation. However, the results of the assay were not consistent as shown by the large deviation in colony numbers.

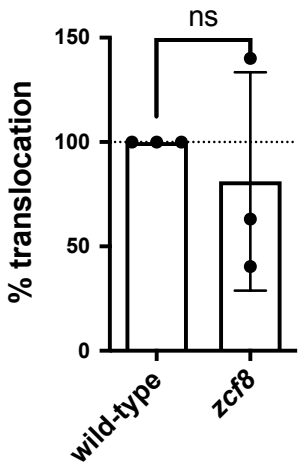

Figure 22: *In vitro* translocation through C2BBe1 cells acts independently of *ZCF8*. Each dot represents the number of *C. albicans* colonies grown in one independent experiment as a proxy for translocation. Plotted is the mean colony number ± SD relative to *C. albicans* wild-type. Three independent experiments are considered. Statistical analysis by Wilcoxon matched-pairs signed rank test.

Cell cytotoxicity of the *zcf8* deletion strain was evaluated by quantifying **l**actate **d**e**h**ydrogenase (LDH) release from the epithelium challenged with C. *albicans*. All animal cells produce LDH to convert lactate to pyruvate. The enzyme is very stable and accumulates after damage or death of the cell in the extracellular matrix. Using a colorimetric assay allows to measure LDH release and to use it as a proxy for cell damage. The epithelial cell lines C2BBe1, TR146 cells, and a mix of HT29-MTX-E12 and C2BBe1 in the ratio 30:70, respectively, were incubated with a wild-type strain and the *zcf8* deletion mutant. Co-culturing HT29-MTX goblet cells and Caco-2 enterocyte in a 30:70 ratio produces a confluent monolayer fully covered by mucus which is believed to mimic the human intestinal epithelium (Wikman-Larhed *et al*., 1995). Untreated epithelial cells served as negative control ("no *Candida*") whereas cells treated with 5% Triton-X 100 were used to determine the

maximal possible release of LDH (100%). Figure 23 shows that the *C. albicans* wild type and *zcf8* deletion mutant exhibited a similar extent of epithelial damage indicating that *ZCF8* did not impact cytotoxicity to the tested epithelia *in vitro*. Although it did not reach statistical significance, the deletion mutant showed a trend towards reduced damage of the oral epithelia which would be consistent with *ZCF8* playing a role in interactions with this particular mucosa.

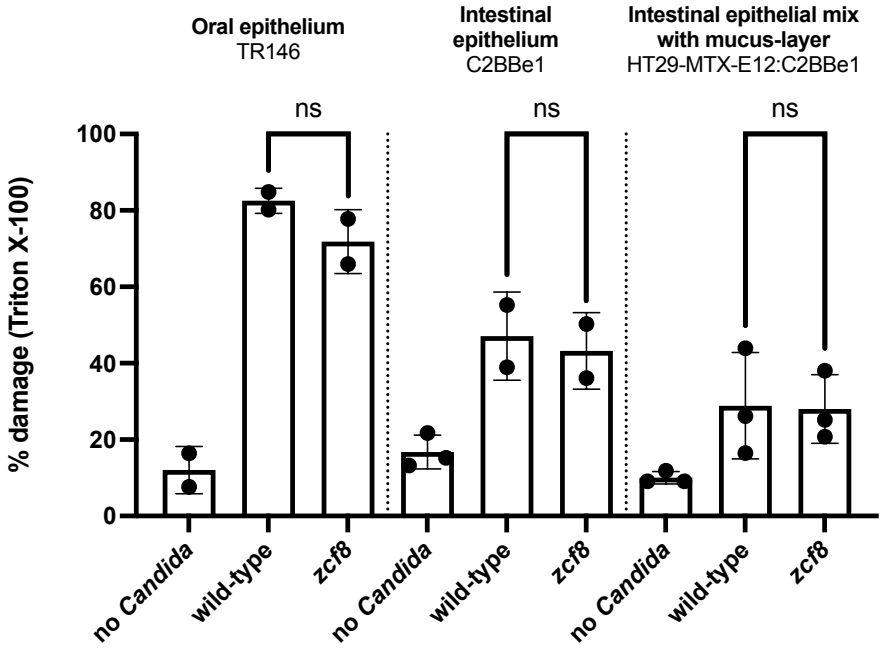

Figure 23: Cell damage remains unaffected by *ZCF8*. Each bar represents the mean LDH release ± SD relative to the epithelial cells treated with Triton X-100. "no *Candida*" are uninfected intact epithelial cells. Each dot represents an independent experiment. Statistical analysis by Mann-Whitney U test.

Overall, the evaluation on translocation and *C. albicans*-dependent epithelial damage determined that *ZCF8* does not have a major effect on either virulence traits independently of the tested epithelium.

3.13 *ZCF8* is a negative regulator of filamentation on host tissues

The results so far suggest that *ZCF8* regulates aspects of vacuolar biology, modulates fungus-host interaction, and is not linked to virulence traits such as translocation or epithelial damage. Nevertheless, the question on how this regulator determines host colonization remains to be established. As mentioned earlier, *C. albicans* interacts with host tissues in different morphologies, and the filamentous form has been described to play a major role during fungal colonization (Gow *et al.*, 2012). In fact, deleting *ZCF8* reduced *Candida* fitness in the murine gut (Böhm *et al.*, 2017) an environment which does not tolerate filamentation well (Pérez, 2019). Moreover, colonies of the *zcf8* deletion mutant formed wrinkles - a proxy for filamentation - when grown under conditions that normally do not induce hyphal growth in *C. albicans* (Böhm *et al.*, 2017). Strikingly, mutations in genes that encode structural components of the fungal vacuole often lead to defects in filamentation in *C. albicans* (Theiss *et al.*, 2002; Veses *et al.*, 2008). Therefore, one explanation for the fitness defect of the deletion mutant might be alterations in filamentation.

Thus, I investigated whether deleting *ZCF8* changed *Candida*'s morphology during colonization of the murine tongue. Histology section of murine tongues infected with either wild-type *Candida* or the *zcf8* deletion mutant (Figure 24A and 24B) were used to (a) quantify the fraction of oval-shaped "yeast" cells as opposed to "filaments" and to (b) determine the average length of the filaments. In contrast to the intestine, filaments are a prominent form of *C. albicans* in the oral cavity (Meir *et al.*, 2018). The proportion of *C. albicans* cells found as filaments increased in the mutant (Figure 24C) indicating that *ZCF8* modulates this trait *in vivo*. This is also supported by the ChIP-Seq data because well-established regulators of yeast-to-filament transition are targeted by Zcf8p (*e.g.*, *BRG1* and *RFG1*) (Table 6). However, the average hyphae length was not impacted by *ZCF8* activity (Figure 24D). Taken together, the results suggest that increased persistence of the mutant during oral infection and the fitness defect are based on an enhanced filamentation

of the deletion mutant. Filamentation is required for fungal interaction of the oral tissue and promotes proliferation of *Candida* as a commensal on this mucosa (Park *et al.*, 2004; Meir *et al.*, 2018). For intestinal colonization, however, the round yeast

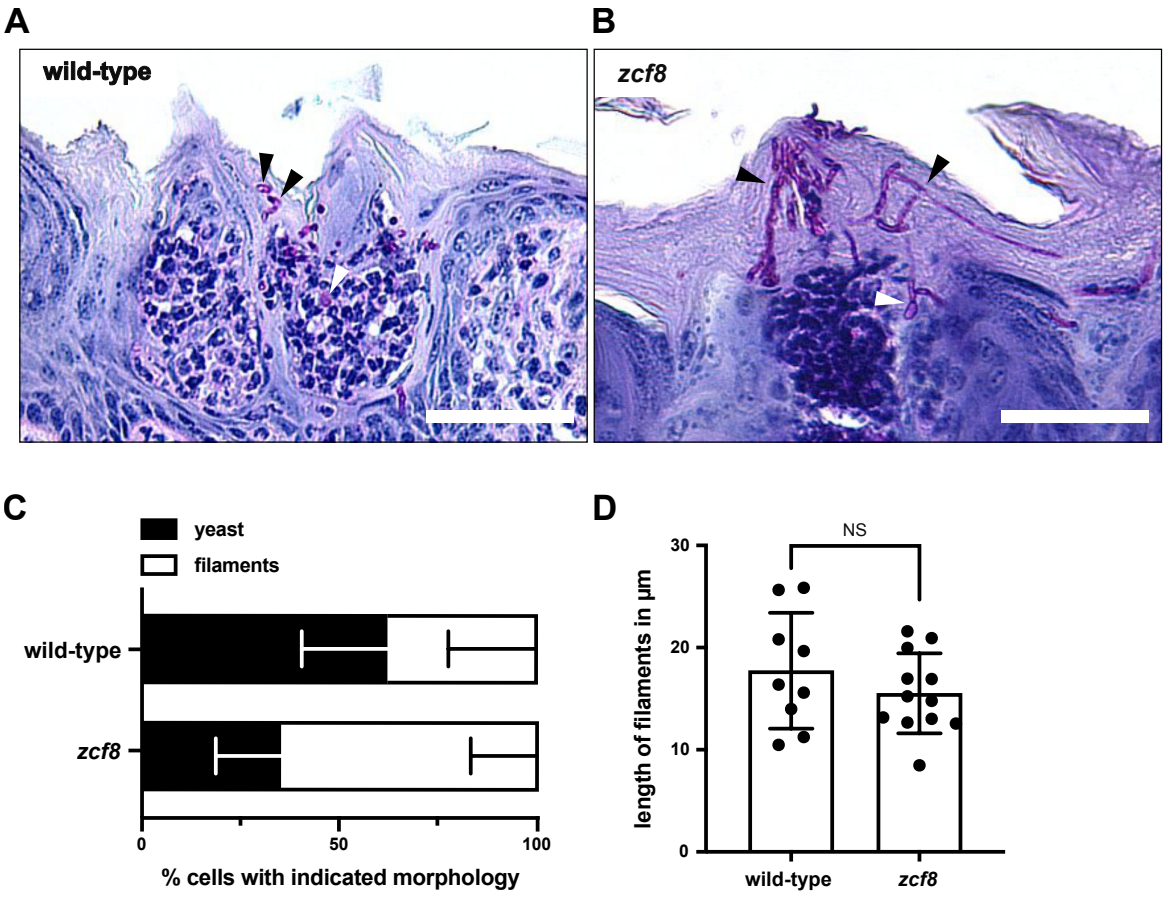

Figure 24: *ZCF8* alters *Candida* morphology during infection of the murine tongue. (A) and (B) show a representative image of PAS-stained sections of infected tongue tissue. *Candida* (purple) resides either in its oval-shaped yeast form (A, arrowhead) or as long filaments (B, arrowhead). Scale bars: 100 µm. (C) Proportion of fungal cells colonizing the murine tongue as "yeast" or "filaments". Cells were considered filamentous when length exceeded twice their diameter. At least 35 fungal cells were evaluated per strain and mouse. Bars represent the mean ± SD. Statistical analyses using the Mann-Whitney U test were carried out to infer significant differences. (D) Length of *Candida* filaments in infected tongues. Plotted is the average filamentation length in µm at each focus of infection (*e.g.*, A or B). Each dot represents one focus of infection. Samples were taken from at least four mice. Bars represent mean ± SD. Statistical analysis by Mann-Whitney U test. (Reuter-Weissenberger *et al.*, *in press*)

form is preferred as it attaches better to the mucus (Böhm *et al.*, 2017). Therefore, *ZCF8* acting as a repressor of filamentation during host interaction could explain the opposing fitness phenotypes in the oral and intestinal mucosae (Figure 25).

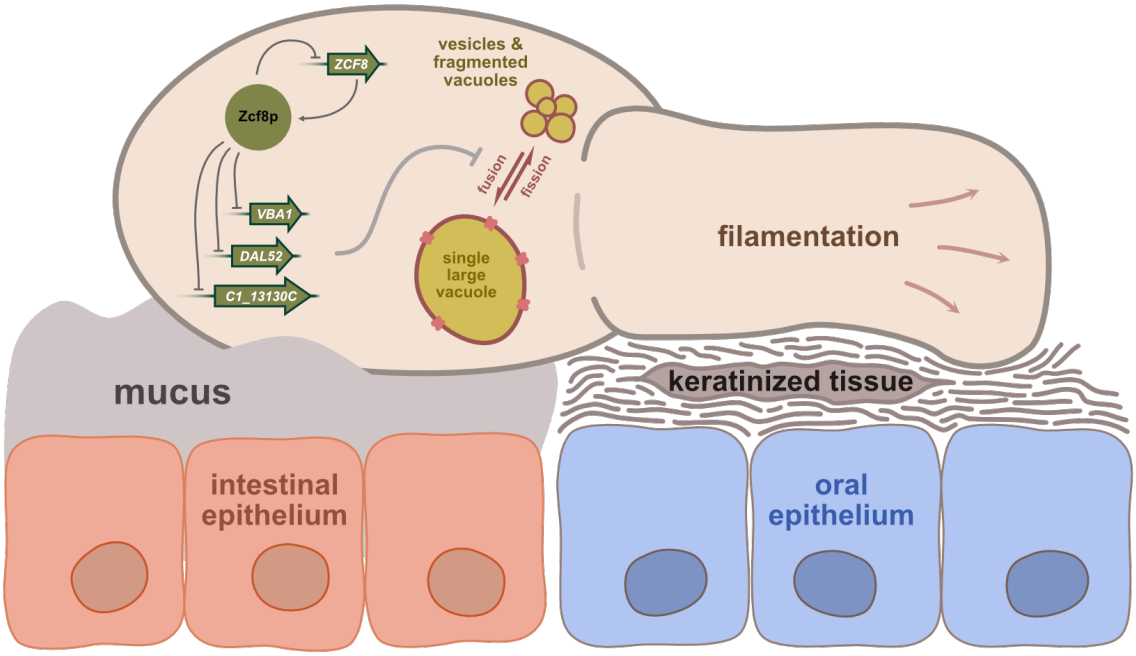

Figure 25: Model depicting *ZCF8*'s role on *C. albicans*-host interplay. Zcf8p-regulated products targeted to the vacuole impinge upon the morphology of the organelle (*i.e.* presence of a single large vacuole or smaller, fragmented compartments), and subsequently on *Candida* attachement to mucosal surfaces. The yeast form of the fungus attaches better to intestinal mucus (Böhm *et al.*, 2017) whereas the filamentous form adheres more efficiently to oral cells (Meir *et al.*, 2018). (Reuter-Weissenberger *et al., in press*)

4 Discussion

4.1 *ZCF8* regulates vacuolar properties in *C. albicans*

The research performed throughout this thesis has been primarily aimed to uncover the role(s) of the transcription regulator *ZCF8* in the human-associated fungus *C. albicans*. Several lines of evidence suggest that the regulator - a determinant of *C. albicans* colonization on mammalian epithelial cells - governs multiple vacuole-associated traits.

Numerous gene targets regulated by Zcf8p are connected to the fungal vacuole. Of all ORFs identified by the ChIP-Seq approach (~50) about a quarter of them had roles connected to vacuole or intracellular vesicle trafficking a process closely associated with the fungal vacuole (Rollenhagen *et al.*, 2020). Furthermore, some of these genes such as *VBA1, CPS1,* and *DAL52* were differentially regulated upon deletion or overexpression of *ZCF8* (Figure 8A and 8B). Furthermore, I carried out additional experiments focusing on the vacuolar properties altered in the *zcf8* deletion mutant strain: When *C. albicans* cells were grown in defined medium lacking any nitrogen source or supplemented with ammonium sulfate, vacuolar morphology as well as vacuolar acidification differed significantly between the mutant and the wild-type strains (Figure 12 and 14). Vacuolar morphology is dictated by fission and fusion events (Li and Kane, 2009), and given that both events rely on vacuolar pH, it is likely that the morphology phenotype is a consequence of changes in luminal acidification affected by Zcf8p. However, the mechanism by which the regulator influences vacuolar acidification remains to be established. Nonetheless, deleting *ZCF8* rendered *C. albicans* cells resistant to nigericin a drug that disrupts vacuolar functions (Jakubkova *et al.*, 2016). Moreover, *ZCF8* has been characterized to negatively regulate fungal filamentation (Böhm *et al.*, 2017) - a process that depends on a functional vacuole (Gow, 1997; Veses *et al.*, 2008; Richards *et al.*, 2010). Therefore, it is plausible that Zcf8p

modulates key properties of the vacuole which influence luminal acidification and, thereby, maintains vacuolar homeostasis in *C. albicans*.

While multiple proteins are known to be involved in vacuole inheritance, dynamics, and vacuole-related biochemical processes (Richards *et al.*, 2010), so far only a few transcription regulators have been shown to regulate this organelle. In a systematic approach aimed at characterizing factors necessary for vacuole fission in *S. cerevisiae*, Michaillat et al. (2013) identified 133 mutants with strong defects in vacuole fragmentation. Only three of those 133 genes, *MOT3, PDR8* and *UME6*, encode known transcription regulators. Mot3p represses genes needed for ergosterol biosynthesis, a process required for multiple functions of the vacuole such as homotypic fusion (Klionsky *et al.*, 1990; Hongay *et al.*, 2002). Its ortholog in *C. albicans*, *CAS5*, is crucial for cell cycle dynamics and cellular response to cell wall stress caused by the antifungal drug caspofungin (Xie *et al.*, 2017; Heredia *et al.*, 2020). Pdr8p is involved in pleiotropic drug resistance (Hikkel *et al.*, 2003). It was shown that *S. cerevisiae MOT3* or *PDR8* deletion mutants grew poorly on alkaline (Hongay *et al.*, 2002) or acidic media (Hikkel *et al.*, 2003), respectively, indicating that the yeast cells failed to maintain a neutral intracellular pH due to defective vacuoles (Klionsky *et al.*, 1990). Ume6p, the third regulator identified to have strong effects on vacuolar fragmentation, negatively regulates autophagy in *S. cerevisiae* a process tightly linked to functions of the fungal vacuole (Bartholomew *et al.*, 2012; Delorme-Axford *et al.*, 2018). Its ortholog in *C. albicans* promotes hyphal formation as its overexpression was shown to stimulate the generation of vacuolated sub-apical compartments in filamenting cells which is proposed to support apical extension and thus hyphal growth (Palmer, 2010). Although Ume6p has been linked to the fungal vacuole, it remains to be established whether it directly controls the expression of any vacuolar component in *Candida*. Another set of transcription regulators identified to regulate vacuolar biology in *S. cerevisiae* are Fkh1p and Fkh2p (Ghavidel *et al.*, 2018). Both Forkhead Box proteins bound upstream of the *VMA6* and *VMA8* genes which encode subunits of the vacuolar ATPase required for vacuolar acidification. *C. albicans* harbors a single Forkhead Box protein, Fkh2p, which does not appear to regulate transcription of any *VMA* gene. Conversely, the *Candida* Fkh2p promotes the

expression of hyphae-specific and pathogenesis-related genes (Bensen *et al.*, 2002; Greig *et al.*, 2015). Therefore, Zcf8p represents one of few transcription regulators that have been shown to control vacuole-related functions in *C. albicans*.

The fact that vacuole physiology is regulated by *ZCF8* a gene present only in the *Candida* clade instead of by a regulator broadly distributed and conserved throughout fungi may sound counterintuitive. However, the regulator might be an example of circuit “rewiring”. In fact, rewiring of transcriptional networks, at least in ascomycete yeast, seems to be a common phenomenon (Habib *et al.*, 2012; Johnson, 2017; Nocedal *et al.*, 2017). Transcription rewiring describes genetic changes in the connections between a regulator and its target genes (Johnson, 2017). In recent years, multiple studies have suggested that the connection between a transcription regulator and a target gene in one organism is probably not preserved in a second closely related species (*e.g.*, last common ancestor 70 - 300 million years ago) (Habib *et al.*, 2012; Johnson, 2017; Nocedal *et al.*, 2017). One example is the regulator Ndt80p which is conserved across a large group of fungal species including *S. cerevisiae and C. albicans* in which it controls meiosis and biofilm formation, respectively (Xu *et al.*, 1995; Nobile *et al.*, 2012). Nocedal *et al.* (2017) showed that only 3 to 12% of the connections between Ndt80p and its target genes are preserved in the two species. Thus, extensive rewiring may explain the apparent lack of a conserved regulator of vacuolar functions amongst fungal species. The few regulators known to act on this organelle in *S. cerevisiae* or *C. albicans* established new genetic connections (*e.g.*, *CAS5*, *FKH2*), are of unknown function, or are absent in the other species (*e.g.*, *PDR8*, *ZCF8*). However, despite the high frequency of transcriptional rewiring, the overall pattern of gene expression - *i.e.* the output of a program - remains relatively stable (Johnson, 2017). A study, which examined transcription networks controlling biofilm formation in *Candida* species, showed that rates of biofilm formation in *C. albicans* and *C. parapsilosis* were rather similar despite the fact that only three of the seven master transcriptional regulators controlling this process in *C. albicans* were also required for biofilm formation in *C. parapsilosis* (Holland *et al.*, 2014; Mancera *et al.*, 2021).

Therefore, transcriptional rewiring provides one explanation for the apparent lack of a conserved regulator of vacuolar physiology.

4.2 *ZCF8* modulates adhesion to host cells and yeast-to-filament transition

The ability of *C. albicans* to adhere to mucosal surfaces is crucial for host colonization. When adherence of fungal cells was probed on multiple epithelial cells, representing either the oral cavity or the intestine, deletion of *ZCF8* resulted in an increased attachment of the fungal cells to the oral epithelial cells while it reduced adherence to the intestinal epithelial cells (Figure 20B). The former result is consistent with a previous study that found that the *zcf8* mutation reduced adherence of *C. albicans* to silicone surfaces *in vitro* (Finkel *et al.*, 2012). The results presented in this thesis show that the deletion mutant formed a larger proportion of filamenting cells *in vivo* (Figure 24B and 24C). Additionally, genome wide protein-DNA interaction data reported in this work identified multiple regulators of yeast-to-hyphae transition (*e.g.*, *BRG1* and *RFG1*) and of cell adhesion (*e.g.*, *AAF1* and *WOR4*) as targets of Zcf8p (although, there is no evidence of changes in transcription levels in any of those ORFs in the RNA-Seq data). One explanation for the opposing adhesion phenotypes might connected those phenotypes to the status of fungal vacuole given that Zcf8p seems to regulate aspects of vacuolar biology. In fact, multiple studies have demonstrated that mutations in genes that encode major structural components of the vacuole often lead to defects in *C. albicans* filamentation (Holmes *et al.*, 1988; Biswas *et al.*, 2003; Biswas *et al.*, 2005; Veses *et al.*, 2008). Thus, it is plausible that deleting *ZCF8* impinges (a) directly on fungal morphology or (b), more likely, in a vacuole-dependent manner which ultimately dictates the attachment of *C. albicans* cells to different mucosal surfaces.

This raises the question of how vacuoles can alter filamentation and cell surface of *C. albicans* cells with consequences for fungal adhesion. Several studies indicate that mutations affecting vacuole function, biogenesis, and inheritance lead

to defects in fungal virulence (Veses *et al.*, 2008; Palmer, 2011; Raines *et al.*, 2013; Olsen, 2014; Khandelwal *et al.*, 2016). In most cases, attenuated virulence of the *C. albicans* mutant was traced back to defects in hypha development. Formation of the germ tube, *i.e.* emerging hyphal evagination upon hyphal induction (Gale and Berman, 2012), involves fundamental enlargement of the vacuole to push the cytoplasm towards the newly developing hyphae (Gow, 1997). Furthermore, the vacuole regulates fungal cell-cycle during hyphal growth as the volume of the organelle is critical for G1 arrest and re-entry into the cell cycle (Veses *et al.*, 2008; Sudbery, 2011). In support of this, multiple studies reported genes that encode kinases and proteins involved in protein sorting to affect vacuole inheritance and translocation with consequences for hyphal development (Bruckmann *et al.*, 2001; Augsten *et al.*, 2002; Cornet *et al.*, 2005; Poltermann *et al.*, 2005; Franke *et al.*, 2006). However, the function of the V-ATPase seems to be of outstanding importance for filamentous growth as several genes that encode subunits of the complex (*e.g.*, *VMA2* ,*VMA3*, *VMA5*) have been identified to be critical for hyphae formation (Braun *et al.*, 2005; Rane *et al.*, 2013, 2014; Zhang *et al.*, 2017; Kim *et al.*, 2019). In agreement with this, the proton pump provides the chemical basis for vacuolar membrane fusion and fission events enabling the vacuole to adapt its morphology (Li and Kane, 2009). As for the transcription regulator *ZCF8*, the results presented throughout this thesis show that the protein controls vacuolar properties such as vacuolar fusion and fission suggesting that the *ZCF8*-dependent vacuolar homeostasis explains the filamentation and adhesion phenotype of the mutant (Figure 25).

The results presented in this work establish that *ZCF8* is a negative regulator (repressor) of filamentation on murine oral tissue. The associated signaling pathway, however, remains to be fully elucidated. Morphogenesis in the fungus is promoted mainly by the cAMP **p**rotein **k**inase **A** (PKA) and the **m**itogen-**a**ctivated **p**rotein **k**inase (MAPK) pathway although other pathways are known to regulate morphogenesis in certain environmental conditions (Basso *et al.*, 2018). Depending on specific environmental factors (*e.g.*, ambient pH, nutrient availability, or the presence of serum), receptors in the plasma membrane or in the cytoplasm start signaling cascades that lead to the activation of transcription factors such as

Efg1p, Flo8p, Tup1p, or Ume6p that form transcriptional circuits influencing the expression of hypha-associated genes (Basso *et al.*, 2018). Therefore, it is likely that Zcf8p works together with other regulators as part of a network that orchestrate filamentation in *C. albicans*. While upstream factors that control the expression of *ZCF8* remain unknown, several genes that are bound by Zcf8p encode transcription regulators of the cAMP-PKA pathway such as *BRG1*, *TEC1* and *NRG1*. In addition, two more targets of Zcf8p, *RFG1* and *NRG1*, are well-known negative regulators of hyphal induction (Kadosh and Johnson, 2001, 2005). Both repressors are known targets of the temperature-sensitive transcriptional network formed by Sfl1p and Sfl2p that antagonistically control morphogenesis in *C. albicans* and, moreover, are required for full pathogenesis and virulence (Znaidi *et al.*, 2013). However, regulation of morphogenesis in the fungus is a complex process and the fact that none of these ORFs showed changes in their transcription level in the RNA-Seq data implies that Zcfp8 plays a minor role in regulating those proteins, if any. Therefore, further studies are needed to shed light on the mechanisms through which Zcf8p regulates filamentation in *C. albicans*.

An environmental factor that likely influences the *ZCF8*-dependent adherence is the presence of a mucus layer produced by the epithelium. In the gut, this physical barrier shields the epithelium from direct contact with colonizing microbes including *C. albicans* (Böhm *et al.*, 2017; Eckstein *et al.*, 2020). Mucus consists of a large group of proteins that have a high affinity to water which gives this layer a gel-like quality (Johansson *et al.*, 2016). When fungal adherence was probed to an oral and two intestinal epithelial cells lines (Figure 20A), no differences were observed for the Caco-2 intestinal cells. In the presence of a mucus layer, however, the deletion mutant adhered significantly less (Figure 20B) which highlights the importance of mucus in fungal-host interplay. Previous studies have suggested that *C. albicans* in its round yeast form attaches better to mucus (Böhm *et al.*, 2017). In contrast, filaments seem to bind more efficiently to keratinocytes as the deletion mutant of *ZCF8* as well as another key determinant of colonization in the oral mucosa *CUP9* form more filaments *in vivo* (Meir *et al.*, 2018) (Figure 24B and 24C). Therefore, these findings suggest that *ZCF8* promotes the attachment of *C. albicans* to the intestinal mucus but weakens binding to keratinocytes.

4.3 Nitrogen homeostasis and *ZCF8*

Several targets of Zcf8p show connections to transport of amino acids and other nitrogen-rich molecules (*e.g.*, allantoate) which raises the possibility of *ZCF8* controlling some aspect(s) of nitrogen metabolism in *C. albicans*. This hypothesis is supported by *C. albicans'* phenotype when exposed to the vacuole-disturbing agent nigericin (Jakubkova *et al.*, 2016): On the one hand, exposing fungal cells to the drug induces the expression of genes related to amino acid metabolism and amino acid dynamics (Figure 18B); while, on the other hand, many genes regulated by *ZCF8* seem to be affected by the drug as well, as transcriptional changes induced by *ZCF8* are diminished in the presence of nigericin (both samples cluster closer together upon nigericin treatment in the PCA in figure 18C). Furthermore, some targets of the regulator such as *VBA1*, a major vacuolar transporter of amino acids, and *DAL52*, a putative allantoate transporter that localizes in the vacuole, contribute to amino acid dynamics in the fungus. Whether these transporters operate by moving their substrate in or out of the vacuole remains to be uncovered. The data on vacuolar morphology and luminal acidification imply that misregulation of those transporters and/or related products can significantly influence vacuolar homeostasis in response to extracellular nitrogen availability. However, this does not necessarily mean that the regulator governs nitrogen and/or amino acid metabolism in the fungus. Nevertheless, Zcf8p controls vacuolar physiology as properties such as morphology and acidification depend on the regulator (Figure 12 and 14). Acidification, in particular, is fundamental for this organelle because many transport, storage, and homeostatic functions rely on it including the storage and recycling of amino acids (Klionsky *et al.*, 1990; Veses *et al.*, 2008). Therefore, it might be possible that amino acid metabolism in *C. albicans* is affected by Zcf8p's activity as a side effect of its major role on vacuolar properties - such as acidification. In agreement with this idea, the gene expression data of the *ZCF8* mutants (Table 7 and 8) shows no evidence of changes in the transcription levels of key regulators of nitrogen metabolism (*e.g.,* Stp1/2p), their respective target genes (*e.g.*, *OPT1*, *GAP1/2*, *CAN1*), or any gene of the general amino acid control

(GCN) pathway (*e.g.*, *GCN4*). Therefore, further studies are needed to prove the existence of a connection between *ZCF8* and nitrogen metabolism in the fungus.

4.4 Fungal vacuole homeostasis and fungal-host interactions

The fungal vacuole impacts traits associated with general cellular homeostasis and fungal morphology. These processes, in turn, impinge upon the interactions that the fungus establishes with host cells. The vacuole is the key organelle that maintains cellular homeostasis in response to extracellular change (Klionsky *et al.*, 1990). *C. albicans* thrives on a variety of environmental niches within its human host which requires that the fungus adapts its physiology to avoid and/or counteract fluctuations in the conditions such as nutrient availability and/or ambient pH (Alves *et al.*, 2020). In fact, metabolic adaptation to those kind of stresses has been shown to contribute to fungal virulence (Brown *et al.*, 2014). Carbon adaptation, for example, is important for cell wall architecture with consequences for host recognition (Ene *et al.*, 2012; Ene and Heilmann, 2012). Furthermore, when nutrient availability in the surroundings is low, the fungus relies on cellular recycling processes such as autophagy. In order to enhance the degradation capacities of the vacuole, the VPS pathway, for example, regulates protein trafficking of hydrolytic enzymes to the vacuole (Bryant *et al.*, 1998; Conibear *et al.*, 1998; Kraft *et al.*, 2012). Multiple VPS pathway genes have been described to influence interactions between *C. albicans* and its host: *VPS34* encodes a phosphatidylinositol 3-kinase and deletion of the gene blocks endocytic vesicle transport and renders the mutant sensitive to temperature and osmotic stress (Bruckmann *et al.*, 2000, 2001); *VPS11* is required for vesicle fusion events at the vacuolar surface and the deletion mutant is defective in filamentation and epithelial adhesion (Wurmser *et al.*, 2000; Palmer *et al.*, 2005, 2007; Wächtler *et al.*, 2011); the deletion mutant of Vac1p shows defective endosomal vesicle transport, increased sensitivity to high concentrations of metal ions such as copper and zinc, and is defective in adherence to epithelial cells (Franke *et al.*, 2006).

Maintaining cellular physiology also implies clearing the cytosol from excessive nutrient and/or toxic molecules. Here, the acidic lumen of the organelle energizes

several transporters that mediate detoxification and maintain the balance of nutrients, metals, and phosphate (Veses, *et al.*, 2008; Li and Kane, 2009; Richards *et al.*, 2010). As mentioned above, vacuolar acidification modulates fungal-host interactions, because several mutations that affect luminal pH such as those in *VMA2*, *VMA3*, and *VMA7* show defective fungal pathology (Poltermann *et al.*, 2005; Rane *et al.*, 2013, 2014). The deletion of genes that encode structural proteins of the V-ATPase in the vacuolar membrane resulted in the same *vma* phenotype regardless of which protein was disrupted (Umemoto *et al.*, 1990; Kane, 2006). The phenotype is characterized by slow growth in neutral or alkaline media, altered sensitivity to Ca^{2+}, and the inability to grow on non-fermentable carbon sources. Repression of *VMA3* in *C. albicans* results in alkalization of the vacuole, reduced filamentation, and attenuated in *in vitro* macrophage killing (Kane, 2006). *C. albicans vma5* mutants had a dysfunctional vacuole, disturbances in calcium homeostasis, were hypersensitive to nitrogen starvation, had weaker adhesion, and were avirulent in a mouse model of systemic candidiasis (Zhang *et al.*, 2017). In other fungi the vacuole also plays an important role in physiology and virulence. When the fungus *Cryptococcus neoformans*, which causes cryptococcal meningitis in immunocompromised individuals, is exposed to conditions that cause an increased level of intracellular reactive oxygen species (ROS) such as high concentrations of iron or other trace metals the fungal vacuole was highly fragmented (Kim *et al.*, 2021). The authors of that study speculate that fragmentation increases the surface-to-volume ratio to provide more docking sites for vacuolar iron transporters which increases uptake into the vacuoles and thus protecting the fungal cell from oxidative stress (Kim *et al.*, 2021).

Several of the above-mentioned vacuole-related mutants (*e.g.*, *vac1*, *vps11*, and *vma3*) share defects in filamentation and/or morphology. Morphology is central for host interaction as *C. albicans* switches between multiple morphological forms depending on each niche (Böhm *et al.*, 2017; Meir *et al.*, 2018; Richardson *et al.*, 2018). Moreover, filamentation of the fungus is a well-established response when cells face conditions with low concentrations of available nitrogen (Tripathi *et al.*, 2002; Biswas *et al.*, 2005); and the fungal vacuole plays an important role during hyphal growth (Veses *et al.*, 2008; Richards *et al.*, 2010). As mentioned earlier,

formation of the germ tube involves fundamental enlargement of the vacuole to push the cytoplasm towards the newly developing hyphae, and the size of the vacuole regulates fungal cell-cycle during hyphal growth (Gow, 1997; Veses *et al.*, 2008; Sudbery, 2011). In fact, Veses *et al.* (2008) proposed that the link between cell-cycle arrest/initiation and vacuolation might be a fungal strategy to adapt growth under nutrient-depleted conditions. Vacuolation of the distal compartment is energetically less costly than synthesizing new cytoplasm, and since these cells remain nucleated they can form a branch after some time in cell-cycle arrest (Barelle *et al.*, 2003). Furthermore, Veses et al. (2008) posit that a functional vacuole is essential for many aspects of pathogenesis in a wide range of plant and human pathogenic fungi.

4.5 Perspectives and future directions

I think the most interesting questions to explore giving the results of this thesis focus on the molecular mechanism(s) that explain(s) the role of Zcf8p on vacuolar properties. Several genes are known to encode structural proteins of the vacuolar ATPase that directly regulates acidification. However, my research shows that neither genome wide protein-DNA interaction nor gene expression data connect Zcf8p to any of those genes coding for subunits of the complex. Moreover, the effect of *ZCF8* on vacuolar pH was, although significant, relatively small. While activity of the V-ATPase is essential for vacuole functionality, there are alternative routes that regulate luminal pH such as endocytic vesicles, for example by the Na^+/H^+ antiporter Nhx1p in *S. cerevisiae* (Brett *et al.*, 2005). It remains to be established if any of the identified targets of regulation such as the transporter Vba1p are sufficient to influence vacuolar acidification. A straightforward approach to test this would be to assess vacuolar acidification and/or gene expression in *Candida* cells exposed to extreme pH as performed for *MOT3* and *PDR8* (Hongay *et al.*, 2002; Hikkel *et al.*, 2003). These experiments could potentially provide additional evidence on Zcf8p's role on vacuolar biology.

Some questions about the transcription regulators identified in the ChIP-Seq data remain also unanswered. Future studies should aim to identify and

characterize transcriptional regulators that bind to *ZCF8* to dissect the molecular mechanism of Zcf8p's own regulation. Like many transcription regulators, it is likely that Zcf8p functions as part of a larger circuit that regulates traits such as vacuole physiology or fungal filamentation. This idea is supported by the fact that well-known regulators of cell adhesion and biofilm formation are targeted by Zcf8p.

A third question which arises from the data relates to the role of the vacuole during fungal-host interaction. As previously mentioned, it is known that the vacuole modulates filamentation (Veses *et al.*, 2008) while it maintains cellular homeostasis in response to extracellular change (Klionsky *et al.*, 1990). Moreover, nitrogen starvation induces filamentation in *C. albicans* which links both traits (Biswas and Morschhäuser, 2005). However, the importance of the vacuole during fungal-host interaction has not been fully elucidated. Multiple of the above mentioned reports show that dysfunctional vacuoles have consequences for virulence because the physiology of those cells was severely affected (Hongay *et al.*, 2002; Johnston *et al.*, 2009; Rane *et al.*, 2014; Khandelwal *et al.*, 2016; Zhang *et al.*, 2017). Therefore, further investigations are needed to characterize the effect of the vacuole on fungal-host interaction. Those approaches should allow, for example, fine tuning of vacuolar properties such as acidification (*e.g.*, through genetic modification of genes encoding subunits of V-ATPase) or homotypic vesicle fusion (*e.g.*, through nutrient starvation) in *C. albicans* cells during infection.

6 Supplementary data

6.1 ChIP-Seq data generated in this study

The results of the genome-wide chromatin immunoprecipitation of a *C. albicans* strain encoding a myc-tagged Zcf8p to identify direct targets of regulation are listed in table 5 and 6. The experimental procedure as well as data analysis is described in 2.5. The data has been deposited in the Gene Expression Omnibus (GEO) database (accession number GSE181652).

Table 5: 42 identified peaks or DNA regions bound by Zcf8p genome wide. “Start” and “end” defines the location of the peak within the respective chromosome of the *C. albicans* genome. “bpeak_name” is the identifier generated by the peak calling function of bPeaks (Merhej *et al.*, 2014). “IP sample” and “control sample” present the local parameter of the peak signal in the IP and control sample, respectively, that are the basis for the log2 fold change calculation (“log2FC”) (Merhej *et al.*, 2014).

Peak	Model	Chromosome	Start	End	bpeak_name	IP sample	control sample	log2FC
peak_1	C_albicans_SC5314	Ca21chr1	892489	892989	allGenome_bPeak_105	42.73	11.31	1.83
peak_2	C_albicans_SC5314	Ca21chr1	1081981	1082481	allGenome_bPeak_46	49.14	10.66	2.11
peak_3	C_albicans_SC5314	Ca21chr1	2227862	2228362	allGenome_bPeak_62	46.87	11.28	1.96
peak_4	C_albicans_SC5314	Ca21chr1	2402668	2403168	allGenome_bPeak_84	44.38	10.22	2.02
peak_5	C_albicans_SC5314	Ca21chr1	2868525	2869025	allGenome_bPeak_20	54.38	10.02	2.31
peak_6	C_albicans_SC5314	Ca21chr1	2870185	2870685	allGenome_bPeak_117	41.53	10.60	1.87
peak_7	C_albicans_SC5314	Ca21chr1	3120303	3120803	allGenome_bPeak_78	44.68	10.98	1.93
peak_8	C_albicans_SC5314	Ca21chr2	163524	164024	allGenome_bPeak_15	54.83	11.27	2.19
peak_9	C_albicans_SC5314	Ca21chr2	517156	517656	allGenome_bPeak_136	39.92	10.69	1.81
peak_10	C_albicans_SC5314	Ca21chr2	522869	523369	allGenome_bPeak_50	48.77	10.66	2.09

peak_11	C_albicans _SC5314	Ca21chr2	829442	829942	allGenome_bPeak _137	39.85	10.11	1.88
peak_12	C_albicans _SC5314	Ca21chr3	284079	284579	allGenome_bPeak _130	40.53	10.56	1.84
peak_13	C_albicans _SC5314	Ca21chr3	866349	866849	allGenome_bPeak _66	46.65	10.57	2.04
peak_14	C_albicans _SC5314	Ca21chr3	953478	953978	allGenome_bPeak _42	49.33	8.80	2.36
peak_15	C_albicans _SC5314	Ca21chr3	1125145	1125645	allGenome_bPeak _111	41.91	11.30	1.80
peak_16	C_albicans _SC5314	Ca21chr3	1475225	1475725	allGenome_bPeak _119	41.48	10.81	1.85
peak_17	C_albicans _SC5314	Ca21chr3	1728087	1728587	allGenome_bPeak _19	54.39	10.56	2.24
peak_18	C_albicans _SC5314	Ca21chr3	1759252	1759752	allGenome_bPeak _44	49.25	10.56	2.12
peak_19	C_albicans _SC5314	Ca21chr4	481556	482056	allGenome_bPeak _21	54.16	9.41	2.39
peak_20	C_albicans _SC5314	Ca21chr4	635845	636345	allGenome_bPeak _45	49.24	10.20	2.16
peak_21	C_albicans _SC5314	Ca21chr4	787888	788388	allGenome_bPeak _2	63.88	11.23	2.39
peak_22	C_albicans _SC5314	Ca21chr4	1504333	1504833	allGenome_bPeak _121	41.12	10.92	1.82
peak_23	C_albicans _SC5314	Ca21chr5	155399	155899	allGenome_bPeak _79	44.65	10.52	1.99
peak_24	C_albicans _SC5314	Ca21chr5	254344	254844	allGenome_bPeak _93	43.48	11.32	1.85
peak_25	C_albicans _SC5314	Ca21chr5	337125	337625	allGenome_bPeak _140	39.60	10.63	1.80
peak_26	C_albicans _SC5314	Ca21chr5	374330	374830	allGenome_bPeak _7	58.17	9.94	2.42
peak_27	C_albicans _SC5314	Ca21chr6	250413	250913	allGenome_bPeak _57	47.44	11.26	1.98
peak_28	C_albicans _SC5314	Ca21chr6	288584	289084	allGenome_bPeak _99	43.06	10.92	1.89
peak_29	C_albicans _SC5314	Ca21chr6	552209	552709	allGenome_bPeak _91	43.79	10.34	1.98
peak_30	C_albicans _SC5314	Ca21chr6	668470	668970	allGenome_bPeak _51	48.64	11.05	2.04
peak_31	C_albicans _SC5314	Ca21chr6	765156	765656	allGenome_bPeak _10	56.60	10.98	2.27
peak_32	C_albicans _SC5314	Ca21chr7	70244	70744	allGenome_bPeak _86	44.22	10.37	1.99
peak_33	C_albicans _SC5314	Ca21chr7	300979	301479	allGenome_bPeak _68	46.17	10.67	2.01
peak_34	C_albicans _SC5314	Ca21chr7	378219	378719	allGenome_bPeak _89	43.84	10.74	1.93
peak_35	C_albicans _SC5314	Ca21chr7	917693	918193	allGenome_bPeak _61	47.18	11.15	1.99
peak_36	C_albicans _SC5314	Ca21chrR	586746	587246	allGenome_bPeak _122	40.98	9.76	1.96
peak_37	C_albicans _SC5314	Ca21chrR	597636	598136	allGenome_bPeak _94	43.43	11.04	1.88

peak_38	C_albicans _SC5314	Ca21chrR	1388511	1389011	allGenome_bPeak _95	43.41	10.44	1.95
peak_39	C_albicans _SC5314	Ca21chrR	1525821	1526321	allGenome_bPeak _26	52.01	9.58	2.32
peak_40	C_albicans _SC5314	Ca21chrR	2105332	2105832	allGenome_bPeak _5	61.32	10.59	2.41
peak_41	C_albicans _SC5314	Ca21chrR	2168711	2169211	allGenome_bPeak _56	47.58	11.54	1.95
peak_42	C_albicans _SC5315	Ca21chrR	2169331	2169831	allGenome_bPeak _60	47.21	10.03	2.13

Table 6: Nearest annotated ORF of each identified peak.

ORF name	Alias	Annotation (CGD)
C3_05180W	*RHB1*	Putative small G protein from the Ras superfamily, controls filamentous growth under nitrogen starvation
C6_03170C	*MDR1*	Plasma membrane MDR/MFS multidrug efflux pump
C6_01290C	*QDR3*	Predicted membrane transporter
C7_01770W		Protein of unknown function
C2_02590W	*ZRT2*	Zinc transporter
CR_06490C	*HSP60*	Heat shock protein
C3_04530C	*TEC1*	TEA/ATTS transcription factor
C1_10850W		Protein of unknown function
C1_14150C	*PAM16*	Putative maltase
C3_04160W	*DAL8*	Putative allantoate permease
C1_10840C		Ortholog(s) have role in retrograde transport
C4_03050C		Ortholog(s) have carboxypeptidase activity, role in nitrogen compound metabolic process
C1_13130C		Putative histidine permease
C3_01330W	*ZCF8*	Predicted Zn(II)2Cys6 transcription factor
CR_02640W	*RFG1*	HMG domain transcriptional repressor of filamentous growth and hyphal genes
C5_01120W		Dubious open reading frame
C5_00680W	*RMT2*	Minor protein arginine methyltransferases
C1_13140C	*TYE7*	bHLH transcription factor
C4_06760W	*GUT2*	Glycerol-3-phosphate dehydrogenase
C1_13150W		Protein of unknown function

C3_07730W	*WOR4*	Predicted C2H2 zinc finger protein
C6_01300W		Putative transferase
C7_00430W		Putative ferric reductase
C5_01510W	*SMD3*	Putative core small nuclear ribonucleoprotein
C1_04300C	*SSA2*	HSP70 family chaperone
C1_14160W		Ortholog(s) have protein-lysine N-methyltransferase activity
C2_02550C		Protein of unknown function
C5_01500C	*ZCF20*	Zn(II)2Cys6 transcription factor
C7_04230W	*NRG1*	Transcription regulator
CR_09880W	*DEF1*	RNA polymerase II regulator
CR_07060C	*CRZ2*	C2H2 transcription factor
C7_01440W		Protein of unknown function
C6_01440C	*FRP5*	Protein with a GPR1/FUN34/yaaH family domain
C6_03600C		Putative cytochrome P450
C7_01760C	*ISU1*	Protein with similarity to proteins involved in the assembly of nitrogenase
CR_02630C		Essential component of the conserved oligomeric Golgi complex
C1_10150W	*WOR1*	Transcription factor
C4_03700W		Predicted membrane transporter
C3_06470W	*AAF1*	Possible regulatory protein
C3_07560W	*TCC1*	Putative transcription regulator
C1_05140W	*BRG1*	Transcription factor
C2_01000W	*HGT7*	Putative MFS glucose transporter
C6_02680W		Ortholog(s) have SNAP receptor activity
C4_03690C		Has domain(s) with predicted role in RNA catabolic process and ribonuclease H2 complex localization
C5_01670W	*DAL52*	Putative allantoate permease
C2_02560W		Planktonic growth-induced gene
C2_03950W		Putative ribosomal protein
C3_07720C		Protein of unknown function

6.2 Gene expression data of *Candida* mutants generated in this study

Results of the transcriptome analysis comparing *C. albicans* wild-type cells with either a *zcf8* deletion (Table 7) or a strain overexpressing *ZCF8* (Table 8) are listed. The experimental procedure as well as data analysis is described in 2.9. The data has been deposited in the GEO database (accession number GSE181653).

Table 7: List of *C. albicans* genes whose expression was up- or down-regulated in the *zcf8* deletion mutant ranked by the log2FC value.

ORF name	Alias	log2FC (*zcf8*/wild-type)	*P*-value	Annotation	Ortholog/ "Best hit" in *S. cerevisiae*
C5_01670W	*DAL52*	4.16	0	Putative allantoate permease	
C4_01340W		3.01	6.80E-81	Protein similar to GPI-linked cell-wall proteins	
C4_01330W		2.52	3.14E-115	Protein of unknown function	
CR_06500C		1.87	8.04E-104	Protein of unknown function	
C2_05360C	*BIO32*	1.58	3.80E-88	Putative class III aminotransferase	
C7_03310W		1.56	2.05E-26	Protein of unknown function	
C3_02750W		1.55	9.07E-60	Protein with a ribonuclease III domain	
C2_01270W	*CHA1*	1.54	4.25E-74	Similar to catabolic ser/thr dehydratases	
CR_07740W		1.54	2.13E-26	Protein of unknown function	
CR_06510W		1.45	1.93E-71	Protein of unknown function	
C6_03320W		1.32	1.17E-84	Stationary phase enriched protein	*YHI9*
CR_02060W		1.31	5.05E-33	Protein of unknown function	
C1_02590C	*SNZ1*	1.20	1.35E-235	Protein of unknown function	*SNZ1*
C2_02550C		1.16	4.27E-20	Protein of unknown function	
C4_03700W		1.08	1.41E-104	Predicted membrane transporter	*VBA1*
C1_02600W	*SNO1*	1.06	2.71E-43	Protein with a predicted role in pyridoxine metabolism	*SNO1*
C3_04340W	*ATF1*	1.00	1.65E-48	Putative alcohol acetyltransferase	
C2_00340C	*ARO8*	0.99	7.22E-112	Aromatic transaminase	*ARO8*

C2_09750W	*LEU42*	0.98	6.71E-97	Putative alpha-isopropylmalate synthase	
C1_08170C	*BUL1*	0.96	1.93E-49	Protein involved in selection of substrates for ubiquitination	
C4_03940C	*PYC2*	0.96	1.79E-128	Putative pyruvate carboxylase	*PYC2*
C4_00650W	*HIS5*	0.95	4.46E-48	Putative histidinol-phosphate aminotransferase	*HIS5*
C1_08790W	*TPO3*	0.91	6.66E-38	Putative polyamine transporter	*TPO2*
C1_10060C		0.90	4.06E-15	Protein of unknown function	
C7_03330C	*SHM1*	0.89	3.09E-123	Mitochondrial serine hydroxymethyltransferase	*SHM1*
C7_03340C	*PRR2*	0.88	8.70E-15	Putative serine/threonine protein kinase	
C1_08400C	*GCV2*	0.85	8.21E-98	Glycine decarboxylase P subunit	*GCV2*
C5_03060C	*TNA1*	0.84	9.26E-63	Putative nicotinic acid transporter	*TNA1*
C2_04460W	*LYS22*	0.82	3.72E-64	Homocitrate synthase	
C3_03070W		-0.80	8.51E-24	Putative transporter similar to MDR proteins	
C4_05580C		-0.80	9.90E-48	Secreted protein	
CR_04220C		-0.82	1.66E-16	Protein of unknown function	
C1_07580C	*PRY1*	-0.86	2.14E-18	Pry family pathogenesis-related protein	
C1_13080W	*OP4*	-0.90	4.55E-83	Protein of unknown function	
C6_03790C	*HGT10*	-1.01	7.18E-62	Glycerol permease involved in glycerol uptake	*STL1*
CR_10320W		-1.09	5.16E-45	Protein of unknown function	
C4_05250W		-1.33	8.86E-11	Putative ubiquitin-protein ligase	
C3_07670W		-1.67	9.60E-168	Protein of unknown function	*YDR090C*

Table 8: List of *C. albicans* genes whose expression is up- or down-regulated in the strain overexpressing *ZCF8* ranked by the log2FC value.

ORF name	**Alias**	**log2FC (overexpression/wild-type)**	***P*-value**	**Annotation**	**Ortholog/ "Best hit" in *S.cerevisiae***
C2_09800C		2.80	0	Protein of unknown function	
C1_06610C	*HAK1*	2.17	1.82E-233	Putative potassium transporter	
CR_10320W		2.02	1.32E-172	Protein of unknown function	
C1_13080W	*OP4*	1.92	0	Protein of unknown function	
C1_07580C	*PRY1*	1.91	6.24E-101	Protein of unknown function	

C4_05580C		1.88	4.89E-284	Secreted protein	
C4_01340W		1.80	6.60E-29	Protein similar to GPI-linked cell-wall proteins	
C6_03170C	*MDR1*	1.80	7.72E-64	Plasma membrane MDR/MFS multidrug efflux pump	*FLR1*
C1_02070W	*HSP31*	1.75	8.74E-12	Putative 30 kda heat shock protein	
C1_12220W	*CDC6*	1.72	5.57E-75	Putative ATP-binding protein with a predicted role in DNA replication	*CDC6*
C1_05890W		1.69	3.32E-258	Protein of unknown function	
C6_00080C		1.67	1.26E-297	Protein of unknown function	
C2_02750C		1.62	1.84E-12	Protein of unknown function	
C1_07330W	*RME1*	1.62	1.13E-18	Zinc finger protein	*RME1*
CR_00180C	*CHT1*	1.57	7.72E-108	Chitinase	
C3_07160W	*PGA32*	1.57	1.12E-158	Putative GPI-anchored adhesin-like protein	
C1_09150W	*AOX2*	1.56	2.22E-278	Alternative oxidase	
C1_02520W	*SCW4*	1.54	3.00E-133	Putative cell wall protein	
C2_02230C		1.53	2.07E-286	Protein with a globin-like domain	
C3_05630W	*GTT1*	1.52	2.01E-37	Putative glutathione S-transferase	
C7_04180W	*FAA2-3*	-1.52	3.41E-110	Predicted acyl CoA synthetase	
C4_03050C		-1.59	1.29E-256	Ortholog(s) have carboxypeptidase activity	*CPS1*
C1_10550C	*GCA2*	-1.61	2.00E-125	Predicted extracellular glucoamylase	
C2_02880C	*EBP7*	-1.62	1.36E-36	Putative NADPH oxidoreductase	
C2_05770W		-1.66	2.71E-112	Zn(II)2Cys6 domain transcription factor	
C1_10290W	*GCA1*	-1.71	2.59E-107	Extracellular/plasma membrane-associated glucoamylase	
CR_04440C	*RBR1*	-1.73	3.78E-48	Glycosylphosphatidylinositol (GPI)-anchored cell wall protein	
C7_01520W	*FLU1*	-1.73	1.69E-156	Multidrug efflux pump of the plasma membrane	*TPO1*
C3_00230C		-1.78	3.54E-12	Putative protein of unknown function	
CR_03280W	*IFR2*	-1.80	0	Zinc-binding dehydrogenase	
C1_01440C	*POX18*	-1.84	2.07E-46	Similar to Pox18, a peroxisomal protein	
CR_05170C	*FDH1*	-1.87	0	Formate dehydrogenase	*FDH1*
C3_00220W	*HGT19*	-1.87	0	Putative MFS glucose/myo-inositol transporter	

C2_04470W	*ADH3*	-1.91	8.86E-70	Putative NAD-dependent (R,R)-butanediol dehydrogenase	
CR_08310C		-1.95	4.03E-57	Protein of unknown function	
C3_03460C		-1.96	4.17E-11	Protein of unknown function	
C2_09590C		-2.09	2.02E-69	Ortholog(s) have copper ion transmembrane transporter activity	*PIC2*
C4_01840C		-2.29	0	Putative dienelactone hydrolase	*AIM2*
CR_10100C	*INO1*	-2.62	7.98E-18	Inositol-1-phosphate synthase	*INO1*
C4_06710W		-3.18	5.32E-141	Putative NADP-dependent oxidoreductase	
C4_06380W	*SOU2*	-3.35	1.52E-96	Protein similar to Sou1	
C2_02550C		-3.54	1.64E-79	Protein of unknown function	
C6_03600C		-4.54	1.74E-135	Putative cytochrome P450	
C5_01670W	*DAL52*	-4.79	1.28E-202	Putative allantoate permease	
C6_03480W	*YMX6*	-5.96	2.11E-15	Putative NADH dehydrogenase	

6.3 Gene expression data of *Candida* cells exposed to nigericin

Results of the transcriptome analysis comparing *C. albicans* wild-type cells or cells of the *zcf8* deletion mutant treated either with nigericin or a mock control are listed in table 9 or table 10, respectively. The data has been deposited in the GEO database (accession number GSE181655). The experimental procedure as well as data analysis is described in 2.9.

Table 9: List of *C. albicans* genes whose expression was significantly altered in response to nigericin treatment in the wild-type reference strain. ORFs labeled in red belong to the list of 19 genes up-regulated in the *zcf8* deletion mutant and in response to nigericin treatment in the wild-type strain.

ORF name	Alias	log2FC (nigericin/ control)	*P*-value	Annotation	Ortholog/ "Best hit" in *S.cerevisiae*
C4_01350W		7.38	1.15E-57	Protein of unknown function	
CR_03920C	*TPO4*	5.57	0	Putative sperimidine transporter	*TPO4*
C1_06870C		5.45	1.71E-14	Protein of unknown function	
C1_03390W	*EHT1*	5.02	0	Putative acyl-coenzymeA:ethanol O-acyltransferase	*EHT1*
C7_00770W		4.91	6.52E-86	Protein of unknown function	
C5_02790C	*GAP1*	4.67	0	Amino acid permease	
C3_03460C		4.60	0	Protein of unknown function	
CR_06550C		4.45	0	Protein of unknown function	
CR_02060W		4.43	0	Protein of unknown function	
C1_02980W	*GOR1*	4.05	0	Role in glyoxylate catabolic process and extracellular region localization	*GOR1*
C5_03500W	*GAP6*	4.03	0	Broad-specificity amino acid permease	
C4_01340W		3.87	4.93E-212	Protein similar to GPI-linked cell-wall proteins	

C1_04450C	*FMA1*	3.86	0	Putative oxidoreductase	
C2_07410W		3.57	0	Ortholog(s) have acylglycerol lipase activity	*MGL2*
CR_08990C	*SLP3*	3.52	0	Plasma membrane protein implicated in stress response	
C1_11480W	*PHO84*	3.50	0	High-affinity phosphate transporter	*PHO84*
C2_01270W	*CHA1*	3.46	0	Similar to catabolic ser/thr dehydratases	
C4_03380C	*DAO2*	3.45	5.57E-23	Putative D-amino acid oxidase	
C1_09300C		3.31	1.27E-57	Has domain(s) with predicted metal ion binding activity	
C6_03540W		3.24	0	Predicted membrane transporter	
C3_04340W	*ATF1*	3.23	0	Putative alcohol acetyltransferase	
CR_06500C		3.20	0	Protein of unknown function	
C7_03570W	*ARG4*	3.19	0	Argininosuccinate lyase	*ARG4*
C1_02970W		3.11	0	Predicted aminotransferase	
C4_03340C		2.99	5.87E-15	Protein with homology to NADH dehydrogenase	
C5_05190W	*PCL5*	2.97	1.65E-95	Putative cyclin for Pho85 kinase	*PCL5*
C6_03230W	*ARG3*	2.96	0	Putative ornithine carbamoyltransferase	*ARG3*
C5_04490C	*CAR1*	2.93	0	Arginase	*CAR1*
C4_06670W		2.92	6.52E-198	Protein of unknown function	
C3_05220W	*CDR1*	2.91	0	Multidrug transporter of ABC superfamily	*PDR5*
C6_03320W		2.91	0	Stationary phase enriched protein	*YHI9*
C3_04890W	*CDR2*	2.91	0	Multidrug transporter	
C5_02000C	*ACH1*	2.89	0	Acetyl-coA hydrolase	*ACH1*
C4_00650W	*HIS5*	2.89	0	Putative histidinol-phosphate aminotransferase	*HIS5*
CR_00620C	*ARG1*	2.89	0	Argininosuccinate synthase	*ARG1*

C1_08410C	*SAM4*	2.86	0	Putative S-adenosylmethionine-homocysteine methyltransferase	*SAM4*
C1_02590C	*SNZ1*	2.85	0	Protein with role in vitamin B synthesis	*SNZ1*
CR_02570C		2.83	0	Role in triglyceride catabolic process	*LPX1*
C2_04460W	*LYS22*	2.82	0	Homocitrate synthase	
C2_04230W	*BAT21*	2.81	0	Putative branched chain amino acid aminotransferase	*BAT2*
C2_02030W	*ARO3*	2.78	0	3-deoxy-D-arabinoheptulosonate-7-phosphate synthase	*ARO3*
C6_01060C	*CAN2*	2.77	2.60E-184	Basic amino acid permease	*CAN1*
C1_04290C	*ACS2*	2.72	0	Acetyl-CoA synthetase	*ACS2*
CR_00210W	*ALK2*	2.71	0	N-Alkane inducible cytochrome P450	
CR_03120W		2.67	0	Ortholog of S. cerevisiae Mpm1	*MPM1*
C2_09060C	*ASN1*	2.65	0	Putative asparagine synthetase	*ASN2*
C2_09750W	*LEU42*	2.64	0	Putative alpha-isopropylmalate synthase	
C6_03700W	*ALS1*	2.59	0	Cell-surface adhesin	
C7_03720C	*HIS7*	2.56	0	Putative imidazole glycerol phosphate synthase	*HIS7*
C4_00140C	*HIS4*	2.56	0	Multifunctional enzyme that catalyzes three steps of histidine biosynthesis	*HIS4*
CR_09920W		2.56	0	Predicted amino acid transport domain	
CR_07740W		2.54	9.71E-93	Protein of unknown function	
C2_06210C	*SER1*	2.54	0	Putative 3-phosphoserine aminotransferase	*SER1*
C6_00330C	*GNP1*	2.53	0	Similar to asparagine and glutamine permease	*AGP1*
C2_04810W	*HIS3*	2.48	9.15E-301	Imidazoleglycerol-phosphate dehydratase	*HIS3*

C3_02750W		2.48	1.13E-201	Protein with a ribonuclease III domain	
C1_10060C		2.46	2.25E-175	Protein of unknown function	
C2_00760C		2.46	0	Protein of unknown function	
C2_01180W	*COX17*	2.43	2.05E-233	Putative copper metallochaperone	*COX17*
CR_06510W		2.43	0	Protein of unknown function	
C4_05400C		2.42	0	D-arabinose 5-phosphate isomerase	
C1_05110C	*ARO4*	2.40	0	3-deoxy-D-arabinoheptulosonate-7-phosphate synthase	*ARO4*
C2_00340C	*ARO8*	2.40	0	Aromatic transaminase	*ARO8*
C1_10360C		2.40	0	Putative protein of unknown function	*YCR061W*
C1_14190C		2.37	1.78E-14	Protein phosphatase inhibitor	*YPI1*
C3_01480C	*RKI1*	2.35	5.49E-284	Ortholog(s) have ribose-5-phosphate isomerase activity and role in pentose-phosphate shunt	*RKI1*
C2_05360C	*BIO32*	2.35	2.25E-254	Putative class III aminotransferase with a predicted role in biotin biosynthesis	
C1_09400C	*FTH1*	2.33	2.72E-204	Protein similar to S. cerevisiae Fth1p, a high affinity iron transporter for intravacuolar stores of iron	*FTH1*
C4_02720C		2.30	0	Putative plasma membrane protein	*SFK1*
C6_04510C		2.29	1.53E-168	Has domain(s) with predicted ATP binding	
C2_09220W	*DDR48*	2.29	0	Immunogenic stress-associated protein	*DDR48*
C3_07220C	*PRO2*	2.28	0	Putative gamma-glutamyl phosphate reductase with a predicted role in proline biosynthesis	*PRO2*

C1_02600W	*SNO1*	2.26	9.37E-276	Protein with a predicted role in pyridoxine metabolism	*SNO1*
C4_01330W		2.26	1.51E-108	Protein of unknown function	
C6_01420C		2.26	0	Putative oxidoreductase	
C1_01740W	*CTN1*	2.24	0	Carnitine acetyl transferase	*YAT1*
C1_02820W	*LYS2*	2.24	0	Heterodimeric alpha-aminoadipate reductase large subunit	*LYS2*
C5_03860W	*HAM1*	2.23	0	Putative deoxyribonucleoside triphosphate pyrophosphohydrolase	*HAM1*
CR_06490C	*HSP60*	2.21	0	Heat shock protein	*HSP60*
C5_00450C	*IFG3*	2.21	0	Putative D-amino acid oxidase	
C1_04470C		2.20	7.40E-157	Protein of unknown function	
C2_04010C	*HSP21*	2.20	0	Small heat shock protein	
C1_11270W		2.19	0	Cell wall protein	
C4_05540W	*HOM3*	2.18	0	Putative L-aspartate 4-P-transferase	*HOM3*
C4_05320W	*LYS1*	2.17	0	Saccharopine dehydrogenase	*LYS1*
C4_01090C		2.15	4.85E-119	Possile protease	
C7_01540W	*ALK6*	2.12	5.37E-39	Putative cytochrome P-450 of N-alkane-induced detoxification	
C4_00160C	*CAR2*	2.11	0	Ornithine aminotransferase	*CAR2*
C5_01800C	*HIP1*	2.10	0	Amino acid permeases	
C2_06470W	*RTA2*	2.10	0	Flippase involved in sphingolipid long chain base release	*RSB1*
C6_04210C	*ATM1*	2.09	8.27E-266	Member of MDR subfamily of ABC family	*ATM1*
C4_03940C	*PYC2*	2.08	0	Putative pyruvate carboxylase	*PYC2*
C7_01170C		2.06	2.67E-207	Putative oxidoreductase	

C7_03230C		2.06	3.72E-43	Protein of unknown function	
CR_09070C		-2.03	2.76E-115	Protein of unknown function	
C7_00630C		-2.03	3.73E-15	Protein of unknown function	
C1_01330C	*DUT1*	-2.04	5.87E-67	dUTP pyrophosphatase	*DUT1*
C3_02700W	*SMC3*	-2.05	1.79E-73	Protein similar to S. cerevisiae Smc3p, which is an ATPase involved in sister chromatid cohesion	*SMC3*
C6_04610C	*NAG3*	-2.07	6.25E-146	Putative MFS transporter	
CR_00930W	*ATO10*	-2.07	5.37E-35	Putative fungal-specific transmembrane protein	
C3_04300C	*POL1*	-2.09	2.03E-221	Putative DNA directed DNA polymerase alpha	*POL1*
C4_04400C		-2.09	2.86E-20	Protein of unknown function	
C3_02480C	*CCP1*	-2.09	0	Cytochrome-c peroxidase N terminus	*CCP1*
C6_03110C		-2.10	2.42E-23	Protein of unknown function	*ASA1*
CR_03470W		-2.10	9.52E-143	Protein of unknown function	*CIP1*
C7_00290C	*HGT13*	-2.15	2.01E-77	Predicted sugar transporter	
C5_00980W	*TRY3*	-2.15	1.68E-206	RING-finger transcription factor	
C2_09020W	*CDC47*	-2.19	0	Phosphorylated protein described as having role in control of cell division	*MCM7*
CR_07820W		-2.26	4.41E-21	Protein with monooxygenase domains	
C4_01770W	*POL30*	-2.26	1.93E-290	Proliferating cell nuclear antigen (PCNA), forms homotrimeric sliding clamp for DNA polymerases	*POL30*
C3_01930W	*PXP2*	-2.28	0	Putative acyl-CoA oxidase; enzyme of fatty acid beta-oxidation	

C2_06680W	*FRP3*	-2.29	0	Putative ammonium transporter	*ATO2*
C6_02250W		-2.30	4.08E-40	Predicted methyltransferase	
CR_00180C	*CHT1*	-2.32	1.99E-104	Chitinase	
C7_03910W	*OGG1*	-2.32	3.16E-70	Mitochondrial glycosylase/lyase	*OGG1*
C1_13630W	*CYB2*	-2.32	0	Putative cytochrome b2 precursor	*CYB2*
C6_00080C		-2.33	1.02E-238	Protein of unknown function	
C1_08900W		-2.33	3.42E-182	Protein of unknown function	
C2_08170W		-2.33	1.32E-164	Putative sterol deacetylase	*SAY1*
CR_08310C		-2.34	1.45E-55	Ortholog is a predicted sulfonate/alpha-ketoglutare dioxygenase	
C5_03310C	*PCL1*	-2.35	1.11E-83	Cyclin homolog	*PCL1*
C4_01250W	*NAT4*	-2.35	8.67E-31	Putative histone acetyltransferase	*NAT4*
C1_09870W	*HCM1*	-2.36	5.82E-76	Protein with forkhead domain	*HCM1*
CR_02110W	*MCM6*	-2.38	4.97E-217	Putative MCM DNA replication initiation complex component	*MCM6*
C5_01360W	*CFL4*	-2.39	7.56E-81	C-terminus similar to ferric reductases	*FRE2*
C6_00070C	*PGA25*	-2.39	3.17E-281	Putative GPI-anchored adhesin-like protein	
C4_00430W	*MEP2*	-2.39	0	Ammonium permease and regulator of nitrogen starvation-induced filamentation	*MEP2*
C3_03580C	*GTT13*	-2.39	5.13E-126	Putative glutathione S-transferase	
C3_03710W	*CCC1*	-2.40	8.45E-233	Manganese transporter	*CCC1*
CR_03830C	*MCM2*	-2.40	5.40E-219	Phosphorylated protein of unknown function	*MCM2*

C1_02110C	*HGT2*	-2.45	0	Putative MFS glucose transporter	
C3_05980C	*FAA2*	-2.46	0	Putative acyl CoA synthetase	
C3_03360W	*FCY2*	-2.47	1.22E-87	Purine-cytosine permease of pyrimidine salvage	
C1_09430W		-2.49	2.73E-172	Putative membrane protein	*RSN1*
C6_03790C	*HGT10*	-2.50	0	Glycerol permease involved in glycerol uptake	*STL1*
CR_04220C		-2.51	1.98E-61	Protein of unknown function	
C2_10350C	*ACS1*	-2.51	0	Acetyl-CoA synthetase	*ACS1*
C4_03620C	*CDR3*	-2.54	1.45E-159	Transporter of the Pdr/Cdr family of the ATP-binding cassette superfamily	
C1_12220W	*CDC6*	-2.57	2.78E-40	Putative ATP-binding protein with a predicted role in DNA replication	*CDC6*
C1_12550C	*CDC54*	-2.61	6.25E-269	Putative pre-replication complex helicase subunit	*MCM4*
C1_02990C	*XOG1*	-2.65	4.20E-73	Exo-1,3-beta-glucanase	*EXG1*
C1_14020W		-2.69	8.11E-77	Putative Rho GDP dissociation inhibitor	
C1_08330C	*ADH2*	-2.71	0	Alcohol dehydrogenase	*ADH1*
C4_04020C		-2.72	5.53E-63	Protein of unknown function	
C2_07350W	*MCM3*	-2.74	0	Putative DNA replication protein	*MCM3*
CR_09050C		-2.75	2.30E-49	Has domain(s) with predicted DNA binding, nucleic acid binding activity	
C7_00870W		-2.76	1.13E-238	Putative guanine deaminase	*GUD1*
C2_06250C	*CDC46*	-2.80	4.22E-273	Putative hexameric MCM complex subunit	*MCM5*
C1_13670W	*OSM2*	-2.84	0	Putative mitochondrial fumarate reductase	*OSM1*
C3_01060W		-2.84	1.28E-45	Protein of unknown function	

C2_06990W		-2.90	7.50E-129	Protein of unknown function	
C4_02230C		-2.96	1.46E-114	Catechol 1,2-dioxygenase (1,2-CTD), involved in degradation of aromatic compounds	
C5_01670W	*DAL52*	-2.99	3.24E-78	Putative allantoate permease	
C1_01440C	*POX18*	-3.04	2.64E-12	Similar to Pox18, a peroxisomal protein	
C5_04220W	*MRV5*	-3.04	1.58E-10	Planktonic growth-induced gene	
C3_01540W		-3.13	4.12E-45	Plasma-membrane-localized protein	
C3_07160W	*PGA32*	-3.16	1.71E-194	Putative GPI-anchored adhesin-like protein	
C1_05080W	*GPT1*	-3.17	1.11E-264	GABA/polyamine transporter	
C1_14220C	*FTR2*	-3.22	0	High-affinity iron permease	
C3_05450C		-3.28	0	Protein of unknown function	
C1_05960W	*PGA45*	-3.36	0	Putative GPI-anchored cell wall protein	
C2_03610W	*FMO2*	-3.37	0	Protein with a monooxygenase domain	
C4_01160W	*CRD2*	-3.55	9.29E-156	Metallothionein	
C6_03360C		-3.69	3.23E-209	Protein of unknown function	
C5_04380C		-3.74	8.60E-30	Protein of unknown function	
C6_03850C	*IHD1*	-3.75	0	GPI-anchored protein	*YFL067W*
C5_01380W	*CFL5*	-3.78	1.03E-27	Ferric reductase	*FRE3*
C2_01540W		-3.78	0	Ortholog is a predicted sulfonate dioxygenase	
C4_01070W	*HGT17*	-3.97	0	Putative MFS family glucose transporter	
C3_05630W	*GTT1*	-4.03	1.95E-56	Putative glutathione S-transferase	
C2_03350W	*PGA17*	-4.06	0	Putative GPI-anchored protein	

C7_03740C		-4.24	1.59E-33	Protein of unknown function	
C2_08260W		-4.51	0	Protein of unknown function	
C6_04620C	*NAG4*	-4.59	1.09E-60	Putative transporter	
C3_00920W	*ATO1*	-4.75	0	Putative fungal-specific transmembrane protein	
C6_01440C	*FRP5*	-5.35	0	Protein with a GPR1/FUN34/yaaH family domain	
C1_05890W		-5.39	0	Protein of unknown function	
CR_03450W	*HXT5*	-5.60	1.35E-39	Putative sugar transporter	
C1_02520W	*SCW4*	-5.68	0	Putative cell wall protein	
C2_02060C	*FMO1*	-5.68	0	Putative oxidoreductase	
CR_03580C		-5.78	7.32E-62	Putative MFS transporter	
C1_07580C	*PRY1*	-5.79	1.13E-113	Pry family pathogenesis-related protein	
C2_02230C		-5.84	0	Protein with a globin-like domain	
C4_05580C		-6.09	3.40E-39	Secreted protein	
C1_13080W	*OP4*	-6.30	0	Protein of unknown function	
C3_06580W	*JEN1*	-6.79	0	Lactate transporter	*JEN1*
C2_09800C		-7.17	8.44E-59	Protein of unknown function	
CR_10320W		-7.94	4.84E-128	Protein of unknown function	
C7_00280W	*HGT12*	-8.85	1.07E-250	Glucose, fructose, mannose transporter	

Table 10: List of C. albicans genes whose expression was significantly altered in response to nigericin treatment in *zcf8* deletion strain.

ORF name	Alias	log2FC (nigericin/ control)	*P*-value	Annotation	Ortholog/ "Best hit" in *S.cerevisiae*
C4_01350W		8.09	6.27E-47	Protein of unknown function	
CR_03920C	*TPO4*	5.63	0	Putative sperimidine transporter	
C1_03390W	*EHT1*	5.23	0	Putative acyl-coenzymeA:ethanol O-acyltransferase	*GOR1*
C7_00770W		4.77	0	Protein of unknown function	
C3_03460C		4.65	0	Protein of unknown function	
CR_06550C		4.33	0	Protein of unknown function	*MCM4*
C1_04450C	*FMA1*	3.98	0	Putative oxidoreductase	
C1_11480W	*PHO84*	3.89	0	High-affinity phosphate transporter	
C5_02790C	*GAP1*	3.86	5.36E-262	Amino acid permease	*HIS4*
C1_02980W	*GOR1*	3.72	0	Ortholog(s) have glyoxylate reductase (NAD+) activity	
C2_07410W		3.67	0	Ortholog(s) have acylglycerol lipase activity	
C5_03500W	*GAP6*	3.65	0	Broad-specificity amino acid permease	*CAN1*
C6_03230W	*ARG3*	3.51	0	Putative ornithine carbamoyltransferase	*ARO3*
CR_08990C	*SLP3*	3.51	0	Plasma membrane protein implicated in stress response	*FTH1*
CR_02060W		3.47	0	Protein of unknown function	
C4_03380C	*DAO2*	3.43	1.60E-230	Putative D-amino acid oxidase	

CR_00620C	*ARG1*	3.41	0	Argininosuccinate synthase	
C7_03570W	*ARG4*	3.22	0	Argininosuccinate lyase	*EXG1*
C1_06870C		3.16	5.16E-33	Protein of unknown function	
C6_03540W		3.12	0	Predicted membrane transporter	*SAY1*
C6_03700W	*ALS1*	3.11	0	Cell-surface adhesin	*CIP1*
C2_05960C		2.99	4.15E-64	Protein of unknown function	*GGC1*
C3_05220W	*CDR1*	2.92	0	Multidrug transporter of ABC superfamily	*TRP5*
C1_14190C		2.78	1.38E-93	Protein phosphatase inhibitor	
C4_06670W		2.77	3.77E-235	Protein of unknown function	
CR_00210W	*ALK2*	2.76	0	N-Alkane inducible cytochrome P450	*SAM4*
C5_02000C	*ACH1*	2.71	0	Acetyl-coA hydrolase	*YCR061W*
CR_02570C		2.71	0	Ortholog(s) have triglyceride lipase activity	
C3_04890W	*CDR2*	2.71	0	Multidrug transporter, ATP-binding cassette (ABC) superfamily	
C5_05190W	*PCL5*	2.68	2.81E-46	Putative cyclin for Pho85 kinase	*ARG1*
C5_04370C	*PGA37*	2.67	1.09E-28	Putative GPI-anchored protein	
CR_09920W		2.66	0	Predicted amino acid transport domain	
C6_00330C	*GNP1*	2.65	0	Similar to asparagine and glutamine permease	
C1_04290C	*ACS2*	2.64	0	Acetyl-CoA synthetase	*HIS5*
CR_03120W		2.61	0	Ortholog of S. cerevisiae Mpm1	*EHT1*
C1_10360C		2.61	0	Putative protein of unknown function	

C1_02970W		2.60	0	Predicted aminotransferase	
C4_05400C		2.58	0	D-arabinose 5-phosphate isomerase	
C1_08410C	*SAM4*	2.55	1.13E-280	Putative S-adenosylmethionine-homocysteine methyltransferase	*JEN1*
C1_11270W		2.53	0	Cell wall protein	
C5_04490C	*CAR1*	2.51	0	Arginase	*MEP2*
C7_03720C	*HIS7*	2.51	0	Putative imidazole glycerol phosphate synthase	*MGL2*
C6_04510C		2.47	9.40E-208	Proten of unknown function	
C1_05110C	*ARO4*	2.45	0	3-deoxy-D-arabinoheptulosonate-7-phosphate synthase	*GLT1*
C1_06000W		2.44	1.19E-13	Putative dicarboxylic amino acid permease	*HIS7*
C3_04340W	*ATF1*	2.43	0	Putative alcohol acetyltransferase	
C2_01180W	*COX17*	2.40	2.20E-118	Putative copper metallochaperone	
C2_00760C		2.40	0	Proten of unknown function	*CCC1*
C2_09060C	*ASN1*	2.38	0	Putative asparagine synthetase	
C2_02030W	*ARO3*	2.36	0	3-deoxy-D-arabinoheptulosonate-7-phosphate synthase	*DDR48*
CR_06490C	*HSP60*	2.36	0	Heat shock protein	*CAR1*
C2_04460W	*LYS22*	2.30	0	Homocitrate synthase	
C4_05070C	*ARG8*	2.28	0	Putative acetylornithine aminotransferase	*PCL1*
C2_06210C	*SER1*	2.28	0	Putative 3-phosphoserine aminotransferase	

C2_04230W	*BAT21*	2.28	6.52E-264	Putative branched chain amino acid aminotransferase	*SFK1*
C4_00650W	*HIS5*	2.26	0	Putative histidinol-phosphate aminotransferase	*TAH11*
C5_01800C	*HIP1*	2.25	0	Amino acid permeases	
CR_05170C	*FDH1*	2.24	0	Formate dehydrogenase	
C4_00140C	*HIS4*	2.24	0	Enzyme of histidine biosynthesis	*ATO2*
C4_02720C		2.23	0	Putative plasma membrane protein	
C7_00760C		2.22	2.14E-14	Protein of unknown function	*MCM3*
C6_01930W	*YHM1*	2.22	0	Putative mitochondrial carrier protein	*PDR5*
C2_04010C	*HSP21*	2.22	0	Small heat shock protein	
C1_04470C		2.21	3.16E-139	Protein of unknown function	
C6_01420C		2.21	7.31E-247	Putative oxidoreductase	
C3_07220C	*PRO2*	2.20	4.48E-259	Putative gamma-glutamyl phosphate reductase	*YPI1*
C4_05540W	*HOM3*	2.18	3.17E-256	Putative L-aspartate 4-P-transferase	
C1_09400C	*FTH1*	2.17	1.36E-151	A high affinity iron transporter for intravacuolar stores of iron	
C4_01550C	*CPA1*	2.17	3.04E-288	Putative carbamoyl-phosphate synthase subunit	
C4_01090C		2.17	3.15E-93	Possile protease	
C1_09290C	*ARG5,6*	2.16	0	Arginine biosynthetic enzyme	*BAT2*
C2_04810W	*HIS3*	2.16	2.73E-207	Imidazoleglycerol-phosphate dehydratase	

C6_01060C	*CAN2*	2.15	6.91E-62	Basic amino acid permease	
C1_09300C		2.11	1.13E-34	Has domain(s) with predicted metal ion binding activity	*RSB1*
CR_05790C	*ACO2*	2.09	4.11E-271	Putative aconitate hydratase 2	*MCM2*
C2_09220W	*DDR48*	2.07	0	Immunogenic stress-associated protein	
C1_12190W	*BUL4*	2.07	8.35E-129	Protein with a predicted BUL1 N-terminal and C-terminal domains	
C4_00860C		2.06	1.43E-148	Protein of unknown function	*ACS1*
C1_02820W	*LYS2*	2.05	0	Heterodimeric alpha-aminoadipate reductase large subunit	
C3_03870C	*SAP9*	2.04	9.89E-263	Secreted aspartyl protease	
C7_01540W	*ALK6*	2.02	1.31E-44	Putative cytochrome P-450 of N-alkane-induced detoxification	
CR_01480W	*PRS*	2.02	2.43E-143	Putative prolyl-tRNA synthetase	*NAT4*
C2_06470W	*RTA2*	2.01	3.09E-157	Flippase involved in sphingolipid long chain base release	*ARG5,6*
C4_06110C	*TRP5*	2.01	0	Predicted tryptophan synthase	
C1_06550W	*GLT1*	-2.01	0	Putative glutamate synthase	
C3_02330C		-2.02	1.22E-11	Protein of unknown function	
C1_14020W		-2.03	5.77E-34	Putative Rho GDP dissociation inhibitor	*OSM1*
C3_03710W	*CCC1*	-2.04	3.17E-130	Manganese transporter	
CR_03470W		-2.04	7.23E-119	Protein of unknown function	*YLR050C*
C3_02700W	*SMC3*	-2.04	8.04E-68	Protein similar to S. cerevisiae Smc3p	

CR_09050C		-2.05	1.44E-28	Protein of unknown function	*HOM3*
C1_02990C	*XOG1*	-2.06	5.11E-31	Exo-1,3-beta-glucanase	
C2_08170W		-2.06	2.87E-102	Putative sterol deacetylase	*ARG4*
C6_03110C		-2.08	3.74E-17	Protein of unknown function	*MPM1*
C6_02130C	*CTF5*	-2.08	4.96E-17	Predicted component of the kinetochore sub-complex COMA	*MCM5*
C2_06530W		-2.09	2.10E-22	DNA replication licensing factor required for pre-replication complex assembly	
C7_03910W	*OGG1*	-2.09	6.07E-42	Mitochondrial glycosylase/lyase	*LYS2*
C4_03620C	*CDR3*	-2.12	5.29E-84	Transporter of the Pdr/Cdr family of the ATP-binding cassette superfamily	
C7_02230W		-2.14	1.30E-12	Protein of unknown function	
C2_06990W		-2.15	3.82E-72	Protein of unknown function	
C3_00930W	*ATO2*	-2.17	0	Putative fungal-specific transmembrane protein	*CDC6*
C6_02450W		-2.21	1.08E-139	N-acetyltransferase	
C5_01360W	*CFL4*	-2.22	4.97E-84	C-terminus similar to ferric reductases	
C4_00080C		-2.22	9.65E-273	Protein of unknown function	
C5_03130W	*SUT1*	-2.23	7.66E-82	Zn2Cys6 transcription factor involved in sterol uptake	
C7_03310W		-2.23	6.57E-44	Protein of unknown function	
CR_02110W	*MCM6*	-2.23	2.07E-135	Putative MCM DNA replication initiation complex component	

CR_09070C		-2.25	3.23E-106	Protein of unknown function	*MCM6*
C4_01250W	*NAT4*	-2.28	4.06E-20	Putative histone acetyltransferase	*YPS1*
C3_00650W	*NGT1*	-2.29	2.72E-27	N-acetylglucosamine (GlcNAc)-specific transporter	
C4_02660W		-2.30	1.13E-46	Protein of unknown function	*TPO4*
CR_08310C		-2.30	3.79E-48	Ortholog is a predicted sulfonate/alpha-ketoglutare dioxygenase	*PCL5*
C4_00430W	*MEP2*	-2.31	7.06E-304	Ammonium permease and regulator of nitrogen starvation-induced filamentation	
CR_02490W	*OPT4*	-2.31	1.48E-59	Oligopeptide transporter	*AGP1*
C5_03310C	*PCL1*	-2.33	1.12E-75	Cyclin homolog	*GUD1*
C3_03360W	*FCY2*	-2.34	1.26E-48	Purine-cytosine permease of pyrimidine salvage	*ACS2*
C1_08900W		-2.35	1.38E-133	Protein of unknown function	*CPA1*
C4_04400C		-2.35	2.89E-28	Protein of unknown function	*ADH1*
C3_05630W	*GTT1*	-2.36	5.98E-17	Putative glutathione S-transferase	
C1_08330C	*ADH2*	-2.39	0	Alcohol dehydrogenase	
C1_09430W		-2.40	3.58E-113	Putative membrane protein	*YFL067W*
C3_01930W	*PXP2*	-2.43	0	Putative acyl-CoA oxidase	
CR_07820W		-2.43	6.36E-29	Protein with monooxygenase domains	
CR_00930W	*ATO10*	-2.44	3.41E-32	Putative fungal-specific transmembrane protein	

C3_03580C	*GTT13*	-2.45	6.72E-129	Putative glutathione S-transferase	*HCM1*
C1_13630W	*CYB2*	-2.48	0	Putative cytochrome b2 precursor	*SER1*
C3_07160W	*PGA32*	-2.56	3.01E-87	Putative GPI-anchored adhesin-like protein	*ACO2*
C1_09870W	*HCM1*	-2.57	1.11E-78	Protein with forkhead domain	
CR_03830C	*MCM2*	-2.57	1.95E-173	Phosphorylated protein of unknown function	
C1_12220W	*CDC6*	-2.61	3.76E-47	Putative ATP-binding protein with a predicted role in DNA replication	
C2_07350W	*MCM3*	-2.62	0	Putative DNA replication protein	
C2_06680W	*FRP3*	-2.64	0	Putative ammonium transporter	*PHO84*
C2_06250C	*CDC46*	-2.65	8.61E-193	Putative hexameric MCM complex subunit	*ARO4*
C1_02110C	*HGT2*	-2.66	0	Putative MFS glucose transporter	*PIN2*
C3_05980C	*FAA2*	-2.68	0	Putative acyl CoA synthetase	
C1_12550C	*CDC54*	-2.68	3.67E-160	Putative pre-replication complex helicase subunit	*ARG8*
C1_05960W	*PGA45*	-2.69	8.41E-125	Putative GPI-anchored cell wall protein	*PRO2*
C1_14220C	*FTR2*	-2.70	2.21E-190	High-affinity iron permease	
C7_00870W		-2.78	5.59E-203	Putative guanine deaminase	*SUT1*
C2_10350C	*ACS1*	-2.78	0	Acetyl-CoA synthetase	*CYB2*
C1_13670W	*OSM2*	-2.83	0	Putative mitochondrial fumarate reductase	
C2_03350W	*PGA17*	-2.93	5.13E-195	Putative GPI-anchored protein	*SMC3*
C1_01440C	*POX18*	-2.94	3.15E-72	Similar to Pox18, a peroxisomal protein	*FDH1*

C2_03610W	*FMO2*	-3.22	0	Protein with a monooxygenase domain	
C1_05080W	*GPT1*	-3.29	6.74E-227	GABA/polyamine transporter	*ACH1*
C5_01670W	*DAL52*	-3.30	0	Putative allantoate permease	
C3_01060W		-3.35	3.29E-55	Protein of unknown function	
C6_03850C	*IHD1*	-3.43	0	GPI-anchored protein	*AIM10*
C3_01540W		-3.45	5.64E-52	Plasma-membrane-localized protein	
C2_01540W		-3.54	0	Ortholog is a predicted sulfonate dioxygenase	
C6_03360C		-3.55	6.42E-180	Protein of unknown function	
C4_02230C		-3.57	1.32E-187	Catechol 1,2-dioxygenase	*ASN2*
C4_01160W	*CRD2*	-3.60	1.70E-144	Metallothionein	*LPX1*
C3_05450C		-3.63	0	Protein of unknown function	
C4_04020C		-3.66	1.33E-118	Protein of unknown function	
C4_01070W	*HGT17*	-3.90	0	Putative MFS family glucose transporter	
C1_07580C	*PRY1*	-3.95	1.52E-57	Pry family pathogenesis-related protein	*FRE2*
C1_05890W		-4.16	5.47E-283	Protein of unknown function	
C5_00540C	*AGA1*	-4.29	1.19E-41	Protein with some similarity to agglutinin subunit	
C2_08260W		-4.34	0	Protein of unknown function	
C5_04380C		-4.59	1.89E-43	Protein of unknown function	*ARG3*
C2_02230C		-4.64	0	Protein with a globin-like domain	
C7_03740C		-4.68	9.54E-27	Putative protein of unknown function	*RSN1*

C1_02520W	*SCW4*	-4.70	3.21E-199	Putative cell wall protein	
C4_05580C		-4.81	2.21E-277	Secreted protein	
C6_04620C	*NAG4*	-4.89	1.57E-71	Putative transporter	
C1_13080W	*OP4*	-4.89	0	Ala- Leu- and Ser-rich protein	*HIS3*
C3_00920W	*ATO1*	-5.19	0	Putative fungal-specific transmembrane protein	
C2_09800C		-5.20	1.24E-48	Protein of unknown function	
C2_02060C	*FMO1*	-5.37	0	Putative oxidoreductase	*HSP60*
C6_01440C	*FRP5*	-5.52	1.65E-161	Protein with a GPR1/FUN34/yaaH family domain	
CR_03450W	*HXT5*	-5.52	6.33E-275	Putative sugar transporter	
CR_10320W		-5.60	1.92E-103	Protein of unknown function	*COX17*
CR_03580C		-5.72	1.54E-58	Putative MFS transporter	*MCM21*
C6_03600C		-6.53	1.04E-94	Putative cytochrome P450	*ASA1*
C3_06580W	*JEN1*	-7.17	1.30E-118	Lactate transporter	*OGG1*

7 Reference

Akache, B. *et al.* (2004) 'Complex interplay among regulators of drug resistance genes in Saccharomyces cerevisiae.', *The Journal of biological chemistry*. United States, 279(27), pp. 27855–27860. doi: 10.1074/jbc.M403487200.

Akache, B. and Turcotte, B. (2002) 'New regulators of drug sensitivity in the family of yeast zinc cluster proteins.', *The Journal of biological chemistry*. United States, 277(24), pp. 21254–21260. doi: 10.1074/jbc.M202566200.

Akaike, H. (1973) 'Information Theory and an Extension of the Maximum Likelihood Principle', in Parzen, E., Tanabe, K., and Kitagawa, G. (eds) *Selected Papers of Hirotugu Akaike*. New York, NY: Springer New York, pp. 199–213. doi: 10.1007/978-1-4612-1694-0_15.

Allert, S. *et al.* (2018) '*Candida albicans*-induced epithelial damage mediates translocation through intestinal barriers', *mBio*, 9(3), pp. 1–20. doi: 10.1128/mBio.00915-18.

Almeida, R. S. *et al.* (2008) 'The hyphal-associated adhesin and invasin Als3 of *Candida albicans* mediates iron acquisition from host ferritin', *PLoS pathogens*, 4(11), p. e1000217. doi: 10.1371/journal.ppat.1000217.

Alvarez, F. J. and Konopka, J. B. (2007) 'Identification of an N-Acetylglucosamine Transporter That Mediates Hyphal Induction in Candida albicans', *Molecular Biology of the Cell*, 18, pp. 965–975. doi: 10.1091/mbc.E06.

Alves, R. *et al.* (2020) 'Adapting to survive: How *Candida* overcomes host-imposed constraints during human colonization', *PLOS Pathogens*. Edited by S. G. Filler, 16(5), p. e1008478. doi: 10.1371/journal.ppat.1008478.

Anders, S., Pyl, P. T. and Huber, W. (2015) 'HTSeq-A Python framework to work with high-throughput sequencing data', *Bioinformatics*. Oxford University Press, 31(2), pp. 166–169. doi: 10.1093/bioinformatics/btu638.

Anderson, S. F. *et al.* (1995) '*UME6*, a negative regulator of meiosis in *Saccharomyces cerevisiae*, contains a C-terminal Zn2Cys6 binuclear cluster that

binds the URS1 DNA sequence in a zinc-dependent manner.', *Protein science : a publication of the Protein Society*, 4(9), pp. 1832–1843. doi: 10.1002/pro.5560040918.

Angus-Hill, M. L. *et al.* (2001) 'A Rsc3/Rsc30 zinc cluster dimer reveals novel roles for the chromatin remodeler RSC in gene expression and cell cycle control.', *Molecular cell*. United States, 7(4), pp. 741–751. doi: 10.1016/s1097-2765(01)00219-2.

Askew, C. *et al.* (2009) 'Transcriptional regulation of carbohydrate metabolism in the human pathogen *Candida albicans*.', *PLoS pathogens*, 5(10), p. e1000612. doi: 10.1371/journal.ppat.1000612.

Aufschnaiter, A. and Büttner, S. (2019) 'The vacuolar shapes of ageing: From function to morphology', *Biochimica et Biophysica Acta - Molecular Cell Research*. Elsevier, 1866(5), pp. 957–970. doi: 10.1016/j.bbamcr.2019.02.011.

Augsten, M. *et al.* (2002) 'Defective Hyphal induction of a Candida albicans phosphatidylinositol 3-phosphate 5-kinase null mutant on solid media does not lead to decreased virulence.', *Infection and immunity*, 70(8), pp. 4462–4470. doi: 10.1128/IAI.70.8.4462-4470.2002.

Baars, T. L. *et al.* (2007) 'Role of the V-ATPase in regulation of the vacuolar fission-fusion equilibrium', *Molecular Biology of the Cell*, 18(10), pp. 3873–3882. doi: 10.1091/mbc.E07-03-0205.

Baba, M. *et al.* (1994) 'Ultrastructural analysis of the autophagic process in yeast: detection of autophagosomes and their characterization.', *The Journal of cell biology*, 124(6), pp. 903–913. doi: 10.1083/jcb.124.6.903.

Banerjee, M. *et al.* (2008) 'UME6, a novel filament-specific regulator of Candida albicans hyphal extension and virulence', *Molecular Biology of the Cell*. Edited by H. Riezman, 19(4), pp. 1354–1365. doi: 10.1091/mbc.E07-11-1110.

Banerjee, S. and Kane, P. M. (2020) 'Regulation of V-ATPase Activity and Organelle pH by Phosphatidylinositol Phosphate Lipids', *Frontiers in Cell and Developmental Biology*, 8, p. 510. doi: 10.3389/fcell.2020.00510.

Barelle, C. J. *et al.* (2003) 'Asynchronous cell cycle and asymmetric vacuolar inheritance in true hyphae of Candida albicans.', *Eukaryotic cell*, 2(3), pp. 398–410.

doi: 10.1128/EC.2.3.398-410.2003.

Barelle, C. J. *et al.* (2006) 'Niche-specific regulation of central metabolic pathways in a fungal pathogen', *Cellular Microbiology*, 8(6), pp. 961–971. doi: 10.1111/j.1462-5822.2005.00676.x.

Bartholomew, C. R. *et al.* (2012) '*Ume6* transcription factor is part of a signaling cascade that regulates autophagy', *Proceedings of the National Academy of Sciences of the United States of America*, 109(28), pp. 11206–11210. doi: 10.1073/pnas.1200313109.

Basso, V. *et al.* (2018) 'From Genes to Networks: The Regulatory Circuitry Controlling Candida albicans Morphogenesis', in, pp. 61–99. doi: 10.1007/82_2018_144.

Bensen, E. S., Filler, S. G. and Berman, J. (2002) 'A forkhead transcription factor is important for true hyphal as well as yeast morphogenesis in *Candida albicans*', *Eukaryotic Cell*, 1(5), pp. 787–798. doi: 10.1128/EC.1.5.787-798.2002.

Biswas, K. and Morschhäuser, J. (2005) 'The Mep2p ammonium permease controls nitrogen starvation-induced filamentous growth in Candida albicans', *Molecular Microbiology*, 56(3), pp. 649–669. doi: 10.1111/j.1365-2958.2005.04576.x.

Biswas, S., Roy, M. and Datta, A. (2003) 'N-acetylglucosamine-inducible CaGAP1 encodes a general amino acid permease which co-ordinates external nitrogen source response and morphogenesis in *Candida albicans*', *Microbiology*, 149(9), pp. 2597–2608. doi: 10.1099/mic.0.26215-0.

Boens, N. *et al.* (2006) 'Photophysics of the fluorescent pH indicator BCECF', *Journal of Physical Chemistry A*, 110(30), pp. 9334–9343. doi: 10.1021/jp0615712.

Böhm, L. *et al.* (2017) 'The yeast form of the fungus *Candida albicans* promotes persistence in the gut of gnotobiotic mice', *PLoS Pathogens*, 13(10), pp. 1–26. doi: 10.1371/journal.ppat.1006699.

Bolger, A. M., Lohse, M. and Usadel, B. (2014) 'Trimmomatic: A flexible trimmer for Illumina sequence data', *Bioinformatics*. Oxford University Press, 30(15), pp. 2114–2120. doi: 10.1093/bioinformatics/btu170.

Bordallo, J. and Suárez-Rendueles, P. (1993) 'Control of Saccharomyces cerevisiae carboxypeptidase S (CPS1) gene expression under nutrient limitation', *Yeast*, 9(4), pp. 339–349. doi: 10.1002/yea.320090404.

Bougnoux, M.-E. *et al.* (2006) 'Multilocus sequence typing reveals intrafamilial transmission and microevolutions of *Candida albicans* isolates from the human digestive tract.', *Journal of clinical microbiology*, 44(5), pp. 1810–1820. doi: 10.1128/JCM.44.5.1810-1820.2006.

Braun, B. R. *et al.* (2005) 'A human-curated annotation of the Candida albicans genome', *PLoS Genetics*. Edited by M. Snyder. Public Library of Science, 1(1), pp. 0036–0057. doi: 10.1371/journal.pgen.0010001.

Brett, C. L. *et al.* (2005) 'The yeast endosomal Na+K+/H+ exchanger Nhx1 regulates cellular pH to control vesicle trafficking.', *Molecular biology of the cell*, 16(3), pp. 1396–1405. doi: 10.1091/mbc.e04-11-0999.

Brett, C. L. and Merz, A. J. (2008) 'Osmotic Regulation of Rab-Mediated Organelle Docking', *Current Biology*, 18(14), pp. 1072–1077. doi: 10.1016/j.cub.2008.06.050.

Bricmont, P. A., Daugherty, J. R. and Cooper, T. G. (1991) 'The *DAL81* gene product is required for induced expression of two differently regulated nitrogen catabolic genes in *Saccharomyces cerevisiae*.', *Molecular and cellular biology*, 11(2), pp. 1161–1166. doi: 10.1128/mcb.11.2.1161-1166.1991.

Brown, A. J., Brown, G. D., *et al.* (2014) 'Metabolism impacts upon candida immunogenicity and pathogenicity at multiple levels', *Trends in Microbiology*. Elsevier Ltd, 22(11), pp. 614–622. doi: 10.1016/j.tim.2014.07.001.

Brown, A. J., Budge, S., *et al.* (2014) 'Stress adaptation in a pathogenic fungus', *Journal of Experimental Biology*. Edited by S. A. Davies, J. A. T. Dow, and K. Lukowiak, 217(1), pp. 144–155. doi: 10.1242/jeb.088930.

Brown, G. D. *et al.* (2012) 'Hidden Killers: Human Fungal Infections', *Science Translational Medicine*, 4(165), pp. 165rv13-165rv13. doi: 10.1126/scitranslmed.3004404.

Bruckmann, A. *et al.* (2000) 'A phosphatidylinositol 3-kinase of *Candida albicans* influences adhesion, filamentous growth and virulence.', *Microbiology (Reading,*

England). England, 146 (Pt 1, pp. 2755–2764. doi: 10.1099/00221287-146-11-2755.

Bruckmann, A. *et al.* (2001) 'The deletion of *CaVPS34* in the human pathogenic yeast *Candida albicans* causes defects in vesicle-mediated protein sorting and nuclear segregation.', *Yeast (Chichester, England)*. England, 18(4), pp. 343–353. doi: 10.1002/1097-0061(20010315)18:4<343::AID-YEA675>3.0.CO;2-Z.

Bryant, N. J. *et al.* (1998) 'Retrograde traffic out of the yeast vacuole to the TGN occurs via the prevacuolar/endosomal compartment.', *The Journal of cell biology*, 142(3), pp. 651–663. doi: 10.1083/jcb.142.3.651.

Bryant, N. J. and Stevens, T. H. (1998) 'Vacuole Biogenesis in *Saccharomyces cerevisiae*: Protein Transport Pathways to the Yeast Vacuole', *Microbiology and Molecular Biology Reviews*, 62(1), pp. 230–247. doi: 10.1128/MMBR.62.1.230-247.1998.

Burri, L. *et al.* (2003) *A SNARE required for retrograde transport to the endoplasmic reticulum*, *Proceedings of the National Academy of Sciences of the United States of America*. doi: 10.1073/pnas.1734000100.

Cain, C. W. *et al.* (2012) 'A conserved transcriptional regulator governs fungal morphology in widely diverged species', *Genetics*. Genetics, 190(2), pp. 511–521. doi: 10.1534/genetics.111.134080.

Cao, F. *et al.* (2006) 'The Flo8 transcription factor is essential for hyphal development and virulence in *Candida albicans*.', *Molecular biology of the cell*, 17(1), pp. 295–307. doi: 10.1091/mbc.e05-06-0502.

Carlberg, C. and Molnár, F. (2020) 'Transcription Factors and Signal Transduction', in *Mechanisms of Gene Regulation: How Science Works*. Cham: Springer International Publishing, pp. 35–57. doi: 10.1007/978-3-030-52321-3_3.

Carlisle, P. L. and Kadosh, D. (2010) '*Candida albicans* Ume6, a filament-specific transcriptional regulator, directs hyphal growth via a pathway involving Hgc1 cyclin-related protein', *Eukaryotic Cell*, 9(9), pp. 1320–1328. doi: 10.1128/EC.00046-10.

Casadevall, A. (2016) 'Thermal Restriction as an Antimicrobial Function of Fever', *PLOS Pathogens*. Edited by D. A. Hogan. Public Library of Science, 12(5), p. e1005577. doi: 10.1371/journal.ppat.1005577.

Chardwiriyapreecha, S. *et al.* (2008) 'Identification of the fnx1 + and fnx2 + genes for vacuolar amino acid transporters in *Schizosaccharomyces pombe*', *FEBS Letters*, 582(15), pp. 2225–2230. doi: 10.1016/j.febslet.2008.05.017.

Chaves, G. M. *et al.* (2007) 'Candida albicans GRX2, encoding a putative glutaredoxin, is required for virulence in a murine model.', *Genetics and molecular research : GMR*. Brazil, 6(4), pp. 1051–1063.

Chen, C. *et al.* (2011) 'An Iron Homeostasis Regulatory Circuit with Reciprocal Roles in Candida albicans Commensalism and Pathogenesis', *Cell Host & Microbe*, 10(2), pp. 118–135. doi: 10.1016/j.chom.2011.07.005.

Chernomor, O., Von Haeseler, A. and Minh, B. Q. (2016) 'Terrace Aware Data Structure for Phylogenomic Inference from Supermatrices', *Systematic Biology*, 65(6), pp. 997–1008. doi: 10.1093/sysbio/syw037.

Childers, D. S. *et al.* (2016) 'The Rewiring of Ubiquitination Targets in a Pathogenic Yeast Promotes Metabolic Flexibility, Host Colonization and Virulence.', *PLoS pathogens*, 12(4), p. e1005566. doi: 10.1371/journal.ppat.1005566.

Childers, D. S. *et al.* (2020) 'Impact of the Environment upon the *Candida albicans* Cell Wall and Resultant Effects upon Immune Surveillance', in Latgé, J.-P. (ed.) *The Fungal Cell Wall : An Armour and a Weapon for Human Fungal Pathogens*. Cham: Springer International Publishing, pp. 297–330. doi: 10.1007/82_2019_182.

Citiulo, F. *et al.* (2012) 'Candida albicans scavenges host zinc via Pra1 during endothelial invasion.', *PLoS pathogens*, 8(6), p. e1002777. doi: 10.1371/journal.ppat.1002777.

Collins, M. P. and Forgac, M. (2018) 'Regulation of V-ATPase Assembly in Nutrient Sensing and Function of V-ATPases in Breast Cancer Metastasis', *Frontiers in Physiology*, 9, p. 902. doi: 10.3389/fphys.2018.00902.

Conibear, E. and Stevens, T. H. (1998) 'Multiple sorting pathways between the late Golgi and the vacuole in yeast.', *Biochimica et biophysica acta*. Netherlands, 1404(1–2), pp. 211–230. doi: 10.1016/s0167-4889(98)00058-5.

Coornaert, D., Vissers, S. and André, B. (1991) 'The pleiotropic UGA35(DURL) regulatory gene of Saccharomyces cerevisiae: cloning, sequence and identity with the

DAL81 gene.', *Gene*. Netherlands, 97(2), pp. 163–171. doi: 10.1016/0378-1119(91)90048-g.

Cornet, M. *et al.* (2005) 'Deletions of endocytic components VPS28 and VPS32 affect growth at alkaline pH and virulence through both RIM101-dependent and RIM101-independent pathways in *Candida albicans*.', *Infection and immunity*, 73(12), pp. 7977–7987. doi: 10.1128/IAI.73.12.7977-7987.2005.

Cornet, M. and Gaillardin, C. (2014) 'pH signaling in human fungal pathogens: a new target for antifungal strategies.', *Eukaryotic cell*, 13(3), pp. 342–352. doi: 10.1128/EC.00313-13.

Cottier, F. *et al.* (2019) 'Remasking of *Candida albicans* β-Glucan in Response to Environmental pH Is Regulated by Quorum Sensing.', *mBio*, 10(5). doi: 10.1128/mBio.02347-19.

Crawford, A. and Wilson, D. (2015) 'Essential metals at the host-pathogen interface: nutritional immunity and micronutrient assimilation by human fungal pathogens.', *FEMS yeast research*, 15(7). doi: 10.1093/femsyr/fov071.

Dalal, C. K. *et al.* (2016) 'Transcriptional rewiring over evolutionary timescales changes quantitative and qualitative properties of gene expression', *eLife*. eLife Sciences Publications Ltd, 5(September2016). doi: 10.7554/eLife.18981.

Davies, S. A. *et al.* (1996) 'Analysis and inactivation of vha55, the gene encoding the vacuolar ATPase B-subunit in *Drosophila melanogaster* reveals a larval lethal phenotype.', *The Journal of biological chemistry*. United States, 271(48), pp. 30677–30684. doi: 10.1074/jbc.271.48.30677.

Davis, D. (2003) 'Adaptation to environmental pH in Candida albicans and its relation to pathogenesis.', *Current genetics*. United States, 44(1), pp. 1–7. doi: 10.1007/s00294-003-0415-2.

Delorme-Axford, E. *et al.* (2015) 'The yeast Saccharomyces cerevisiae: an overview of methods to study autophagy progression', *Methods*, 75, pp. 3–12. doi: 10.1016/j.ymeth.2014.12.008.

Delorme-Axford, E. and Klionsky, D. J. (2018) 'Transcriptional and post-transcriptional regulation of autophagy in the yeast *Saccharomyces cerevisiae*',

Journal of Biological Chemistry, 293(15), pp. 5396–5403. doi: 10.1074/jbc.R117.804641.

Denis, V. and Cyert, M. S. (2002) 'Internal Ca(2+) release in yeast is triggered by hypertonic shock and mediated by a TRP channel homologue.', *The Journal of cell biology*, 156(1), pp. 29–34. doi: 10.1083/jcb.200111004.

Dilcher, M. *et al.* (2003) 'Use1p is a yeast SNARE protein required for retrograde traffic to the ER', *EMBO Journal*, 22(14), pp. 3664–3674. doi: 10.1093/emboj/cdg339.

Dimitrov, K. and Sazer, S. (1998) 'The Role of fnx1, a Fission Yeast Multidrug Resistance Protein, in the Transition of Cells to a Quiescent G0 State', *Molecular and Cellular Biology*, 18(9), pp. 5239–5246. doi: 10.1128/MCB.18.9.5239.

Dinter, A. and Berger, E. G. (1998) 'Golgi-disturbing agents', *Histochemistry and Cell Biology*, 109(5–6), pp. 571–590. doi: 10.1007/s004180050256.

Dobin, A. *et al.* (2013) 'STAR: Ultrafast universal RNA-seq aligner', *Bioinformatics*. Bioinformatics, 29(1), pp. 15–21. doi: 10.1093/bioinformatics/bts635.

Douzery, E. J. P. *et al.* (2004) 'The timing of eukaryotic evolution: does a relaxed molecular clock reconcile proteins and fossils?', *Proceedings of the National Academy of Sciences of the United States of America*, 101(43), pp. 15386–15391. doi: 10.1073/pnas.0403984101.

Eckstein, M. T., Moreno-Velásquez, S. D. and Pérez, J. C. (2020) 'Gut Bacteria Shape Intestinal Microhabitats Occupied by the Fungus *Candida albicans*', *Current Biology*. Cell Press, 30(23), pp. 4799-4807.e4. doi: 10.1016/j.cub.2020.09.027.

Edgar, R. C. (2004) 'MUSCLE: Multiple sequence alignment with high accuracy and high throughput', *Nucleic Acids Research*, 32(5), pp. 1792–1797. doi: 10.1093/nar/gkh340.

Efe, J. A., Botelho, R. J. and Emr, S. D. (2005) 'The Fab1 phosphatidylinositol kinase pathway in the regulation of vacuole morphology', *Current Opinion in Cell Biology*. England, 17(4), pp. 402–408. doi: 10.1016/j.ceb.2005.06.002.

Van Ende, M., Wijnants, S. and Van Dijck, P. (2019) 'Sugar Sensing and Signaling in *Candida albicans* and *Candida glabrata*.', *Frontiers in microbiology*, 10, p. 99. doi:

10.3389/fmicb.2019.00099.

Ene, I. V, Heilmann, C. J., *et al.* (2012) 'Carbon source-induced reprogramming of the cell wall proteome and secretome modulates the adherence and drug resistance of the fungal pathogen *Candida albicans*.', *Proteomics*, 12(21), pp. 3164–3179. doi: 10.1002/pmic.201200228.

Ene, I. V, Adya, A. K., *et al.* (2012) 'Host carbon sources modulate cell wall architecture, drug resistance and virulence in a fungal pathogen.', *Cellular microbiology*, 14(9), pp. 1319–1335. doi: 10.1111/j.1462-5822.2012.01813.x.

Enjalbert, B. *et al.* (2006) 'Role of the Hog1 stress-activated protein kinase in the global transcriptional response to stress in the fungal pathogen Candida albicans.', *Molecular biology of the cell*, 17(2), pp. 1018–1032. doi: 10.1091/mbc.e05-06-0501.

Enjalbert, B. *et al.* (2007) 'Niche-specific activation of the oxidative stress response by the pathogenic fungus Candida albicans.', *Infection and immunity*, 75(5), pp. 2143–2151. doi: 10.1128/IAI.01680-06.

Finkel, J. S. *et al.* (2012) 'Portrait of Candida albicans adherence regulators', *PLoS Pathogens*, 8(2). doi: 10.1371/journal.ppat.1002525.

Fitzpatrick, D. A. *et al.* (2010) 'Analysis of gene evolution and metabolic pathways using the *Candida* Gene Order Browser', *BMC Genomics*, 11(1), p. 290. doi: 10.1186/1471-2164-11-290.

Franke, K., Nguyen, M., Härtl, A., Dahse, H.-M., Vogl, G., Würzner, R., Zipfel, Peter F, *et al.* (2006) 'The vesicle transport protein Vac1p is required for virulence of Candida albicans.', *Microbiology (Reading, England)*. England, 152(Pt 10), pp. 3111–3121. doi: 10.1099/mic.0.29115-0.

Franke, K., Nguyen, M., Härtl, A., Dahse, H.-M., Vogl, G., Würzner, R., Zipfel, Peter F., *et al.* (2006) 'The vesicle transport protein Vac1p is required for virulence of *Candida albicans*.', *Microbiology*. England, 152(10), pp. 3111–3121. doi: 10.1099/mic.0.29115-0.

Frazer, C., Hernday, A. D. and Bennett, R. J. (2019) 'Monitoring Phenotypic Switching in *Candida albicans* and the Use of Next-Gen Fluorescence Reporters', *Current Protocols in Microbiology*, 53(1), pp. 1–27. doi: 10.1002/cpmc.76.

Freimoser, F. M. *et al.* (2006) 'Systematic screening of polyphosphate (poly P) levels in yeast mutant cells reveals strong interdependence with primary metabolism.', *Genome biology*. BioMed Central, 7(11), pp. 986–994. doi: 10.1186/gb-2006-7-11-r109.

Gale, C. A. and Berman, J. (2012) 'Cell Cycle and Growth Control in Canidda Species', in Calderone, R. A. and Clancy, C. J. (eds) *Candida and Candidiasis*. 2nd edn. Washington, DC, USA: ASM Press, pp. 101–124.

Gancedo, J. M. (1998) 'Yeast Carbon Catabolite Repression', *Microbiology and Molecular Biology Reviews*, 62(2), pp. 334–361. doi: 10.1128/MMBR.62.2.334-361.1998.

Gerami-Nejad, M. *et al.* (2012) 'Analysis of protein function in clinical *C. albicans* isolates', *Yeast*. John Wiley & Sons, Ltd, 29(8), pp. 303–309. doi: 10.1002/yea.2910.

Gerwien, F. *et al.* (2018) 'Metals in fungal virulence', *FEMS Microbiology Reviews*, 42(1), pp. 1–21. doi: 10.1093/femsre/fux050.

Ghavidel, A. *et al.* (2018) 'Rapid nuclear exclusion of HCM1 in aging *Saccharomyces cerevisiae* leads to vacuolar alkalization and replicative senescence', *G3: Genes, Genomes, Genetics*, 8(5), pp. 1579–1592. doi: 10.1534/g3.118.200161.

Gillum, A. M., Tsay, E. Y. H. and Kirsch, D. R. (1984) 'Isolation of the *Candida albicans* gene for orotidine-5′-phosphate decarboxylase by complementation of *S. cerevisiae ura3* and *E. coli* pyrF mutations', *MGG Molecular & General Genetics*. Springer-Verlag, 198(1), pp. 179–182. doi: 10.1007/BF00328721.

Giosa, D. *et al.* (2017) 'Whole RNA-sequencing and transcriptome assembly of Candida albicans and Candida africana under chlamydospore-inducing conditions', *Genome Biology and Evolution*, 9(7), pp. 1971–1977. doi: 10.1093/gbe/evx143.

Gow, N. A. (1997) 'Germ tube growth of Candida albicans.', *Current topics in medical mycology*. Spain, 8(1–2), pp. 43–55.

Gow, N. A. R. *et al.* (2012) 'Candida albicans morphogenesis and host defence: Discriminating invasion from colonization', *Nature Reviews Microbiology*, pp. 112–122. doi: 10.1038/nrmicro2711.

Gow, N. A. R. and Yadav, B. (2017) 'Microbe Profile: Candida albicans: a shape-changing, opportunistic pathogenic fungus of humans', *Microbiology*. Microbiology Society, 163(8), pp. 1145–1147. doi: 10.1099/mic.0.000499.

Graf, K. *et al.* (2019) 'Keeping Candida commensal: how lactobacilli antagonize pathogenicity of Candida albicans in an in vitro gut model.', *Disease models & mechanisms*, 12(9). doi: 10.1242/dmm.039719.

Greig, J. A. *et al.* (2015) 'Cell Cycle-Independent Phospho-Regulation of Fkh2 during Hyphal Growth Regulates *Candida albicans* Pathogenesis', *PLoS Pathogens*. Edited by X. Lin, 11(1), pp. 1–31. doi: 10.1371/journal.ppat.1004630.

Gropp, K. *et al.* (2009) 'The yeast *Candida albicans* evades human complement attack by secretion of aspartic proteases.', *Molecular immunology*. England, 47(2–3), pp. 465–475. doi: 10.1016/j.molimm.2009.08.019.

Ha, N., Hellauer, K. and Turcotte, B. (1996) 'Mutations in target DNA elements of yeast *HAP1* modulate its transcriptional activity without affecting DNA binding.', *Nucleic acids research*, 24(8), pp. 1453–1459. doi: 10.1093/nar/24.8.1453.

Habib, N. *et al.* (2012) 'A functional selection model explains evolutionary robustness despite plasticity in regulatory networks.', *Molecular systems biology*, 8, p. 619. doi: 10.1038/msb.2012.50.

Hall, R. A. (2015) 'Dressed to impress: impact of environmental adaptation on the *Candida albicans* cell wall', *Molecular Microbiology*, 97(1), pp. 7–17. doi: 10.1111/mmi.13020.

Van Den Hazel, H. B., Kielland-Brandt, M. C. and Winther, J. R. (1996) 'Review: biosynthesis and function of yeast vacuolar proteases.', *Yeast (Chichester, England)*. England, 12(1), pp. 1–16. doi: 10.1002/(sici)1097-0061(199601)12:1<1::aid-yea902>3.0.co;2-n.

Heredia, M. Y. *et al.* (2020) 'An expanded cell wall damage signaling network is comprised of the transcription factors Rlm1 and Sko1 in Candida albicans', *PLoS Genetics*, 16(7), pp. 1–23. doi: 10.1371/journal.pgen.1008908.

Hernday, A. D. *et al.* (2010) 'Genetics and molecular biology in *Candida albicans*', *Methods in Enzymology*. 2nd edn. Elsevier Inc, 470(C), pp. 737–758. doi:

10.1016/S0076-6879(10)70031-8.

Hikkel, I. *et al.* (2003) 'A general strategy to uncover transcription factor properties identifies a new regulator of drug resistance in yeast.', *The Journal of biological chemistry*. United States, 278(13), pp. 11427–11432. doi: 10.1074/jbc.M208549200.

Holland, L. M. *et al.* (2014) 'Comparative phenotypic analysis of the major fungal pathogens Candida parapsilosis and Candida albicans.', *PLoS pathogens*, 10(9), p. e1004365. doi: 10.1371/journal.ppat.1004365.

Holmes, A. R. and Shepherd, M. G. (1988) 'Nutritional factors determine germ tube formation in *Candida albicans*', *Medical Mycology*, 26(2), pp. 127–131. doi: 10.1080/02681218880000181.

Homann, O. R. *et al.* (2009) 'A phenotypic profile of the Candida albicans regulatory network', *PLoS Genetics*, 5(12). doi: 10.1371/journal.pgen.1000783.

Homann, O. R. and Johnson, A. D. (2010) 'MochiView: Versatile software for genome browsing and DNA motif analysis', *BMC Biology*, 8. doi: 10.1186/1741-7007-8-49.

Hongay, C. *et al.* (2002) 'Mot3 is a transcriptional repressor of ergosterol biosynthetic genes and is required for normal vacuolar function in Saccharomyces cerevisiae', *EMBO Journal*, 21(15), pp. 4114–4124. doi: 10.1093/emboj/cdf415.

Hood, M. I. and Skaar, E. P. (2012) 'Nutritional immunity: transition metals at the pathogen-host interface.', *Nature reviews. Microbiology*, 10(8), pp. 525–537. doi: 10.1038/nrmicro2836.

Hromatka, B. S., Noble, S. M. and Johnson, A. D. (2005) 'Transcriptional response of Candida albicans to nitric oxide and the role of the YHB1 gene in nitrosative stress and virulence', *Molecular Biology of the Cell*, 16(10), pp. 4814–4826. doi: 10.1091/mbc.E05-05-0435.

Issi, L. *et al.* (2017) 'Zinc cluster transcription factors alter virulence in Candida albicans', *Genetics*, 205(2), pp. 559–576. doi: 10.1534/genetics.116.195024.

Itapary Dos Santos, C. *et al.* (2019) 'Antifungal and Antivirulence Activity of Vaginal Lactobacillus Spp. Products against Candida Vaginal Isolates.', *Pathogens (Basel,*

Switzerland), 8(3). doi: 10.3390/pathogens8030150.

Jackson, J. C. and Lopes, J. M. (1996) 'The yeast *UME6* gene is required for both negative and positive transcriptional regulation of phospholipid biosynthetic gene expression.', *Nucleic acids research*, 24(7), pp. 1322–1329. doi: 10.1093/nar/24.7.1322.

Jakubkova, M. *et al.* (2016) 'Identification of yeast mutants exhibiting altered sensitivity to valinomycin and nigericin demonstrate pleiotropic effects of ionophores on cellular processes', *PLoS ONE*, 11(10), pp. 1–24. doi: 10.1371/journal.pone.0164175.

Jang, S. J. *et al.* (2019) 'Vaginal lactobacilli inhibit growth and hyphae formation of Candida albicans.', *Scientific reports*, 9(1), p. 8121. doi: 10.1038/s41598-019-44579-4.

Johansson, M. E. V. and Hansson, G. C. (2016) 'Immunological aspects of intestinal mucus and mucins', *Nature Reviews Immunology*. Nature Publishing Group, 16(10), pp. 639–649. doi: 10.1038/nri.2016.88.

Johnson, A. D. (2017) 'The rewiring of transcription circuits in evolution.', *Current opinion in genetics & development*, 47, pp. 121–127. doi: 10.1016/j.gde.2017.09.004.

Johnson, R. M. *et al.* (2010) 'Identification of inhibitors of vacuolar proton-translocating ATPase pumps in yeast by high-throughput screening flow cytometry', *Analytical Biochemistry*. Elsevier Inc., 398(2), pp. 203–211. doi: 10.1016/j.ab.2009.12.020.

Johnston, D. A. *et al.* (2009) 'Role for endosomal and vacuolar GTPases in Candida albicans pathogenesis', *Infection and Immunity*, 77(6), pp. 2343–2355. doi: 10.1128/IAI.01458-08.

Jones, E. W. (1991) 'Three proteolytic systems in the yeast *Saccharomyces cerevisiae*.', *The Journal of biological chemistry*. United States, 266(13), pp. 7963–7966.

Kadosh, D. and Johnson, A. D. (2001) 'Rfg1, a protein related to the Saccharomyces cerevisiae hypoxic regulator Rox1, controls filamentous growth and virulence in Candida albicans.', *Molecular and cellular biology*, 21(7), pp. 2496–2505.

doi: 10.1128/MCB.21.7.2496-2505.2001.

Kadosh, D. and Johnson, A. D. (2005) 'Induction of the Candida albicans filamentous growth program by relief of transcriptional repression: a genome-wide analysis.', *Molecular biology of the cell*, 16(6), pp. 2903–2912. doi: 10.1091/mbc.e05-01-0073.

Kalyaanamoorthy, S. *et al.* (2017) 'ModelFinder: Fast model selection for accurate phylogenetic estimates', *Nature Methods*, 14(6), pp. 587–589. doi: 10.1038/nmeth.4285.

Kane, P. M. (2006) 'The Where, When, and How of Organelle Acidification by the Yeast Vacuolar H+-ATPase', *Microbiology and Molecular Biology Reviews*, 70(1), pp. 177–191. doi: 10.1128/mmbr.70.1.177-191.2006.

Kanneganti, V., Kama, R. and Gerst, J. E. (2011) 'Btn3 is a negative regulator of Btn2-mediated endosomal protein trafficking and prion curing in yeast', *Molecular Biology of the Cell*, 22(10), pp. 1648–1663. doi: 10.1091/mbc.E10-11-0878.

Katoh, K. and Standley, D. M. (2013) 'MAFFT multiple sequence alignment software version 7: Improvements in performance and usability', *Molecular Biology and Evolution*, 30(4), pp. 772–780. doi: 10.1093/molbev/mst010.

Katzmann, D. J. *et al.* (1994) 'Transcriptional control of the yeast PDR5 gene by the PDR3 gene product.', *Molecular and cellular biology*, 14(7), pp. 4653–4661. doi: 10.1128/mcb.14.7.4653-4661.1994.

Katzmann, D. J. *et al.* (1996) 'Multiple Pdr1p/Pdr3p binding sites are essential for normal expression of the ATP binding cassette transporter protein-encoding gene PDR5.', *The Journal of biological chemistry*. United States, 271(38), pp. 23049–23054. doi: 10.1074/jbc.271.38.23049.

Kawano-Kawada, M., Kakinuma, Y. and Sekito, T. (2018) 'Transport of amino acids across the vacuolar membrane of yeast: Its mechanism and physiological role', *Biological and Pharmaceutical Bulletin*, 41(10), pp. 1496–1501. doi: 10.1248/bpb.b18-00165.

Khandelwal, N. K. *et al.* (2016) 'Pleiotropic effects of the vacuolar ABC transporter MLT1 of Candida albicans on cell function and virulence', *The Biochemical journal*,

473(11), p. 1537—1552. doi: 10.1042/bcj20160024.

Kim, D. *et al.* (2021) 'Oxidative Stress Causes Vacuolar Fragmentation in the Human Fungal Pathogen Cryptococcus neoformans.', *Journal of fungi (Basel, Switzerland)*, 7(7). doi: 10.3390/jof7070523.

Kim, J. and Klionsky, D. J. (2000) 'Autophagy, cytoplasm-to-vacuole targeting pathway, and pexophagy in yeast and mammalian cells.', *Annual review of biochemistry*. United States, 69, pp. 303–342. doi: 10.1146/annurev.biochem.69.1.303.

Kim, S. W. *et al.* (2019) 'Subunits of the vacuolar H+-ATPase complex, Vma4 and Vma10, are essential for virulence and represent potential drug targets in Candida albicans.', *Fungal biology*. Netherlands, 123(10), pp. 709–722. doi: 10.1016/j.funbio.2019.06.002.

Klein, M. *et al.* (2002) 'The ATP-binding cassette (ABC) transporter Bpt1p mediates vacuolar sequestration of glutathione conjugates in yeast.', *FEBS letters*. England, 520(1–3), pp. 63–67. doi: 10.1016/s0014-5793(02)02767-9.

Klionsky, D. J., Herman, P. K. and Emr, S. D. (1990) 'The fungal vacuole: Composition, function, and biogenesis', *Microbiological Reviews*, pp. 266–292. doi: 10.1128/mmbr.54.3.266-292.1990.

Knight, S. A. B. *et al.* (2005) 'Iron acquisition from transferrin by Candida albicans depends on the reductive pathway.', *Infection and immunity*, 73(9), pp. 5482–5492. doi: 10.1128/IAI.73.9.5482-5492.2005.

Knop, M. *et al.* (1993) 'Vacuolar/lysosomal proteolysis: proteases, substrates, mechanisms.', *Current opinion in cell biology*. England, 5(6), pp. 990–996. doi: 10.1016/0955-0674(93)90082-2.

Kraft, C. and Martens, S. (2012) 'Mechanisms and regulation of autophagosome formation.', *Current opinion in cell biology*. England, 24(4), pp. 496–501. doi: 10.1016/j.ceb.2012.05.001.

Kucejova, B. *et al.* (2005) 'A screen for nigericin-resistant yeast mutants revealed genes controlling mitochondrial volume and mitochondrial cation homeostasis', *Genetics*, 171(2), pp. 517–526. doi: 10.1534/genetics.105.046540.

Kushnirov, V. V. (2000) 'Rapid and reliable protein extraction from yeast', *Yeast*, 16(9), pp. 857–860. doi: 10.1002/1097-0061(20000630)16:9<857::AID-YEA561>3.0.CO;2-B.

Kuznets, G. *et al.* (2014) 'A relay network of extracellular heme-binding proteins drives C. albicans iron acquisition from hemoglobin.', *PLoS pathogens*, 10(10), p. e1004407. doi: 10.1371/journal.ppat.1004407.

Langmead, B. and Salzberg, S. (2013) 'Bowtie2', *Nature methods*, 9(4), pp. 357–359. doi: 10.1038/nmeth.1923.Fast.

Leach, M. D. *et al.* (2012) 'Modelling the Regulation of Thermal Adaptation in *Candida albicans*, a Major Fungal Pathogen of Humans', *PLOS ONE*. Public Library of Science, 7(3), pp. 1–14. doi: 10.1371/journal.pone.0032467.

Li, C. X. *et al.* (2015) '*Candida albicans* adapts to host copper during infection by swapping metal cofactors for superoxide dismutase.', *Proceedings of the National Academy of Sciences of the United States of America*, 112(38), pp. E5336-42. doi: 10.1073/pnas.1513447112.

Li, H. *et al.* (2009) 'The Sequence Alignment/Map format and SAMtools', *Bioinformatics*, 25(16), pp. 2078–2079. doi: 10.1093/bioinformatics/btp352.

Li, L. *et al.* (2001) 'CCC1 is a transporter that mediates vacuolar iron storage in yeast.', *The Journal of biological chemistry*. United States, 276(31), pp. 29515–29519. doi: 10.1074/jbc.M103944200.

Li, L. and Kaplan, J. (2004) 'A mitochondrial-vacuolar signaling pathway in yeast that affects iron and copper metabolism.', *The Journal of biological chemistry*. United States, 279(32), pp. 33653–33661. doi: 10.1074/jbc.M403146200.

Li, S. C. and Kane, P. M. (2009) 'The yeast lysosome-like vacuole: Endpoint and crossroads', *Biochimica et Biophysica Acta - Molecular Cell Research*, pp. 650–663. doi: 10.1016/j.bbamcr.2008.08.003.

Lindquist, S. (1992) 'Heat-shock proteins and stress tolerance in microorganisms.', *Current opinion in genetics & development*. England, 2(5), pp. 748–755. doi: 10.1016/s0959-437x(05)80135-2.

Loh, E. and Hong, W. (2004) 'The binary interacting network of the conserved oligomeric Golgi tethering complex', *Journal of Biological Chemistry*, 279(23), pp. 24640–24648. doi: 10.1074/jbc.M400662200.

Love, M. I., Huber, W. and Anders, S. (2014) 'Moderated estimation of fold change and dispersion for RNA-seq data with DESeq2', *Genome Biology*. BioMed Central Ltd., 15(12), p. 550. doi: 10.1186/s13059-014-0550-8.

MacDiarmid, C. W., Gaither, L. A. and Eide, D. (2000) 'Zinc transporters that regulate vacuolar zinc storage in *Saccharomyces cerevisiae*.', *The EMBO journal*, 19(12), pp. 2845–2855. doi: 10.1093/emboj/19.12.2845.

MacDiarmid, C. W., Milanick, M. A. and Eide, D. J. (2002) 'Biochemical Properties of Vacuolar Zinc Transport Systems of *Saccharomyces cerevisiae*', *Journal of Biological Chemistry*. United States, 277(42), pp. 39187–39194. doi: 10.1074/jbc.M205052200.

MacIsaac, K. D. *et al.* (2006) 'An improved map of conserved regulatory sites for *Saccharomyces cerevisiae*.', *BMC bioinformatics*, 7, p. 113. doi: 10.1186/1471-2105-7-113.

MacPherson, S., Larochelle, M. and Turcotte, B. (2006) 'A Fungal Family of Transcriptional Regulators: the Zinc Cluster Proteins', *Microbiology and Molecular Biology Reviews*, 70(3), pp. 583–604. doi: 10.1128/mmbr.00015-06.

Maguire, S. L. *et al.* (2013) 'Comparative genome analysis and gene finding in *Candida* species using CGOB', *Molecular Biology and Evolution*, 30(6), pp. 1281–1291. doi: 10.1093/molbev/mst042.

Mamane, Y. *et al.* (1998) 'A linker region of the yeast zinc cluster protein leu3p specifies binding to everted repeat DNA.', *The Journal of biological chemistry*. United States, 273(29), pp. 18556–18561. doi: 10.1074/jbc.273.29.18556.

Mancera, E. *et al.* (2021) 'Evolution of the complex transcription network controlling biofilm formation in <i>Candida<i/> species.', *eLife*, 10. doi: 10.7554/eLife.64682.

Marmorstein, R. *et al.* (1992) 'DNA recognition by GAL4: structure of a protein-DNA complex.', *Nature*. England, 356(6368), pp. 408–414. doi: 10.1038/356408a0.

Martínez-Muñoz, G. A. and Kane, P. (2008) 'Vacuolar and plasma membrane proton pumps collaborate to achieve cytosolic pH homeostasis in yeast.', *The Journal of biological chemistry*, 283(29), pp. 20309–20319. doi: 10.1074/jbc.M710470200.

Martínez, P. and Ljungdahl, P. O. (2005) 'Divergence of Stp1 and Stp2 Transcription Factors in Candida albicans Places Virulence Factors Required for Proper Nutrient Acquisition under Amino Acid Control', *Molecular and Cellular Biology*, 25(21), pp. 9435–9446. doi: 10.1128/MCB.25.21.9435-9446.2005.

Meir, J. *et al.* (2018) 'Identification of Candida albicans regulatory genes governing mucosal infection', *Cellular Microbiology*, 20(8), pp. 1–17. doi: 10.1111/cmi.12841.

Merhej, J. *et al.* (2014) 'bPeaks: A bioinformatics tool to detect transcription factor binding sites from ChIPseq data in yeasts and other organisms with small genomes', *Yeast*. John Wiley and Sons Ltd, 31(10), pp. 375–391. doi: 10.1002/yea.3031.

Michaillat, L., Baars, T. L. and Mayer, A. (2012) 'Cell-free reconstitution of vacuole membrane fragmentation reveals regulation of vacuole size and number by *TORC1*', *Molecular Biology of the Cell*. Edited by A. Nakano, 23(5), pp. 881–895. doi: 10.1091/mbc.e11-08-0703.

Michaillat, L. and Mayer, A. (2013) 'Identification of Genes Affecting Vacuole Membrane Fragmentation in Saccharomyces cerevisiae', *PLoS ONE*, 8(2). doi: 10.1371/journal.pone.0054160.

Mijaljica, D. *et al.* (2007) 'Autophagy and vacuole homeostasis: A case for self-degradation?', *Autophagy*, 3(5), pp. 417–421. doi: 10.4161/auto.4441.

Minh, B. Q. *et al.* (2020) 'IQ-TREE 2: New Models and Efficient Methods for Phylogenetic Inference in the Genomic Era', *Molecular Biology and Evolution*. Edited by E. Teeling, 37(5), pp. 1530–1534. doi: 10.1093/molbev/msaa015.

Miseta, A. *et al.* (1999) 'The vacuolar Ca 2+ /H + exchanger Vcx1p/Hum1p tightly controls cytosolic Ca 2+ levels in S. cerevisiae', *FEBS Letters*, 451(2), pp. 132–136. doi: 10.1016/S0014-5793(99)00519-0.

Moreno-Velásquez, S. D. *et al.* (2020) 'The Regulatory Proteins Rtg1/3 Govern Sphingolipid Homeostasis in the Human-Associated Yeast Candida albicans', *Cell Reports*, 30(3), pp. 620-629.e6. doi: 10.1016/j.celrep.2019.12.022.

Mukaiyama, H. *et al.* (2010) 'Autophagy in the fission yeast *Schizosaccharomyces pombe*', *FEBS Letters*. Federation of European Biochemical Societies, 584(7), pp. 1327–1334. doi: 10.1016/j.febslet.2009.12.037.

Naseem, S. *et al.* (2017) 'Regulation of Hyphal Growth and N-Acetylglucosamine Catabolism by Two Transcription Factors in Candida albicans', *Genetics*, 206(1), pp. 299–314. doi: 10.1534/genetics.117.201491.

Navabi, N., McGuckin, M. A. and Lindén, S. K. (2013) 'Gastrointestinal Cell Lines Form Polarized Epithelia with an Adherent Mucus Layer when Cultured in Semi-Wet Interfaces with Mechanical Stimulation', *PLoS ONE*. Edited by B. Foligne, 8(7), p. e68761. doi: 10.1371/journal.pone.0068761.

Nguyen, L. T. *et al.* (2015) 'IQ-TREE: A fast and effective stochastic algorithm for estimating maximum-likelihood phylogenies', *Molecular Biology and Evolution*, 32(1), pp. 268–274. doi: 10.1093/molbev/msu300.

Nobile, C. J. *et al.* (2008) '*Candida albicans* transcription factor Rim101 mediates pathogenic interactions through cell wall functions', *Cellular Microbiology*, 10(11), pp. 2180–2196. doi: 10.1111/j.1462-5822.2008.01198.x.

Nobile, C. J. *et al.* (2012) 'A recently evolved transcriptional network controls biofilm development in *Candida albicans*', *Cell*. Elsevier Inc., 148(1–2), pp. 126–138. doi: 10.1016/j.cell.2011.10.048.

Noble, S. M. and Johnson, A. D. (2005) 'Strains and strategies for large-scale gene deletion studies of the diploid human fungal pathogen *Candida albicans*', *Eukaryotic Cell*, 4(2), pp. 298–309. doi: 10.1128/EC.4.2.298-309.2005.

Nocedal, I., Mancera, E. and Johnson, A. D. (2017) 'Gene regulatory network plasticity predates a switch in function of a conserved transcription regulator.', *eLife*. eLife Sciences Publications Ltd, 6. doi: 10.7554/eLife.23250.

Okonechnikov, K., Conesa, A. and García-Alcalde, F. (2016) 'Qualimap 2: Advanced multi-sample quality control for high-throughput sequencing data', *Bioinformatics*, 32(2), pp. 292–294. doi: 10.1093/bioinformatics/btv566.

del Olmo Toledo, V. *et al.* (2018) 'Diversification of DNA binding specificities enabled SREBP transcription regulators to expand the repertoire of cellular functions

that they govern in fungi', *PLoS Genetics*, 14(12), pp. 1–26. doi: 10.1371/journal.pgen.1007884.

Olsen, I. (2014) 'Attenuation of *Candida albicans* virulence with focus on disruption of its vacuole functions', *Journal of Oral Microbiology*, 6(1), pp. 1–6. doi: 10.3402/jom.v6.23898.

Owen, D. H. and Katz, D. F. (1999) 'A vaginal fluid simulant', *Contraception*, 59(2), pp. 91–95. doi: https://doi.org/10.1016/S0010-7824(99)00010-4.

Palmer, G. E. (2010) 'Endosomal and AP-3-dependent vacuolar trafficking routes make additive contributions to *Candida albicans* hyphal growth and pathogenesis', *Eukaryotic Cell*, 9(11), pp. 1755–1765. doi: 10.1128/EC.00029-10.

Palmer, G. E. (2011) 'Vacuolar trafficking and Candida albicans pathogenesis', *Communicative and Integrative Biology*, 4(2), pp. 240–242. doi: 10.4161/cib.4.2.14717.

Palmer, G. E., Kelly, M. N. and Sturtevant, J. E. (2005) 'The *Candida albicans* vacuole is required for differentiation and efficient macrophage killing', *Eukaryotic Cell*, 4(10), pp. 1677–1686. doi: 10.1128/EC.4.10.1677-1686.2005.

Palmer, G. E., Kelly, M. N. and Sturtevant, J. E. (2007) 'Autophagy in the pathogen Candida albicans', *Microbiology*, 153(1), pp. 51–58. doi: 10.1099/mic.0.2006/001610-0.

Pande, K., Chen, C. and Noble, S. M. (2013) 'Passage through the mammalian gut triggers a phenotypic switch that promotes *Candida albicans* commensalism', *Nature Genetics*, 45(9), pp. 1088–1091. doi: 10.1038/ng.2710.

Park, H. *et al.* (2004) 'Role of the fungal Ras-protein kinase A pathway in governing epithelial cell interactions during oropharyngeal candidiasis', *Cellular Microbiology*. England, 7(4), pp. 499–510. doi: 10.1111/j.1462-5822.2004.00476.x.

Park, Y.-N. and Morschhäuser, J. (2005) 'Tetracycline-Inducible Gene Expression and Gene Deletion in *Candida albicans*', *Eukaryotic Cell*, 4(8), pp. 1328–1342. doi: 10.1128/EC.4.8.1328-1342.2005.

Pérez, J. C. (2019) 'Candida albicans dwelling in the mammalian gut', *Current*

Opinion in Microbiology. Elsevier Ltd, pp. 41–46. doi: 10.1016/j.mib.2019.04.007.

Pérez, J. C., Kumamoto, C. A. and Johnson, A. D. (2013) '*Candida albicans* Commensalism and Pathogenicity Are Intertwined Traits Directed by a Tightly Knit Transcriptional Regulatory Circuit', *PLoS Biology*. Edited by J. Heitman, 11(3), p. e1001510. doi: 10.1371/journal.pbio.1001510.

Peterson, M. D. and Mooseker, M. S. (1992) 'Characterization of the enterocyte-like brush border cytoskeleton of the C2BBe clones of the human intestinal cell line, Caco-2', *Journal of Cell Science*, 102(3), pp. 581–600. doi: 10.1242/jcs.102.3.581.

Petrezselyova, S. *et al.* (2008) 'A collection of yeast mutants selectively resistant to ionophores acting on mitochondrial inner membrane.', *Mitochondrion*. Netherlands, 8(2), pp. 117–129. doi: 10.1016/j.mito.2007.10.003.

Pinto, M. *et al.* (1983) 'Enterocyte-like differentiation and polarization of the human-colon carcinoma cell-line Caco-2 in culture', *Biology of the Cell*, 47(3), pp. 323–330.

Polke, M. *et al.* (2018) 'Farnesol signalling in Candida albicans–more than just communication', *Critical Reviews in Microbiology*, pp. 230–243. doi: 10.1080/1040841X.2017.1337711.

Polke, M. and Jacobsen, I. D. (2017) 'Quorum sensing by farnesol revisited', *Current Genetics*. Springer Berlin Heidelberg, 63(5), pp. 791–797. doi: 10.1007/s00294-017-0683-x.

Poltermann, S. *et al.* (2005) 'The putative vacuolar ATPase subunit Vma7p of *Candida albicans* is involved in vacuole acidification, hyphal development and virulence.', *Microbiology*. England, 151(5), pp. 1645–1655. doi: 10.1099/mic.0.27505-0.

Pradhan, A. *et al.* (2017) 'Elevated catalase expression in a fungal pathogen is a double-edged sword of iron.', *PLoS pathogens*, 13(5), p. e1006405. doi: 10.1371/journal.ppat.1006405.

Pradhan, A. *et al.* (2018) 'Hypoxia Promotes Immune Evasion by Triggering β-Glucan Masking on the Candida albicans Cell Surface via Mitochondrial and cAMP-Protein Kinase A Signaling.', *mBio*, 9(6). doi: 10.1128/mBio.01318-18.

Quinlan, A. R. and Hall, I. M. (2010) 'BEDTools: A flexible suite of utilities for comparing genomic features', *Bioinformatics*, 26(6), pp. 841–842. doi: 10.1093/bioinformatics/btq033.

Raines, S. M. *et al.* (2013) 'Deletion of vacuolar proton-translocating ATPase Voa isoforms clarifies the role of vacuolar pH as a determinant of virulence-associated traits in Candida albicans', *Journal of Biological Chemistry*. Â© 2013 ASBMB. Currently published by Elsevier Inc; originally published by American Society for Biochemistry and Molecular Biology., 288(9), pp. 6190–6201. doi: 10.1074/jbc.M112.426197.

Ram, R. J., Li, B. and Kaiser, C. A. (2002) 'Identification of Sec36p, Sec37p, and Sec38p: Components of yeast complex that contains Sec34p and Sec35p', *Molecular Biology of the Cell*, 13(5), pp. 1484–1500. doi: 10.1091/mbc.01-10-0495.

Ramírez, M. A. and Lorenz, M. C. (2009) 'The transcription factor homolog *CTF1* regulates ß-oxidation in *Candida albicans*.', *Eukaryotic cell*, 8(10), pp. 1604–1614. doi: 10.1128/EC.00206-09.

Ramsay, L. M. and Gadd, G. M. (1997) 'Mutants of *Saccharomyces cerevisiae* defective in vacuolar function confirm a role for the vacuole in toxic metal ion detoxification.', *FEMS microbiology letters*. England, 152(2), pp. 293–298. doi: 10.1111/j.1574-6968.1997.tb10442.x.

Rane, H. S. *et al.* (2013) 'Candida albicans VMA3 is necessary for V-ATPase assembly and function and contributes to secretion and filamentation', *Eukaryotic Cell*, 12(10), pp. 1369–1382. doi: 10.1128/EC.00118-13.

Rane, H. S. *et al.* (2014) 'The Contribution of *Candida albicans* Vacuolar ATPase Subunit V 1 B, Encoded by *VMA2* , to Stress Response, Autophagy, and Virulence Is Independent of Environmental pH', *Eukaryotic Cell*, 13(9), pp. 1207–1221. doi: 10.1128/EC.00135-14.

Rebbeor, J. F. *et al.* (1998) 'ATP-dependent transport of reduced glutathione on YCF1, the yeast orthologue of mammalian multidrug resistance associated proteins.', *The Journal of biological chemistry*. United States, 273(50), pp. 33449–33454. doi: 10.1074/jbc.273.50.33449.

Régnacq, M. *et al.* (2001) 'SUT1p interaction with Cyc8p(Ssn6p) relieves hypoxic genes from Cyc8p-Tup1p repression in *Saccharomyces cerevisiae*.', *Molecular microbiology*. England, 40(5), pp. 1085–1096. doi: 10.1046/j.1365-2958.2001.02450.x.

Reuß, O. *et al.* (2004) 'The SAT1 flipper, an optimized tool for gene disruption in Candida albicans', *Gene*, 341(1–2), pp. 119–127. doi: 10.1016/j.gene.2004.06.021.

Richards, A., Gow, N. A. R. and Veses, V. (2012) 'Identification of vacuole defects in fungi', *Journal of Microbiological Methods*, 91(1), pp. 155–163. doi: 10.1016/j.mimet.2012.08.002.

Richards, A., Veses, V. and Gow, N. A. R. (2010) 'Vacuole dynamics in fungi', *Fungal Biology Reviews*. Elsevier Ltd, 24(3–4), pp. 93–105. doi: 10.1016/j.fbr.2010.04.002.

Richardson, J. P., Ho, J. and Naglik, J. R. (2018) 'Candida–epithelial interactions', *Journal of Fungi*, 4(1), p. 22. doi: 10.3390/jof4010022.

Rollenhagen, C. *et al.* (2020) 'The Role of Secretory Pathways in Candida albicans Pathogenesis', *Journal of Fungi*, 6(1), p. 26. doi: 10.3390/jof6010026.

Rowland, I. *et al.* (2018) 'Gut microbiota functions: metabolism of nutrients and other food components', *European Journal of Nutrition*, 57(1), pp. 1–24. doi: 10.1007/s00394-017-1445-8.

Rupniak, H. T. *et al.* (1985) 'Characteristics of four new human cell lines derived from squamous cell carcinomas of the head and neck.', *Journal of the National Cancer Institute*. United States, 75(4), pp. 621–635.

Russnak, R., Konczal, D. and McIntire, S. L. (2001) 'A Family of Yeast Proteins Mediating Bidirectional Vacuolar Amino Acid Transport', *Journal of Biological Chemistry*, 276(26), pp. 23849–23857. doi: 10.1074/jbc.M008028200.

Sandai, D. *et al.* (2012) 'The evolutionary rewiring of ubiquitination targets has reprogrammed the regulation of carbon assimilation in the pathogenic yeast *Candida albicans*.', *mBio*, 3(6). doi: 10.1128/mBio.00495-12.

Sarry, J.-E. *et al.* (2007) 'Analysis of the vacuolar luminal proteome of

Saccharomyces cerevisiae.', *The FEBS journal*. England, 274(16), pp. 4287–4305. doi: 10.1111/j.1742-4658.2007.05959.x.

Schillig, R. and Morschhäuser, J. (2013) 'Analysis of a fungus-specific transcription factor family, the Candida albicans zinc cluster proteins, by artificial activation', *Molecular Microbiology*, 89(5), pp. 1003–1017. doi: 10.1111/mmi.12327.

Schindelin, J. *et al.* (2012) 'Fiji: an open-source platform for biological-image analysis', *Nature Methods*, 9(7), pp. 676–682. doi: 10.1038/nmeth.2019.

Schneider, C. A., Rasband, W. S. and Eliceiri, K. W. (2012) *NIH Image to ImageJ: 25 years of image analysis*, *Nature Methods*. doi: 10.1038/nmeth.2089.

Sellam, A. *et al.* (2010) 'Role of transcription factor CaNdt80p in cell separation, hyphal growth, and virulence in <l>Candida albicans</i>.', *Eukaryotic cell*, 9(4), pp. 634–644. doi: 10.1128/EC.00325-09.

Setiadi, E. R. *et al.* (2006) 'Transcriptional response of *Candida albicans* to hypoxia: linkage of oxygen sensing and Efg1p-regulatory networks.', *Journal of molecular biology*. England, 361(3), pp. 399–411. doi: 10.1016/j.jmb.2006.06.040.

Shapiro, R. S., Robbins, N. and Cowen, L. E. (2011) 'Regulatory Circuitry Governing Fungal Development, Drug Resistance, and Disease', *MICROBIOLOGY AND MOLECULAR BIOLOGY REVIEWS*, 75(2), pp. 213–267. doi: 10.1128/MMBR.00045-10.

Sharma, K. G. *et al.* (2002) 'Localization, regulation, and substrate transport properties of Bpt1p, a *Saccharomyces cerevisiae* MRP-type ABC transporter.', *Eukaryotic cell*, 1(3), pp. 391–400. doi: 10.1128/EC.1.3.391-400.2002.

Sherrington, S. L. *et al.* (2017) 'Adaptation of Candida albicans to environmental pH induces cell wall remodelling and enhances innate immune recognition', *PLoS Pathogens*, 13(5), pp. 1–28. doi: 10.1371/journal.ppat.1006403.

Shimazu, M. *et al.* (2005) 'A family of basic amino acid transporters of the vacuolar membrane from *Saccharomyces cerevisiae*', *Journal of Biological Chemistry*, 280(6), pp. 4851–4857. doi: 10.1074/jbc.M412617200.

Simm, C. *et al.* (2007) '*Saccharomyces cerevisiae* Vacuole in Zinc Storage and

Intracellular Zinc Distribution', *Eukaryotic Cell*, 6(7), pp. 1166 LP – 1177. doi: 10.1128/EC.00077-07.

Singh, A., Kaur, N. and Kosman, D. J. (2007) 'The metalloreductase Fre6p in Fe-efflux from the yeast vacuole.', *The Journal of biological chemistry*. United States, 282(39), pp. 28619–28626. doi: 10.1074/jbc.M703398200.

Skrzypek, M. S. *et al.* (2017) 'The *Candida* Genome Database (CGD): incorporation of Assembly 22, systematic identifiers and visualization of high throughput sequencing data', *Nucleic Acids Research*, 45(D1), pp. D592–D596. doi: 10.1093/nar/gkw924.

Solis, N. V. and Filler, S. G. (2012) 'Mouse model of oropharyngeal candidiasis', *Nature Protocols*. Nature Publishing Group, 7(4), pp. 637–642. doi: 10.1038/nprot.2012.011.

Speth, C. *et al.* (2008) 'Complement and fungal pathogens: an update', *Mycoses*, 51(6), pp. 477–496. doi: 10.1111/j.1439-0507.2008.01597.x.

Stephan, J., Franke, J. and Ehrenhofer-Murray, A. E. (2013) 'Chemical genetic screen in fission yeast reveals roles for vacuolar acidification, mitochondrial fission, and cellular GMP levels in lifespan extension', *Aging Cell*, 12(4), pp. 574–583. doi: 10.1111/acel.12077.

Stichternoth, C. and Ernst, J. F. (2009) 'Hypoxic adaptation by Efg1 regulates biofilm formation by *Candida albicans*.', *Applied and environmental microbiology*, 75(11), pp. 3663–3672. doi: 10.1128/AEM.00098-09.

Strømhaug, P. E. *et al.* (2004) 'Atg21 is a phosphoinositide binding protein required for efficient lipidation and localization of Atg8 during uptake of aminopeptidase I by selective autophagy.', *Molecular biology of the cell*, 15(8), pp. 3553–3566. doi: 10.1091/mbc.e04-02-0147.

Su, C., Lu, Y. and Liu, H. (2016) 'N-acetylglucosamine sensing by a GCN5-related N-acetyltransferase induces transcription via chromatin histone acetylation in fungi', *Nature Communications*, 7(1), p. 12916. doi: 10.1038/ncomms12916.

Subramanian Vignesh, K. *et al.* (2013) 'Zinc sequestration: arming phagocyte defense against fungal attack.', *PLoS pathogens*, 9(12), p. e1003815. doi: 10.1371/journal.ppat.1003815.

Sudbery, P. E. (2011) 'Growth of Candida albicans hyphae', *Nature Reviews Microbiology*. Nature Publishing Group, 9(10), pp. 737–748. doi: 10.1038/nrmicro2636.

Sun-Wada, G. *et al.* (2000) 'Acidic endomembrane organelles are required for mouse postimplantation development.', *Developmental biology*. United States, 228(2), pp. 315–325. doi: 10.1006/dbio.2000.9963.

Synnott, J. M. *et al.* (2010) 'Regulation of the hypoxic response in *Candida albicans*.', *Eukaryotic cell*, 9(11), pp. 1734–1746. doi: 10.1128/EC.00159-10.

Tao, L. *et al.* (2014) 'Discovery of a "White-Gray-Opaque" Tristable Phenotypic Switching System in *Candida albicans*: Roles of Non-genetic Diversity in Host Adaptation', *PLoS Biology*. Edited by J. Heitman. Public Library of Science, 12(4), p. e1001830. doi: 10.1371/journal.pbio.1001830.

Tebung, W. A. *et al.* (2016) 'Rewiring of the Ppr1 Zinc Cluster Transcription Factor from Purine Catabolism to Pyrimidine Biogenesis in the *Saccharomycetaceae*.', *Current biology : CB*. England, 26(13), pp. 1677–1687. doi: 10.1016/j.cub.2016.04.064.

Teichert, U. *et al.* (1989) 'Lysosomal (vacuolar) proteinases of yeast are essential catalysts for protein degradation, differentiation, and cell survival.', *The Journal of biological chemistry*. United States, 264(27), pp. 16037–16045.

Theiss, S. *et al.* (2002) 'Functional analysis of a vacuolar ABC transporter in wild-type Candida albicans reveals its involvement in virulence.', *Molecular microbiology*. England, 43(3), pp. 571–584. doi: 10.1046/j.1365-2958.2002.02769.x.

Thomas, M. R. and O'Shea, E. K. (2005) 'An intracellular phosphate buffer filters transient fluctuations in extracellular phosphate levels', *Proceedings of the National Academy of Sciences of the United States of America*, 102(27), pp. 9565–9570. doi: 10.1073/pnas.0501122102.

Torggler, R., Papinski, D. and Kraft, C. (2017) 'Assays to Monitor Autophagy in Saccharomyces cerevisiae', *Cells*, 6(3), p. 23. doi: 10.3390/cells6030023.

Tripathi, G. *et al.* (2002) 'Gcn4 co-ordinates morphogenetic and metabolic responses to amino acid starvation in Candida albicans.', *The EMBO journal*, 21(20),

pp. 5448–5456. doi: 10.1093/emboj/cdf507.

Tso, G. H. W. *et al.* (2018) 'Experimental evolution of a fungal pathogen into a gut symbiont.', *Science (New York, N.Y.)*. United States, 362(6414), pp. 589–595. doi: 10.1126/science.aat0537.

Tuch, B. B. *et al.* (2008) 'The evolution of combinatorial gene regulation in fungi', *PLoS Biology*. Edited by L. D. Hurst. Public Library of Science, 6(2), pp. 0352–0364. doi: 10.1371/journal.pbio.0060038.

Umemoto, N. *et al.* (1990) 'Roles of the *VMA3* gene product, subunit c of the vacuolar membrane H(+)-ATPase on vacuolar acidification and protein transport. A study with VMA3-disrupted mutants of *Saccharomyces cerevisiae*.', *The Journal of biological chemistry*. United States, 265(30), pp. 18447–18453.

Underhill, D. M. and Iliev, I. D. (2014) 'The mycobiota: Interactions between commensal fungi and the host immune system', *Nature Reviews Immunology*. Nature Publishing Group, 14(6), pp. 405–416. doi: 10.1038/nri3684.

Urban, C. F. *et al.* (2009) 'Neutrophil extracellular traps contain calprotectin, a cytosolic protein complex involved in host defense against Candida albicans.', *PLoS pathogens*, 5(10), p. e1000639. doi: 10.1371/journal.ppat.1000639.

Vashee, S. *et al.* (1993) 'How do "Zn2 cys6" proteins distinguish between similar upstream activation sites? Comparison of the DNA-binding specificity of the *GAL4* protein in vitro and in vivo.', *The Journal of biological chemistry*. United States, 268(33), pp. 24699–24706.

Vater, C. A. *et al.* (1992) 'The VPS1 protein, a homolog of dynamin required for vacuolar protein sorting in *Saccharomyces cerevisiae* is a GTPase with two functionally separable domains.', *The Journal of cell biology*, 119(4), pp. 773–786. doi: 10.1083/jcb.119.4.773.

Veses, V., Richards, A. and Gow, N. A. (2008) 'Vacuoles and fungal biology', *Current Opinion in Microbiology*, 11(6), pp. 503–510. doi: 10.1016/j.mib.2008.09.017.

Vida, T. A. and Emr, S. D. (1995) 'A new vital stain for visualizing vacuolar membrane dynamics and endocytosis in yeast', *Journal of Cell Biology*, 128(5), pp. 779–792. doi: 10.1083/jcb.128.5.779.

Wächtler, B. *et al.* (2011) 'From attachment to damage: Defined genes of Candida albicans mediate adhesion, invasion and damage during interaction with oral epithelial cells', *PLoS ONE*, 6(2). doi: 10.1371/journal.pone.0017046.

Warren, G. and Wickner, W. (1996) 'Organelle inheritance', *Cell*, 84(3), pp. 395–400. doi: 10.1016/S0092-8674(00)81284-2.

Weber, R. W. S. (2002) 'Vacuoles and the fungal lifestyle', *Mycologist*, 16(1), pp. 10–20. doi: 10.1017/S0269915X02006110.

Wendland, B., Emr, S. D. and Riezman, H. (1998) 'Protein traffic in the yeast endocytic and vacuolar protein sorting pathways.', *Current opinion in cell biology*. England, 10(4), pp. 513–522. doi: 10.1016/s0955-0674(98)80067-7.

White, C. and Gadd, G. (1986) 'Uptake and cellular distribution of copper, cobalt and cadmium in strains of *Saccharomyces cerevisiae* cultured on elevated concentrations of these metals', *FEMS Microbiology Letters*, 38(5), pp. 277–283. doi: 10.1016/0378-1097(86)90003-0.

Wikman-Larhed, A. and Artursson, P. (1995) 'Co-cultures of human intestinal goblet (HT29-H) and absorptive (Caco-2) cells for studies of drug and peptide absorption', *European Journal of Pharmaceutical Sciences*, 3(3), pp. 171–183. doi: 10.1016/0928-0987(95)00007-Z.

Williams, D. W. *et al.* (2013) 'Interactions of *Candida albicans* with host epithelial surfaces', *Journal of Oral Microbiology*, 5(1), p. 22434. doi: 10.3402/jom.v5i0.22434.

Wullschleger, S., Loewith, R. and Hall, M. N. (2006) 'TOR signaling in growth and metabolism.', *Cell*. United States, 124(3), pp. 471–484. doi: 10.1016/j.cell.2006.01.016.

Wurmser, A. E., Gary, J. D. and Emr, S. D. (1999) 'Phosphoinositide 3-kinases and their FYVE domain-containing effectors as regulators of vacuolar/lysosomal membrane trafficking pathways.', *The Journal of biological chemistry*. United States, 274(14), pp. 9129–9132. doi: 10.1074/jbc.274.14.9129.

Wurmser, A. E., Sato, T. K. and Emr, S. D. (2000) 'New Component of the Vacuolar Class C-Vps Complex Couples Nucleotide Exchange on the Ypt7 Gtpase to Snare-Dependent Docking and Fusion', *Journal of Cell Biology*, 151(3), pp. 551–562. doi:

10.1083/jcb.151.3.551.

Xie, J. L. *et al.* (2017) 'The *Candida albicans* transcription factor Cas5 couples stress responses, drug resistance and cell cycle regulation.', *Nature communications*, 8(1), p. 499. doi: 10.1038/s41467-017-00547-y.

Xu, H. and Ren, D. (2015) 'Lysosomal Physiology', *Annual Review of Physiology*, 77(1), pp. 57–80. doi: 10.1146/annurev-physiol-021014-071649.

Xu, L. *et al.* (1995) 'NDT80, a meiosis-specific gene required for exit from pachytene in Saccharomyces cerevisiae.', *Molecular and cellular biology*, 15(12), pp. 6572–6581. doi: 10.1128/MCB.15.12.6572.

Zhang, K. *et al.* (2017) 'Contribution of *VMA5* to vacuolar function, stress response, ion homeostasis and autophagy in Candida albicans.', *Future microbiology*. England, 12, pp. 1147–1166. doi: 10.2217/fmb-2017-0029.

Zhu, A., Ibrahim, J. G. and Love, M. I. (2019) 'Heavy-Tailed prior distributions for sequence count data: Removing the noise and preserving large differences', *Bioinformatics*. Edited by O. Stegle, 35(12), pp. 2084–2092. doi: 10.1093/bioinformatics/bty895.

Znaidi, S. *et al.* (2013) 'A comprehensive functional portrait of two heat shock factor-type transcriptional regulators involved in Candida albicans morphogenesis and virulence.', *PLoS pathogens*, 9(8), p. e1003519. doi: 10.1371/journal.ppat.1003519.

Zordan, R. E. *et al.* (2007) 'Interlocking transcriptional feedback loops control white-opaque switching in Candida albicans', *PLoS Biology*. Public Library of Science, 5(10), pp. 2166–2176. doi: 10.1371/journal.pbio.0050256.

Zwolińska-Wcisło, M. *et al.* (1998) 'Fungal colonization of the stomach and its clinical relevance.', *Mycoses*. Germany, 41(7–8), pp. 327–334. doi: 10.1111/j.1439-0507.1998.tb00346.x.

List of publication

Publications included in this thesis

Philipp Reuter-Weissenberger, Juliane Meir, J. Christian Pérez (*in press*). A fungal transcription regulator of vacuolar function modulates *Candida alb*icans interactions with host epithelial cells. *Accepted October 15th by mBio*.

Affidavit

I hereby confirm that my thesis entitled “The role of a fungal-specific transcription regulator on vacuolar biology and host interaction in *Candida albicans*” is the result of my own work. I did not receive any help or support form commercial consultants. Al sources and / or materials applied are listed and specified in the thesis.

Furthermore, I confirm that this thesis has not yet been submitted as part of another examination process neither in identical nor in similar form.

Würzburg, 19.11.2021

Eidesstattliche Erklärung

Hiermit erkläre ich an Eides statt, die Dissertation „Die Rolle eines pilzspezifischen Transkriptionsfaktors für die Vakuole und Wirtsinteraktion bei *Candida albicans*„ eigenständig, d.h. insbesondere selbständig und ohne Hilfe eines kommerziellen Promotionsberaters, angefertigt und keine anderen als die von mir angegebenen Quellen und Hilfsmittel verwendet zu haben.

Ich erklären außerdem, dass die Dissertation weder in gleicher noch in ähnlicher Form bereits in einem anderen Prüfungsverfahren vorgelegt wurde.

Würzburg, 19.11.2021